

FUNDAMENTAL ADHESIVE STUDIES OF BLOCK COPOLYMERS

by

Margaret Mary Sheridan

Dissertation submitted to the Faculty of the
Virginia Polytechnic Institute and State University
in partial fulfillment of the requirements for the degree of
Doctor of Philosophy
in
Chemistry

APPROVED:

T.C. Ward, Chairman

D.W. Dwight

M.A. Oglioruso

J.E. McGrath

J.P. Wightman

October, 1985

Blacksburg, Virginia

FUNDAMENTAL ADHESIVE STUDIES OF BLOCK COPOLYMERS

by

Margaret Mary Sheridan

T.C. Ward, Chairman

Chemistry

(ABSTRACT)

Models of multiple component, multiple phase adhesives were developed to examine the conflicting demands placed on modern adhesion technology. Styrene and isoprene based block copolymers were investigated in order to understand their adhesive properties. The structure of the microphase separated morphology of the materials studied was found to influence the adhesive behavior in applications as hot melt/structural type adhesives and as pressure sensitive adhesives.

The thermal and the dynamic mechanical behavior of linear styrene/isoprene/styrene triblock copolymers (40% and 50% by weight styrene) was determined for free films and for films bonding together two rigid adherends. Damping phenomena indicated a broader mechanical relaxation spectrum occurring at higher temperatures in the bonded assemblies. Microphase separation in the melts of these triblock materials was interpreted as contributing to the formation of residual stresses in both free films and bonded joints under appropriate thermal and pressure histories,

MCR
10/30/86

illustrating the importance of sample preparation in the evaluation of multiple phase adhesive systems.

Surface and bulk physical characterization studies of a series of radial styrene and isoprene based block copolymers (25% by weight styrenic block) were conducted in order to decipher their effectiveness as pressure sensitive adhesives. The chosen materials included polymers based on p-tert-butylstyrene and isoprene, (TBS-I)*, p-methylstyrene and isoprene, (PMS-I)*, and finally styrene and isoprene (S-I)*. Such a series was an excellent model system to study in terms of microphase separation-property response. Based on solubility parameter arguments, and supported by dynamic mechanical and thermal mechanical analysis, the polymers based on p-tert-butylstyrene and isoprene, (TBS-I)*, were the most microphase intermixed of the three systems, while the styrene and isoprene, radial block polymer, (S-I)*, had the highest degree of phase separation, and the p-methylstyrene and isoprene, (PMS-I)*, fell between these limits in terms of degree of delineation of its morphology. In two separate preparations, the three block copolymers were synthesized in a manner which either yielded 100% radial (star) blocks or which combined radial blocks with about 20% of diblock copolymer.

Investigations were also conducted on a number of hydrogenated forms of the p-tert-butylstyrene and isoprene radial based block copolymers (25% by weight

p-tert-butylstyrene). Hydrogenation of the isoprene phase converted a reasonably compatible pair of component blocks into a system likely to have a higher degree of microphase separation.

The uniqueness of the two sets of investigated polymers lies in the variation of the trade-off between tack and holding power, both necessary for PSAs. Holding power was partially derived from the light crosslinked structure in the isoprene phase, deriving from the radial topology, as well as the development of microphase separation. Tack was related to the compliance of each material. The pressure sensitive adhesive properties of the polymers were found to be closely tied to the final morphology exhibited which was related to the overall compatibility of the component blocks affected by the chemistry of the respective blocks as well as choice of casting solvent. Furthermore, the presence of residual diblock material was found to be an important factor in overall adhesive performance.

This dissertation is dedicated to my parents
for their love, their prayers,
and their support throughout the course of my work.

ACKNOWLEDGEMENTS

This dissertation represents the results of a coordinated effort on the part of many people and organizations. I, the author, would like to acknowledge these people and express my sincere gratitude, for without them, this work would not have been possible.

I would like to thank:

Mr. Jim Hoover for his cooperation and synthetic expertise in preparing the excellent model adhesive systems without which this work would not have been successful;

Dr. James E. McGrath for his guidance in my research and my career objectives;

the Polymer Materials and Interfaces Laboratory, of which I was a member, for the multidisciplinary interaction it provided;

the Center for Adhesion Science, of which I was a member, for the interaction and assistance of its four principal members: the Surface Chemistry Group, the Materials Engineering Group, the Engineering Science and Mechanics Group, and the Polymer Physical Chemistry Group;

the Industrial Organizations, who viewed my work, for their comments and suggestions which greatly helped in my developing an overall approach to my work;

Drs. David W. Dwight, James E. McGrath, Mark A. Oglioruso, James P. Wightman and Thomas C. Ward for serving on my graduate committee;

Dr. James F. Wolfe, Chemistry Department Head, for his kindness;

my colleagues in the Polymer Physical Chemistry Group for their friendship and their assistance in my work;

the Graduate School and Dean Teekell, Dean of the Graduate School, for honoring me with a Cunningham Fellowship for the 1984-85 academic year;

and _____ for her patience in typing this dissertation.

Since my arrival at Virginia Tech and now upon the completion of my graduate studies through the guidance of my research advisor Dr. Thomas C. Ward and the friendship of his family, I have learned that education is much more than studies and research, it is very much the relationships that are built along the way and to Dr. Ward and his family and also to _____ and her family I express my sincere gratitude. Lastly, and certainly not least, I would also like to express my sincere gratitude to my family and friends for their love, their prayers and their support throughout the course of my work.

TABLE OF CONTENTS

CHAPTER I. INTRODUCTION	1
CHAPTER II. NONDESTRUCTIVE EVALUATION OF SOME BONDED JOINTS	7
Abstract	7
Introduction	7
Experimental	14
Results	20
Discussion and Conclusions	36
References	41
CHAPTER III. BLOCK COPOLYMER ADHESIVE STUDIES	43
Abstract	43
Introduction	43
Experimental	49
Results and Discussion	51
References	63
CHAPTER IV. APPLICATION OF COMPRESSIVE CREEP COMPLIANCE MASTER CURVES AS A PREDICTIVE TOOL IN EVALUATING PRESSURE SENSITIVE ADHESIVES	65
Abstract	65
Introduction	67
A. Pressure Sensitive Adhesives - Property of Tack	67
B. Time and Temperature Dependence on Polymeric	

Systems	68
i. Temperature Dependence	69
ii. Time Dependence	72
iii. Time-Temperature Superposition Principle	74
Experimental	87
A. Synthesis	87
B. Sample Preparation	88
C. Instrumentation	90
Results	95
A. Creep Compliance Measurements	95
B. Master Curve Construction	97
Discussion	101
References	104

CHAPTER V. ROLE OF MICROPHASE SEPARATION IN

ADHESION, I	106
Abstract	106
Background	107
A. Block Copolymers	108
i. Composition	109
ii. Sample Preparation	110
iii. Molecular Weight	111
iv. Temperature	111
v. Chemical Nature of the Phase	112
vi. Radial vs. Linear Topology	115
B. Block Copolymer Based Pressure Sensitive Adhesives	116
i. Shear Holding Power	116

ii. Tack	117
Introduction	122
Experimental	124
A. Synthesis and Characterization	124
B. Characterization of Bulk Polymer Properties	127
i. Dynamic Mechanical Thermal Analysis	127
ii. Thermal Mechanical Analysis	128
C. Surface Characterization	129
D. Adhesive Performance Testing	130
Results and Discussion	134
A. Polymer Characterization	134
B. Microphase Separation	134
C. Surface and Bulk Polymer Properties	140
i. Surface Characterization	141
ii. Bulk Polymer Characterization	144
D. Adhesive Performance	145
References	150

CHAPTER VI. ROLE OF MICROPHASE SEPARATION IN

ADHESION, II	157
Abstract	157
Background on Pressure Sensitive Adhesives	158
A. Tack	159
B. Peel	162
i. Transition from Cohesive to Adhesive Failure	164
ii. Transition to Oscillating Failure	169
C. Long-Term Creep or Shear Creep Resistance	170

i.	Chemical Crosslinks	171
ii.	Physical Crosslinks	172
Introduction	173
Experimental	174
A.	Synthesis and Characterization	174
B.	Characterization of Bulk Polymer Properties . . .	175
C.	Surface Characterization	175
D.	Adhesive Performance Testing	177
Results and Discussion	177
A.	Polymer Characterization	177
B.	Part I: Surface and Bulk Polymer Characterization Related to Adhesive Performance	178
i.	Surface Characterization	180
ii.	Bulk Polymer Characterization and Adhesive Performance	182
C.	Part II: Creep Phenomena	189
i.	Tack	191
ii.	Peel	194
iii.	Shear Creep Resistance	199
References	200
 CHAPTER VII. ROLE OF MICROPHASE SEPARATION IN		
ADHESION, III		204
Abstract	204
Introduction	205
Experimental	208
A.	Synthesis and Characterization	208

B.	Characterization of Bulk Polymer Properties	211
i.	Dynamic Mechanical Thermal Analysis	211
ii.	Thermal Mechanical Analysis	211
C.	Adhesive Performance Testing	212
Results and Discussion		212
A.	Part I	215
B.	Part II	221
i.	Dynamic Mechanical Properties	221
ii.	Adhesive Performance	224
References		232
CHAPTER VIII.	CONCLUSIONS	237
References		241
CHAPTER IX.	FUTURE WORK	242
References		245
APPENDIX A.	ESCA TAKE-OFF ANGLE STUDIES	246
Introduction		246
Experimental		247
Results		248
APPENDIX B.	POLYMER BLENDS	252
Introduction		252
Experimental		252
Results		254

APPENDIX C. SOLID STATE NMR	260
Introduction	260
Experimental	261
A. Samples	261
B. Sample Preparation	261
C. NMR	262
Results	263
References	265
VITA	266

LIST OF FIGURES

Figure 1.	Lap shear bond assembly for mounting in Rheovibron.	15
Figure 2.	Modified lap shear assembly with controlled bond thickness for mounting in Rheovibron. .	16
Figure 3.	Dynamic mechanical storage modulus and damping for epoxy free film (at 110 Hz).	21
Figure 4.	Dynamic mechanical relative shear modulus and damping for epoxy bonded joint assembly (at 110 Hz).	22
Figure 5.	Dynamic mechanical storage modulus and damping for polyester/polysulfone block copolymer film (at 110 Hz).	24
Figure 6.	Dynamic mechanical relative shear modulus and damping for polyester/polysulfone block copolymer adhesively bonded joint	25
Figure 7.	Dynamic mechanical storage modulus and damping for poly(ethyl 2-cyanoacrylate) film (at 110 Hz).	26
Figure 8.	Dynamic mechanical relative shear modulus and damping of poly(ethyl 2-cyanoacrylate) bonded adhesive joint (at 110 Hz).	27
Figure 9.	Dynamic mechanical relative shear modulus and damping of a poly(allyl 2-cyanoacrylate) bonded adhesive joint (at 110 Hz).	29
Figure 10.	Dynamic mechanical damping of 50% styrene S/I/S bonded joint and free film at 110 Hz.	32
Figure 11.	Dynamic mechanical damping of 40% styrene S/I/S bonded joint and free film at 110 Hz.	33
Figure 12.	Dynamic mechanical damping of 50% styrene S/I/S free films, cooled with >5000 psi pressure.	35
Figure 13.	Dynamic mechanical damping of 50% styrene S/I/S free films of 0.1 mm thickness	37
Figure 14.	Modified lap shear assembly for mounting in Rheovibron.	50
Figure 15.	Dynamic mechanical storage modulus for S/I/S free films.	55

Figure 16.	Dynamic mechanical storage modulus free film.	56
Figure 17.	Dynamic mechanical damping of 50% styrene S/I/S bonded joint and free film at 110 Hz.	57
Figure 18.	Dynamic mechanical damping of 50% styrene S/I/S (D3) free films, cooled with >5000 PSI pressure.	58
Figure 19.	Dynamic mechanical damping of a block copolymer film.	60
Figure 20.	First run DSC curves for sample E1.	61
Figure 21.	Schematic modulus-temperature curve showing the four regions of viscoelastic behavior.	70
Figure 22.	Preparation of a stress relaxation master curve from experimentally measured modulus-time curves at various temperatures.	76
Figure 23.	Compressive creep compliance data and master curve for styrene and isoprene radial block copolymer, (S-I)* as cast from cyclohexane.	81
Figure 24.	Compressive creep compliance data and master curve for the (TBS-I)* radial block copolymer as cast from cyclohexane.	82
Figure 25.	Perkin Elmer TMS-2.	91
Figure 26.	Schematic representation of compressive creep compliance experiment.	94
Figure 27.	Experimental shift factor plots for styrene and isoprene, (S-I)*, and p-tert-butylstyrene and isoprene, (TBS-I)*, radial block copolymers as cast from cyclohexane.	100
Figure 28.	GPC trace of p-tert-butylstyrene and isoprene radial block copolymer.	126
Figure 29.	Schematic representation of the construction of the 180° peel specimen.	133
Figure 30.	Viscoelastic properties of styrene, p-methylstyrene and p-tert-butylstyrene and isoprene radial block copolymers (1 Hz).	136
Figure 31.	Thermal mechanical analysis of styrene, p-methylstyrene and p-tert-butylstyrene and isoprene radial block copolymers.	137

Figure 32.	Contact angle measurements for styrene, p-methylstyrene and p-tert-butylstyrene and isoprene radial block copolymers. . . .	143
Figure 33.	Creep response of a styrene-diene block copolymer, untackified (-) and tackified (--).	163
Figure 34.	Generalized peel force versus peel rate behavior.	165
Figure 35.	The dependence of peel force on temperature showing the transition from adhesive to cohesive failure.	167
Figure 36.	GPC trace of p-tert-butylstyrene and isoprene block copolymer.	176
Figure 37.	Viscoelastic properties of styrene, p-methylstyrene and p-tert-butylstyrene and isoprene radial block copolymers. . . .	183
Figure 38.	Viscoelastic properties of styrene and isoprene radial block copolymer as cast from cyclohexane, toluene and dichloroethane. .	187
Figure 39.	Compressive creep compliance data and master curve for p-tert-butylstyrene and isoprene radial block copolymers.	192
Figure 40.	Compressive creep compliance data and master curve for styrene and isoprene radial block copolymer.	193
Figure 41.	Shift factor plots for styrene and isoprene and p-tert-butylstyrene and isoprene radial block copolymers.	196
Figure 42.	Peel force versus peel rate for p-tert-butylstyrene and isoprene radial block copolymer.	197
Figure 43.	Peel force versus peel rate for p-tert-butylstyrene and isoprene radial block copolymer.	198
Figure 44.	FTIR spectra of p-tert-butylstyrene and isoprene radial block copolymer and a hydrogenated form for determination of degree of hydrogenation.	210
Figure 45.	Viscoelastic properties of p-tert-butylstyrene and isoprene radial block	

	copolymers having poly(p-tert-butylstyrene) molecular weights of 1.0×10^4 , 1.5×10^4 , and 2.5×10^4 of 1 mole (1 Hz).	214
Figure 46.	Viscoelastic properties of p-tert-butylstyrene and isoprene radial block copolymer and p-tert-butylstyrene and ethylene propylene alternating copolymer (1 Hz). . .	216
Figure 47.	Thermal mechanical analysis of p-tert-butylstyrene and isoprene radial block copolymer and p-tert-butylstyrene and ethylene propylene alternating copolymer. . .	217
Figure 48.	Viscoelastic properties of polyisoprene and ethylene propylene alternating copolymer (1 Hz).	220
Figure 49.	Tan δ of series of hydrogenated p-tert-butylstyrene and isoprene radial block copolymers.	222
Figure 50.	Dynamic storage moduli of series of hydrogenated p-tert-butylstyrene and isoprene radial block copolymers (1 Hz).	223
Figure 51.	Typical stress-strain relations of a series of hydrogenated p-tert-butylstyrene and isoprene radial block copolymers.	225
Figure 52.	Peel force versus peel rate of p-tert-butylstyrene and isoprene radial block copolymer.	228
Figure 53.	Peel force versus peel rate of p-tert-butylstyrene and isoprene radial block copolymer hydrogenated 5%.	229
Figure 54.	Peel force versus peel rate of p-tert-butylstyrene and isoprene radial block copolymer hydrogenated 23%.	230
Figure 55.	Peel force versus peel rate of p-tert-butylstyrene and isoprene radial block copolymer hydrogenated 43.	231

LIST OF TABLES

Table 1. Materials	52
Table 2. Orientation Study	53
Table 3. Characterization of Radial Block Copolymers	90
Table 4. WLF Parameters	101
Table 5. Characterization of Radial Block Copolymers	136
Table 6. Glass Transitions of Homopolymers (DMTA, 1Hz)	140
Table 7. Critical Surface Tensions	143
Table 8. Peel Force	148
Table 9. Characterization of Series C Radial Block Copolymers	180
Table 10. Critical Surface Tensions	183
Table 11. Peel Force	186
Table 12. Peel Force	191
Table 13. Glass Transitions of Homopolymers	220

CHAPTER I

INTRODUCTION

The research presented in this dissertation represents contributions to the interdisciplinary approach toward adhesion science undertaken by the Center for Adhesion Science at Virginia Tech. The primary purpose of the Center is to encourage the interaction between the disciplines of Chemistry, Materials, and Mechanics such that control, analysis, and property predictions for adhesive bonds can be approached utilizing a combination of principles from these respective fields. Representing contributions from the Polymer Physical Chemistry Group, this research concentrated on further establishing the principles and then proceeded with fundamental polymer adhesive work on block copolymer model adhesives. Such materials are multicomponent, multiphase systems, representative of most real adhesives.

The initial efforts reported in this dissertation (Chapters II and III) were a continuation of studies previously undertaken by two students who pioneered efforts in establishing the initial research involving the fundamentals of polymer adhesion. Chapter II addresses the question "do the results from a bulk property test reliably represent the response behavior of the same polymer in a thin bond line, typical of the type encountered in a structural adhesive application, and of the entire bonded structure?"

Nondestructive evaluation of both the free and the bonded adhesives was applied, given that it is generally appreciated that linear viscoelastic behavior may be related to many of the experimentally observed ultimate properties. In Chapter III, the thermal and dynamic mechanical behavior of styrene/isoprene/styrene (SIS) triblock copolymers were investigated in order to understand their adhesive properties. Both block copolymer free films and bonded films were found to have thermal and mechanical response that was strongly dependent on joint preparation. Microphase separation in the melts of these triblock materials was determined to contribute to the observed phenomena.

Based on research in this dissertation, and consistent with the literature, a very important relationship exists between the morphologies of block copolymers and their properties as adhesives. For example, Widmaier and Meyer (1) reported work on the relationship between the morphology of SIS block copolymers and their properties as heat activated films. For each SIS studied, they reported that resistance to break was maximal at a well defined melt application temperature. They attributed this effect to an evolution of the SIS morphology toward phase miscibility which increased with joint formation temperature. Similar conclusions established the principal theme of this dissertation; namely, evaluating the influence of the compatibility of the component blocks of well characterized block copolymers on

subsequent adhesive performance. Chapters IV through VII are the result of the fundamental polymer adhesive investigations on the block copolymer model adhesives referred to above.

As a further outline of this dissertation, a study was undertaken, addressed in Chapters V and VI, which featured the replacement of polystyrene by poly (p-methylstyrene) and poly (p-tert-butylstyrene) in radial styrene and isoprene block polymers. By modifying the chemistry of the styrenic block, all other parameters held constant, it was possible to vary the degree of compatibility of the component blocks of this series of block copolymers. The extent of compatibility affects the degree of resulting microphase separation and, hence, the integrity of the domains. The goal was to translate the effect of block compatibility into the adhesive performance of the copolymers. The polymers of this study were also modified in their morphology through the choice of casting solvent selected to prepare specimens.

In Chapter V, the three radial block copolymers of the above paragraph were synthesized in a fashion which left about 20% residual diblock copolymer. In a later preparation presented in Chapter VI, the block materials were synthesized in a manner which yielded nearly 100% radial, or star, blocks. The presence or absence of the diblock material alters the polymer morphology and the adhesive behavior. Its presence or absence provides a sharp contrast for the results contained in Chapters V and VI. Both chapters emphasize the

dynamic mechanical and thermal properties of the bulk materials which are used to establish relative degrees of microphase separation in the copolymers. The surface aspects of block copolymer adhesion were also examined through utilization of the facilities of the Surface Chemistry Group and the Materials Engineering Department. Evaluation of adhesive performance was based solely on peel adhesion. The results were interpreted in terms of the surface and bulk material properties, again presented in Chapters V and VI.

The need for a fundamental adhesive performance testing method led to the development of the modified probe tack test as reported in Chapter III. The design of the DMA-2, accessory of the Perkin-Elmer TMS-2 Thermomechanical Analyzer, allowed for evaluation of tack on a fundamental and novel level. Compressive creep compliance master curves were constructed and used as a predictive tool in the evaluation of pressure sensitive adhesive performance in terms of tack, adhesion and shear creep resistance over an extended range of times and temperatures. This work, unique in character, appears in both Chapters IV and VI.

To expand and further develop the evaluation of the role of microphase separation in adhesion a quite different polymer series was investigated and is reported in Chapter VI. Investigations were conducted on a series of hydrogenated forms of the p-tert-butylstyrene and isoprene radial block copolymers. Hydrogenation of the isoprene phase

converts a reasonably compatible pair of block components into a system likely to have a high degree of microphase separation. This series was an excellent model system to study in terms of microphase separation - property response. The modified copolymers were indeed found to vary in the degree of microphase separation, systematically influenced by the degree of hydrogenation, and in adhesive character.

The research presented in Chapters IV through VII on the role of microphase separation in adhesion is a result of a combined effort on the part of the author, as a member of the Polymer Physical Chemistry Group, and Mr. Jim Hoover, a member of the Polymer Synthesis Group. Jim performed the synthesis and characterization of the model block copolymer adhesives. This cooperative character of the research led to strong positive benefits: (i. work proceeded with model adhesives whose compositions are well characterized and (ii. further advances occurred in the interdisciplinary approach to adhesion science undertaken by the Center.

This introduction serves as a guide to the chronological development of the progress of this dissertation, whereas the dissertation itself is presented in a slightly different order. Hopefully, it reinforces the important contributions made by other disciplines in an effort to promote a better understanding of adhesion science.

REFERENCES

1. J.M. Widmaier and G.C. Meyer, *Polymer*, 18, 587 (1977).

CHAPTER II

NONDESTRUCTIVE EVALUATION OF SOME BONDED JOINTS

ABSTRACT

Free films and lap-shear bonded metal joints were compared with respect to their linear dynamic viscoelastic behavior. Thermosetting and thermoplastic adhesives were investigated. Damping phenomena and relative shear moduli indicated a broader mechanical dispersion occurring at higher temperatures in the bonded assemblies. Triblock copolymer model adhesives were used to illustrate the importance of sample preparation in the evaluation of bonded materials.

INTRODUCTION

In terms of a total systems analysis approach to adhesive bonding (1) there exists, among others, one clear role with which polymer scientists might identify, namely, that of evaluating proper material response functions and their connection to joint failure events. This work was motivated, to some extent, by a desire to explore a particular response function, the linear viscoelastic quantity $\tan \delta$, which is widely used by polymer researchers to characterize primary and secondary relaxations in bulk polymers, most notably the glass transition, T_g .

It is important to recognize that the molecular dispersions associated with maxima in the $\tan \delta$ function for

glass containing composites are highly time (or frequency) dependent in any geometry of testing. These maxima indicate changes in the response of the entire assembly undergoing testing; hence, they may originate from a number of sources, but not from a transition in the viscoelastic response of the polymer. Only the kinetic events associated with the relaxations are modified by a new time-temperature set of variables. At more rapid strain rates, polymeric materials respond as if the temperature had been lowered. Thus, it is well accepted that quantities such as high speed impact strength of bulk polymers are quite sensitive to test rate and temperature. In particular, for amorphous glasses, such as epoxies, functions based on the reduced temperature, $T-T_g$, best fit the evidence concerning the variation of impact properties on heating of the polymer once test rates are specified. Hence, any mechanically perceived alteration of the glassy relaxation is of paramount importance in bonded joint performance.

One of the fundamental questions in adhesion science is whether or not the results from a bulk property test will reliably represent the response behavior of the same polymer in a thin bond line (typical of the type encountered in a structural adhesive application) and of the entire bonded structure. Over the past few years, investigations have been underway in our labs which suggest that some caution is appropriate when transferring test results obtained on free

polymer samples into situations where the polymer may be (geometrically) under more severe constraints. Other workers have cited data to indicate that adhesive joints often do not perform as predicted from properties of the bulk polymer adhesive (2). However, some researchers (3) have reported good correlation between in situ and bulk properties, on American Cyanamid's FM-73 in the cited case. In this dissertation, observations on different bonded and free polymer adhesives are presented to help clarify this situation, particularly in the case of rapid strain rates (110 Hz) being applied at low amplitude strains.

Overall, two major objectives were defined for this investigation. First, nondestructive evaluation using very small strain deformations of both the free and the bonded adhesives was of interest. Although fracture and failure must be accurately modeled in real systems by nonlinear mechanics, it is generally appreciated that linear viscoelastic behavior is indicative not only of the kinetics of molecular motions in a Boltzmann superposition sense, but may also be related to many of the experimentally observed ultimate properties. Furthermore, most of the design of polymer molecular architectures is based on knowledge gained from examining unsupported polymers. In other words, our ideas about structure/property correlations in polymeric adhesives originate many times from research on samples

which, when tested, differ physically from the configurations encountered in actual applications.

A second objective of this work was to focus on bond thickness and bond thermal and stress history vis-a-vis the nondestructive type of test. There are many citations in the literature which deal with adhesive bond line thickness (4,5), of course, but usually with regard to ultimate properties; G_{1C} 's and time's-to-failure are good examples. Work on epoxy bonded systems at the Naval Research Labs (6,7) over the years has emphasized that, depending on testing rate and temperature, mode I fracture energies may be optimized by selection of bond thicknesses in the range of 0.02-0.07 cm. The viscoelastic natures of these adhesives was often cited in the models which were formulated by these workers to explain the observed performance of the bonds. Indeed, various master curves were developed relating quantities such as $\tan \delta$ to test frequency and temperature. Shifts of a few degrees in the T_g for CTBN modified epoxies were found to vary the reduced frequency (time) scale's of the unbounded adhesive by as much as a decade (7). From the point of view of the impact strength of an adhesively bonded system, such shifts would be of major significance. The occurrence of such shifts, or changes of the breadth and shape of the $\tan \delta$ vs. temperature curves themselves by virtue of the bonding process was also an item to be explored in our work. Particularly when long term environmental effects on

adhesively bonded joints are of interest, it is important to know how the composite joint behaves viscoelastically relative to the bulk adhesive in order that accelerated testing procedures might be developed; the shifts in relaxations would play a role in the analysis.

There is conflicting evidence on the influence of a rigid substrate or filler on the small strain viscoelastic properties of a thin bond line. Recent modeling has predicted a shift in the relaxation maxima of $\tan \delta$ curves which was attributed to changes in boundary layer properties of the polymer molecules (8). Such modeling involves the application of a three-phase system, effectively a composite, for predicting conditions for the shift and resolution of relaxation maxima of $\tan \delta$ curves. The three phases are the boundary-layer polymer, the bulk polymer, and the filler. Calculation of the glass transition temperature of filled polymers follows from two assumptions. First, the boundary layer, having properties differing from the bulk polymer due to the action of the filler surface, and the bulk polymer have different glass transition temperatures. Second, the filler, whose concentration determines the concentration ratio of boundary layer polymer to bulk polymer, also affects the shape of $\tan \delta$ curves because of its high modulus (8). Experimental work by Lipatov et al. (9) showed the addition of glass beads into epoxy resin resulted in a shift in the glass transition temperature to higher temperatures and a

decrease in the maxima values of $\tan \delta$. Similar results were observed for epoxy resins filled with quartz powder. For poly(butyl methacrylate) filled with glass beads there was a considerable decrease and some broadening of the relaxation maxima. However, there was no shift in the glass transition temperature for this latter system. Their results were explained in terms of a decreased molecular mobility of the boundary-layer polymer due to the effect of the filler.

The idea of an "interphase" of polymer with modified properties has frequently been referred to in reports on filler or substrate modification or polymer response near T_g 's (10). However, there is comment in the literature which seriously questions the ability of a high modulus surface to influence macromolecules at any significant distance from the interface (11). Indeed, it is clear that because of the high possibility of residual stress fields due to thermal or curing operations in the preparation of filled or bonded polymer systems it may be quite difficult to identify mechanistically the origin of any anomalous behavior. Nevertheless, mathematical modeling of the interphase to allow for increases or decreases in the T_g of a filled composite has now appeared (12). Theocaris and Spathis predict that strong bonding between a filler and its matrix material results in a higher composite T_g , weak bonding leading in the opposite direction (12).

In summary of the above review, it is apparent that one may not easily anticipate the outcome of a linear viscoelastic test scheme on a bonded joint assembly, even if the polymeric adhesive has well documented properties. There is one salient feature of such comparisons, on the other hand, which must be kept in mind. As was clearly pointed out recently concerning the mechanical response of a nonhomogeneous viscoelastic glassy composite undergoing heating, the relaxations (or dispersions) of the entire assembly may mistakenly be solely identified with macromolecular motions; whereas, in fact, an interjection of instrumental factors into the observed behavior may have occurred (13,14). These papers on the torsion braid experimental method emphasize that a fiber glass braid/amorphous polymer composite exhibits quite different $\tan \delta$ functions of temperature at approximately constant frequency than does the neat resin itself (13,14). In order to avoid this kind of misinterpretation it must be emphasized that in the present research we were investigating from precisely the opposite point of view: namely, while concerned about molecular dispersions in the resin, the response of the joint as a whole was of major concern. Clearly, this is an important question from a design criterion, one seldom addressed in the past.

EXPERIMENTAL

Since adhesive joints are most commonly designed, tested and used in a lap shear mode, we chose a test specimen which in some cases was formed from two degreased stainless-steel plates adhering at the overlap. The thickness of adhesive layer (h) was usually 0.02 cm, but could be in the range of 0.01 to 0.06 cm. In the initial phase of the study, the bond thickness was not controlled but simply allowed to vary about the 0.02 cm value. Details of the bonded assembly appear in Figure 1. Tensile forces were applied to the non-lapped ends of the joint by a Rheovibron.

In the later work, only on the triblock styrene/isoprene/styrene adhesive described below, a second design for the joint which is shown in Figure 2 was developed. Shims were used to control bond thickness at exactly 0.3, 0.5 or 0.7 mm. Each end of the joint then was fitted into new clamps on the Rheovibron having slots offset as indicated in the figure. The entire assembly was rigidly screwed together. Titanium 6,4 alloy (phosphate fluoride etch) was used for the bonded substrates in this case.

The Rheovibron viscoelastometer, introduced by Takayanagi (15), has found broad application for dynamic tensile testing of polymeric films and fibers. Recently it has been used by Murayama (16,17) for measurement of the dynamic shear and dynamic compression mechanical properties

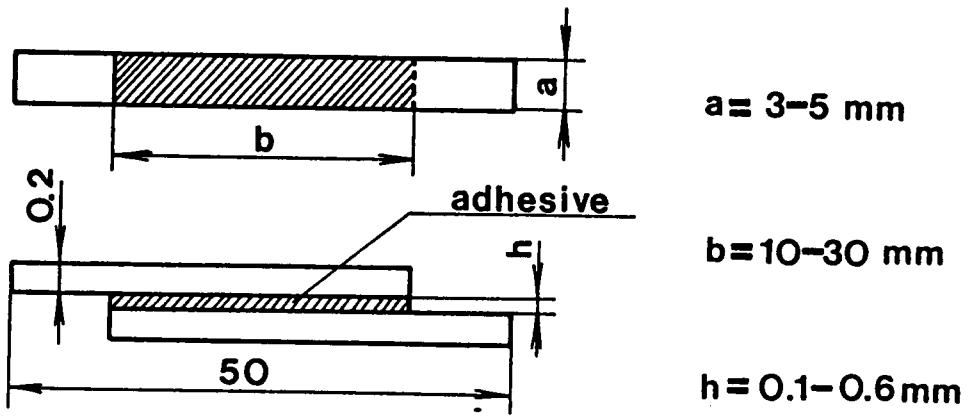


Figure 1. Lap shear bond assembly for mounting in Rheovibron. All dimensions in mm's.

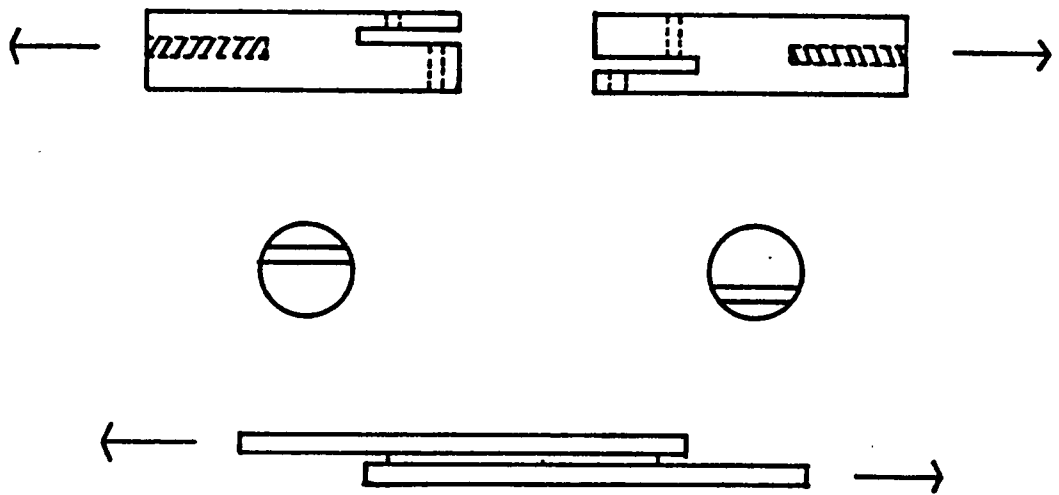


Figure 2. Modified lap shear assembly with controlled bond thickness for mounting in Rheovibron. Dimensions are similar to those in Figure 1. Middle and bottom views are of new clamps for Rheovibron.

of materials. For this purpose special shear and compression grips were developed. Two other reports of use of the Rheovibron in a mode where a viscoelastic material was sheared between parallel plates have been cited; however, in both cases the temperatures were such that only rubbery and liquid-like materials were examined (18,19). In this present paper, the tensile motion of the Rheovibron instrument clamps was transformed into strains in the adhesive that closely approximate those of simple shear, with a calculated magnitude of approximately 10^{-3} . A frequency of 110 Hz and a heating rate of $1^{\circ}\text{C}/\text{min}$ were selected for all testing except on the triblock copolymers where the rate was $1/2^{\circ}\text{C}/\text{min}$. Inertial effects and bending moments in the joint were not observed during any tests. In the materials examined in this study, the Massa correction (20) was not applied.

After the adhesive material was subjected to sinusoidal shear strains, calculations of modulus proceeded according to theory (21). Taking into account the construction of the Rheovibron the dynamic complex shear modulus, G^* in dynes/cm^2 , would be (22):

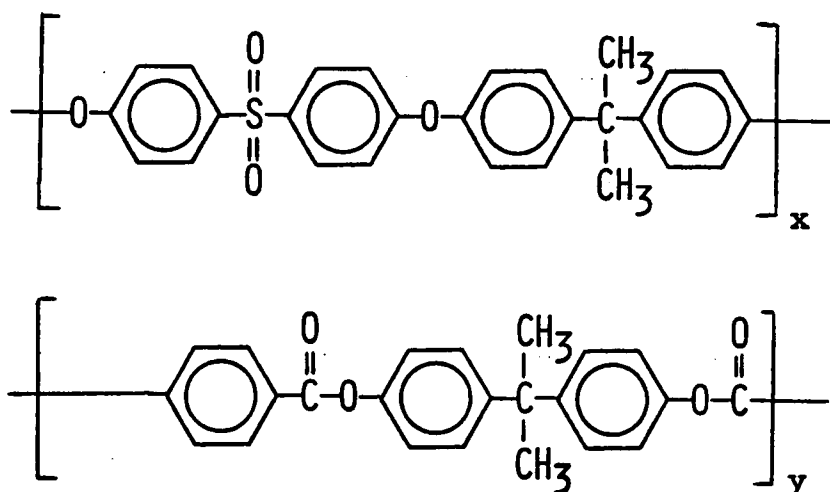
$$G^* = \frac{10^9 h}{ADab} \quad (2.1)$$

where A is the amplitude factor, D is the corrected value of the dynamic force, h is the thickness of adhesive layer, a is the width, and b the length of the adhesive layer. After recording the $\tan \delta$ value, the storage and loss moduli were calculated in the usual fashion. In some cases, however, due to a discrepancy between the sample geometry and the instrument's working range, the calculated values of G^* were observed to be too low. But, decreasing the values of "a" and "b" led to poor result reproducibility, while the magnitude of h was limited by the co-axiality of the clamps and by the actual thickness of the adhesive line for practical comparisons. We found that good qualitative results were obtained by plotting the ratio of the observed value of the shear modulus to its initial value at room temperature, G'/G'_{in} , as a function of increasing temperature.

Two crosslinking adhesive systems were investigated. First a Shell Epon 828 resin was cured with a stoichiometric amount of bis(p-aminocyclohexyl) methane (PACM-20, DuPont) for 2.5 hours at 150°C. Also the crosslinking of an allyl 2-cyanoacrylate was examined (23). Use of this material as opposed to the alkyl ester is known to produce improved thermal resistance, created by thermally induced crosslinking of the anionically cured 2-cyanoacrylate monomer (24).

Several thermoplastic adhesives were melted between the appropriate substrates in a compression mold and cooled to

form the adhesive joint. These were: (1) poly(ethyl 2-cyanoacrylate), (2) styrene/isoprene/styrene (S/I/S) triblock copolymers of varying composition kindly provided by the Phillips Petroleum Co., and (3) a novel polysulfone/polyester block copolymer having the following structure (25), with a 50/50 (wt.) % composition and an overall molecular weight of 25,000 g/mole.



The joint preparation conditions corresponding to the numbers above were (1) room temperature, slight pressure; (2) various pressure and temperature cycles which are discussed below, (3) 220°C, 2000 psi, slow cooling.

The S/I/S samples were selected to have narrow molecular weight distributions, $M_w/M_n = 65000/63000$, and $M_w/M_n = 86000/83000$ containing 50% and 40% by weight of styrene, respectively. These samples were found to be highly

microphase separated in structure and to have a lamellae type morphology.

For polymer tested in the bulk (free) form in the usual Rheovibron tensile geometry, typical sample dimensions of 0.2 to 0.6 mm thickness, 3-5 cm length and 0.5 cm width were chosen. Thus, the polymer part of the composite joint was comparable in size to the free film. Calculations of $\tan \delta$ and storage modulus E' proceeded in the usual way for free films.

RESULTS

Figure 3 and Figure 4 show the results obtained for the common epoxy resin tested as a film in a tensile geometry and then as an adhesive bond between metal substrates in the shear mode. The $\tan \delta$ maximum appeared at 187°C in the bulk neat material and at 5°C higher than this in the bonded adhesive system. However, there was a substantial broadening of the latter peak, reminiscent of the changes produced by adding mineral fillers to thermosets. The maximum damping in the bonded joint is lower by almost a factor of ten. Less dramatic was the larger drop in the free film's storage modulus before a plateau appeared in the relaxation.

Comparisons of the polysulfone/polyester block copolymer mechanical spectra appear in Figure 5 and Figure 6, with the free film results in the former. The

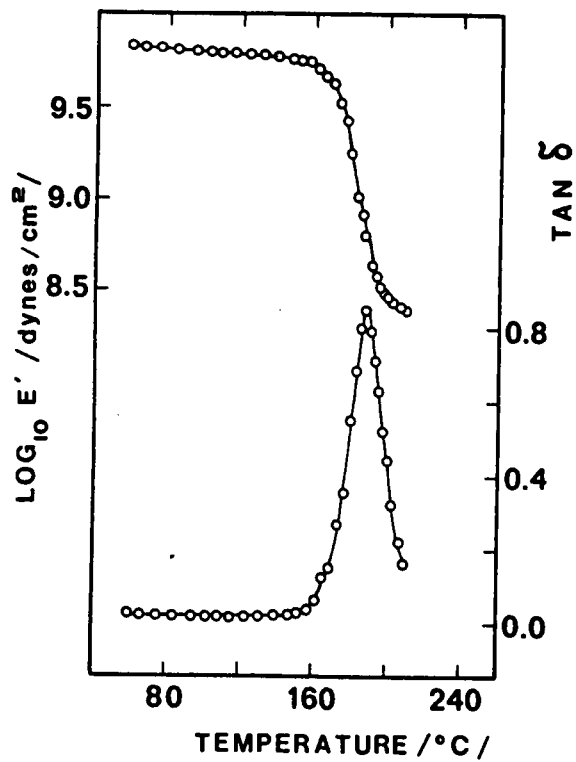


Figure 3. Dynamic mechanical storage modulus and damping for epoxy free film (at 110 Hz).

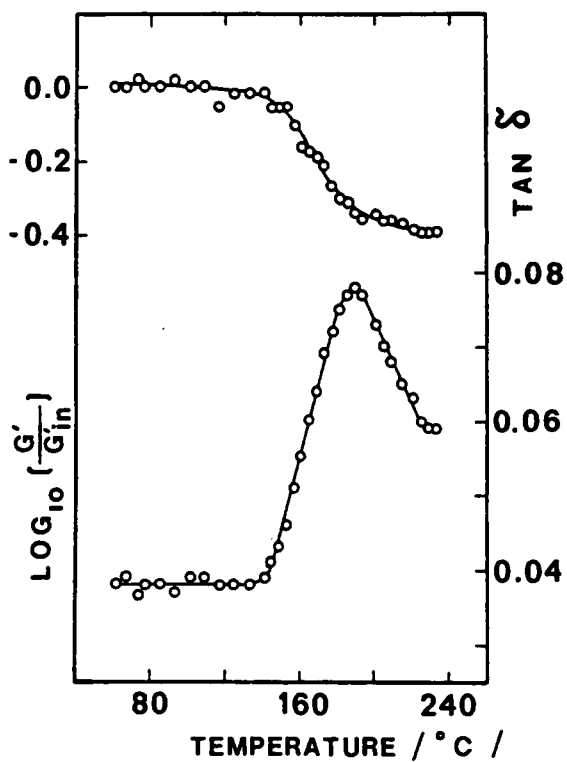


Figure 4. Dynamic mechanical relative shear modulus and damping for epoxy bonded joint assembly (at 110 Hz).

single glass transition indicated at above 200°C was intermediate between those recorded for either homopolymer also tested at 110 Hz and heated at 1°C/min. As observed in the epoxy systems, the maximum in $\tan \delta$ appeared 5°C higher when the lap shear geometry was employed for testing. Furthermore, the difference in the magnitude of the mechanical damping in the two samples was even larger than for the epoxy. Again, the temperature range of the relaxation was broadened as detected in the joint, while the storage modulus drop was approximately equivalent to that for the unconstrained film.

Dynamic mechanical testing of poly(ethyl 2-cyanoacrylate) produced results shown in Figure 7 and Figure 8 in the unbonded and bonded configurations, respectively. The sharp relaxation with a maximum at about 110°C for the free film was modified in the bonded joint to become a quite broad temperature response at this test frequency, with a more complex shape. The magnitude of the higher temperature damping maximum in the joint is approaching the absolute values described above for the free films. In addition, the first peak found on heating is about 20°C higher than in the unrestricted film. In previous work we have noted that the poly(ethyl 2-cyanoacrylate) was found to have very poor thermal stability, showing a total loss of

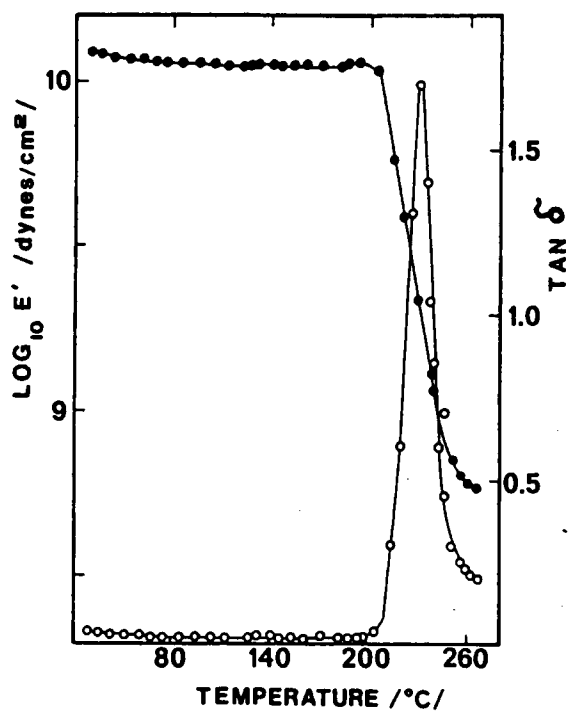


Figure 5. Dynamic mechanical storage modulus and damping for polyester/polysulfone block copolymer film (at 110 Hz).

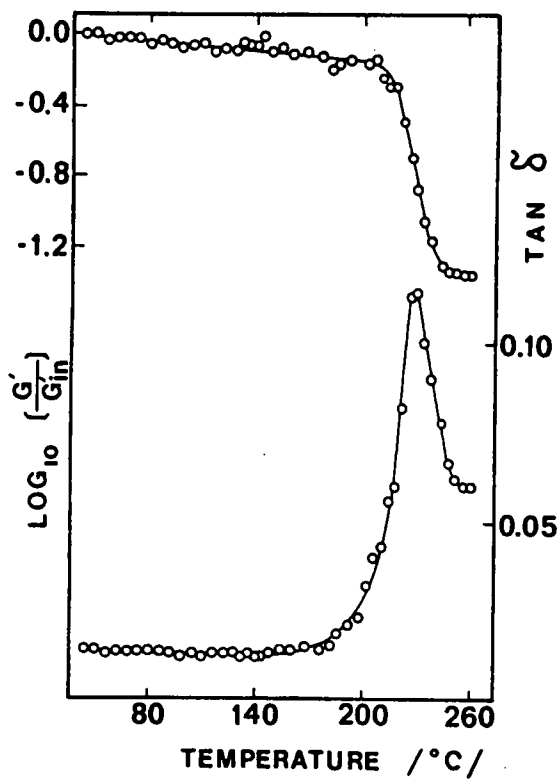


Figure 6. Dynamic mechanical relative shear modulus and damping for polyester/polysulfone block copolymer adhesively bonded joint (at 110 Hz).

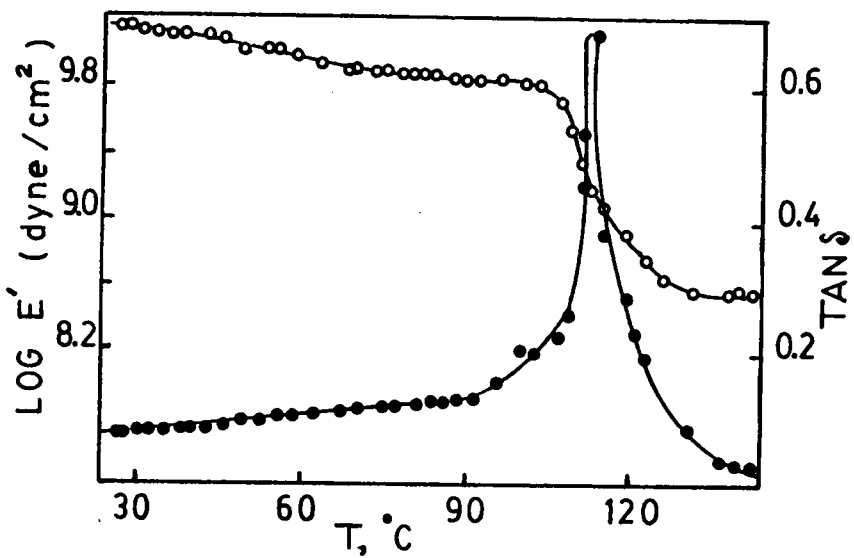


Figure 7. Dynamic mechanical storage modulus and damping for poly(ethyl 2-cyanoacrylate) film (at 110 Hz).

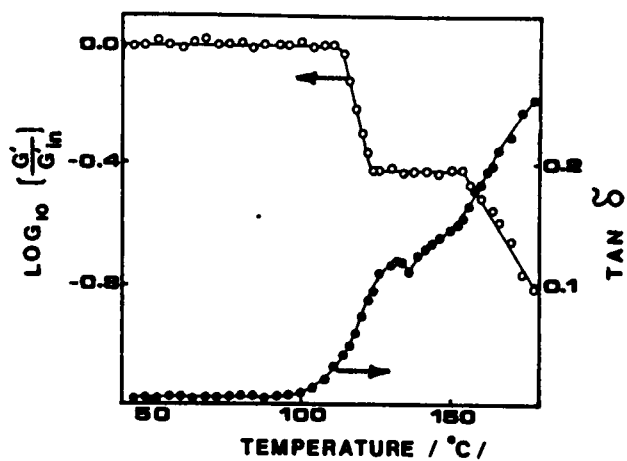


Figure 8. Dynamic mechanical relative shear modulus and damping of poly(ethyl 2-cyanoacrylate) bonded adhesive joint (at 110 Hz).

tensile lap shear strength on aging for 24 hours at 150°C (24).

In contrast to the alkyl 2-cyanoacrylate adhesive, the allyl version had quite different mechanical response as is presented in Figure 9. The maximum in $\tan \delta$ for the bonded system is about 8°C higher in temperature than that seen for the alkyl version, but then decreases gradually with continued heating. More striking is the recovery of the initial shear storage modulus to its original value on heating. Previously, we determined that a thermally induced crosslinking was responsible for this behavior (24). As the vitrification due to network formation proceeded, the glassy storage modulus was approached, in spite of the increase in temperature at 1°C/min (which apparently was slower than the progress of the chemical reaction). The fully-cured allyl ester adhesive was found to have a T_g greater than 200°C (24).

The final experimental results were obtained on the triblock (styrene/isoprene/styrene) thermoplastics, and represent a second phase of the research in which bond thickness was tightly controlled rather than varying around a nominal value of 0.2 mm. The design of Figure 2 was employed for all of this work.

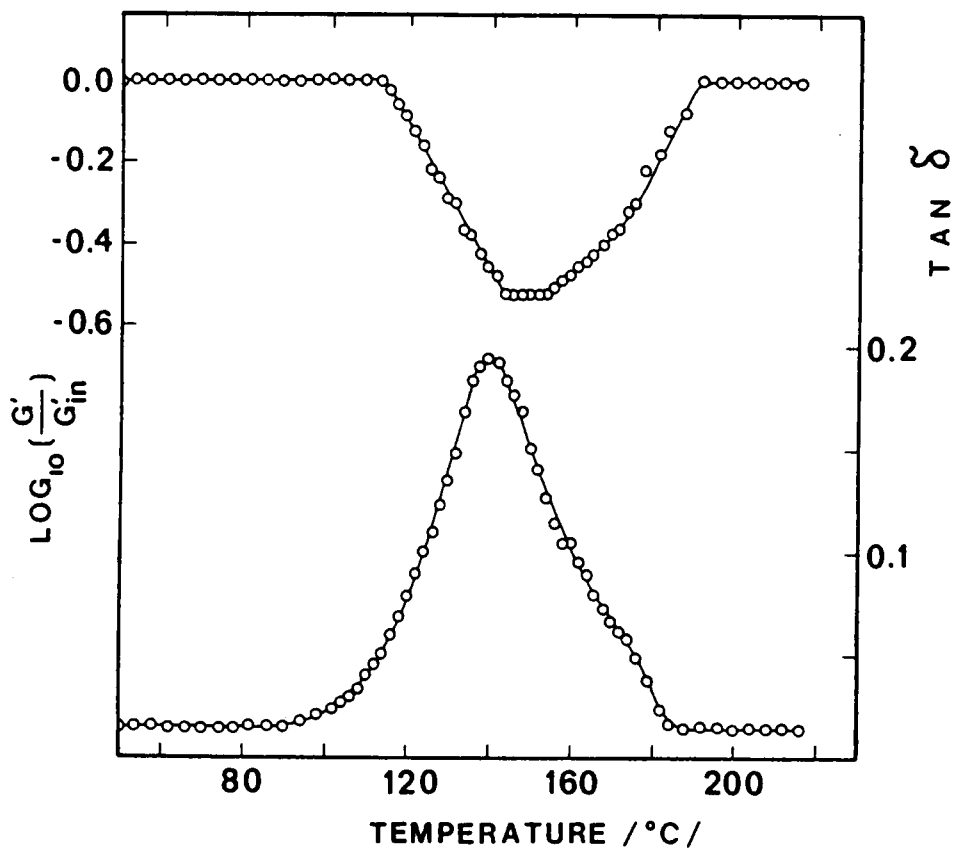


Figure 9. Dynamic mechanical relative shear modulus and damping of a poly(allyl 2-cyanoacrylate) bonded adhesive joint (at 110 Hz).

Preparation of the adhesively bonded joints with the S/I/S polymers was extremely important because of the sensitivity of the polymer morphology to thermal history. For example, we were able to extrude films of similar triblock materials which showed different free film storage moduli (almost a factor of two) in the extruded and transverse directions (25). Also, using DSC we sometimes noted unexpected thermal response of these materials at about 20°C below the glass transition temperature which was attributed to a "stress release phenomenon." It was demonstrated that differences in the compression molding operation could be associated with either the presence or the absence of such stress release events (25). Thus, the S/I/S materials served as model adhesives with which to evaluate the trends in the results for the other polymers described above.

Results of experiments on S/I/S free films and on S/I/S bonded joints with the thermoplastic glue line at 0.3, 0.5 and 0.7 mm appear together in Figure 10. All preparations were made with the 50% styrene content polymer. The preparation temperature was 150°C and at least 5000 psi was applied in the molding. Pressure was maintained during cooling. The $\tan \delta$'s are enlarged in Figure 10 compared to the usual presentation in order to emphasize sample differences. An increase in the rate of the molecular relaxations seems to appear in the bulk free film (B) on

heating, with a very rapid increase in damping in the vicinity of 100°C. For this unbonded film the $\tan \delta$ passed out of the range of the instrument (for these sample dimensions) at about 108°C. In contrast, for all three bond thicknesses investigated the damping of the joint assembly was lower than that of the free film at equivalent temperatures, while the onset of very high damping shifted upward approximately 20 degrees depending on bond thickness. It is apparent that in the very thin bond-line joints there are indications of several temperature ranges where small maxima or details in the damping appear. These results were independent of heating rate and reproducible as long as the same joint preparation conditions were observed. A major question of concern was whether the small peaks were real or artifacts.

When the experiments represented by Figure 10 were repeated with the 40 weight % styrene S/I/S block copolymer, similar observations were again recorded. These results appear in Figure 11. Preparation conditions were the same as in Figure 10. As expected, the magnitude of the damping was higher overall due to the increased isoprene fraction in the copolymer. However, the major features of the previous curves were retained. These are (1) higher temperatures required for appearance of damping maxima in joints as opposed to free films (2) unusual behavior of the $\tan \delta$ prior

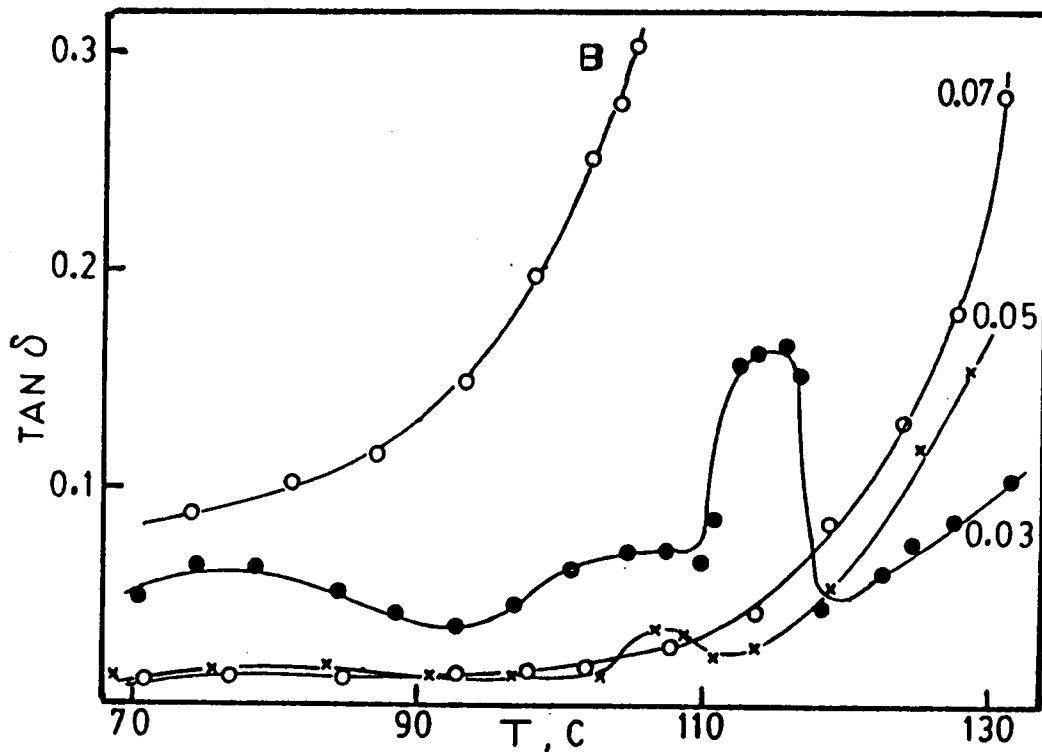


Figure 10. Dynamic mechanical damping of 50% styrene S/I/S bonded joint and free film at 110 Hz. Bond thicknesses shown on curves are in cm for joints. Free film = B.

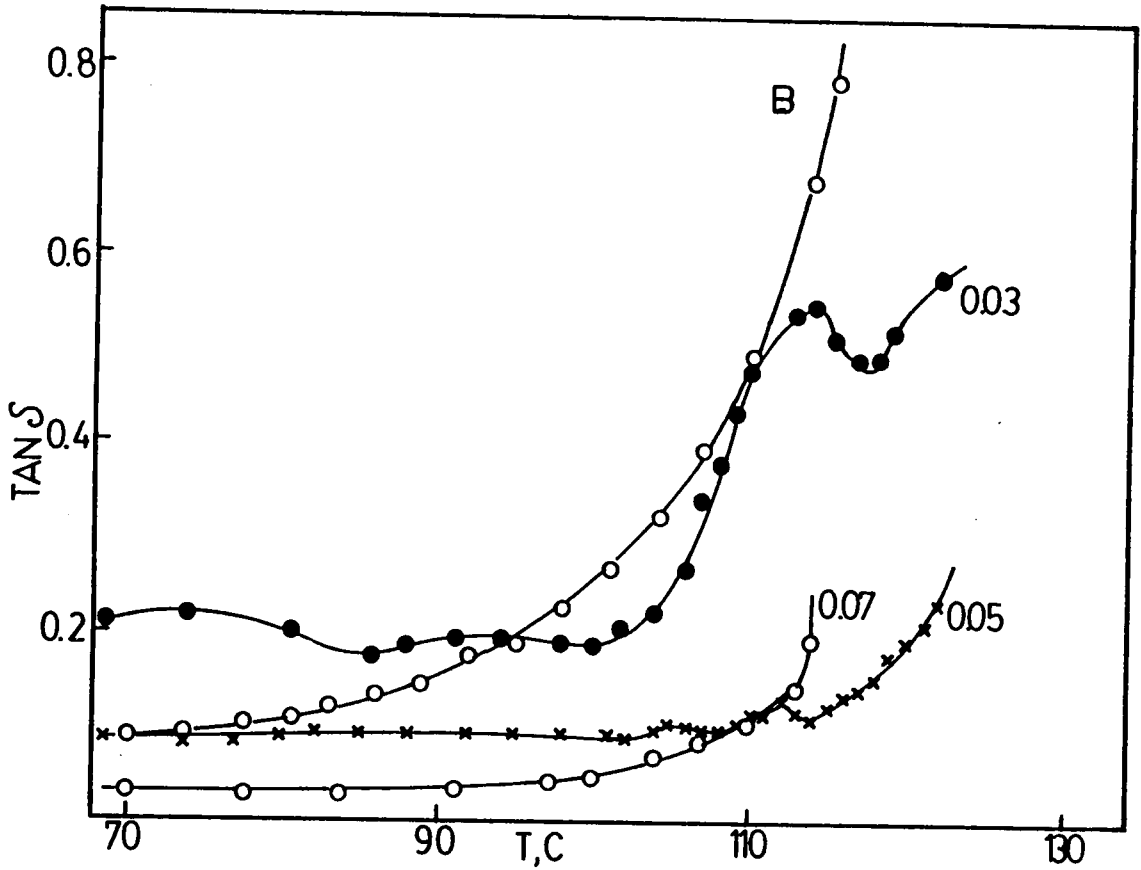


Figure 11. Dynamic mechanical damping of 40% styrene S/I/S bonded joint and free film at 110 Hz. Bond thicknesses shown on curves are in cm for joints. Free film = B.

to very high damping phenomena, which seems to depend on bond thickness in the joints as opposed to the free film (B).

Further experiments were conducted on the 50% styrene content S/I/S copolymer. Modifications of the molding procedure for the S/I/S adhesives were made in an attempt to understand the behavior of the fabricated joints as a whole. The major changes were to provide for slow cooling of the free films with and without any application of external pressure and to vary sample thickness. As a consequence of this new manufacturing process, the mechanical behavior was also altered. It was reasoned that if pressure-induced frozen stress changed mechanical response in bonded composites, a very thin free film prepared under conditions identical to those in the joints might also exhibit similar response. Confirmation of this hypothesis appears in Figure 12, where data on two free films are shown. The curve labeled P,0.1 represents results on a 0.1 mm thick, cooled-with-pressure sample. In the other curve (B), a 0.6 mm thick, cooled-with-pressure, material response is indicated. These latter data are replicates of those in Figure 10. Influence of the sample thickness is striking in this figure.

A final set of experiments on the 50% styrene S/I/S materials is summarized in Figure 13. Both curves shown depict the outcome of tests on free films. Now, holding the

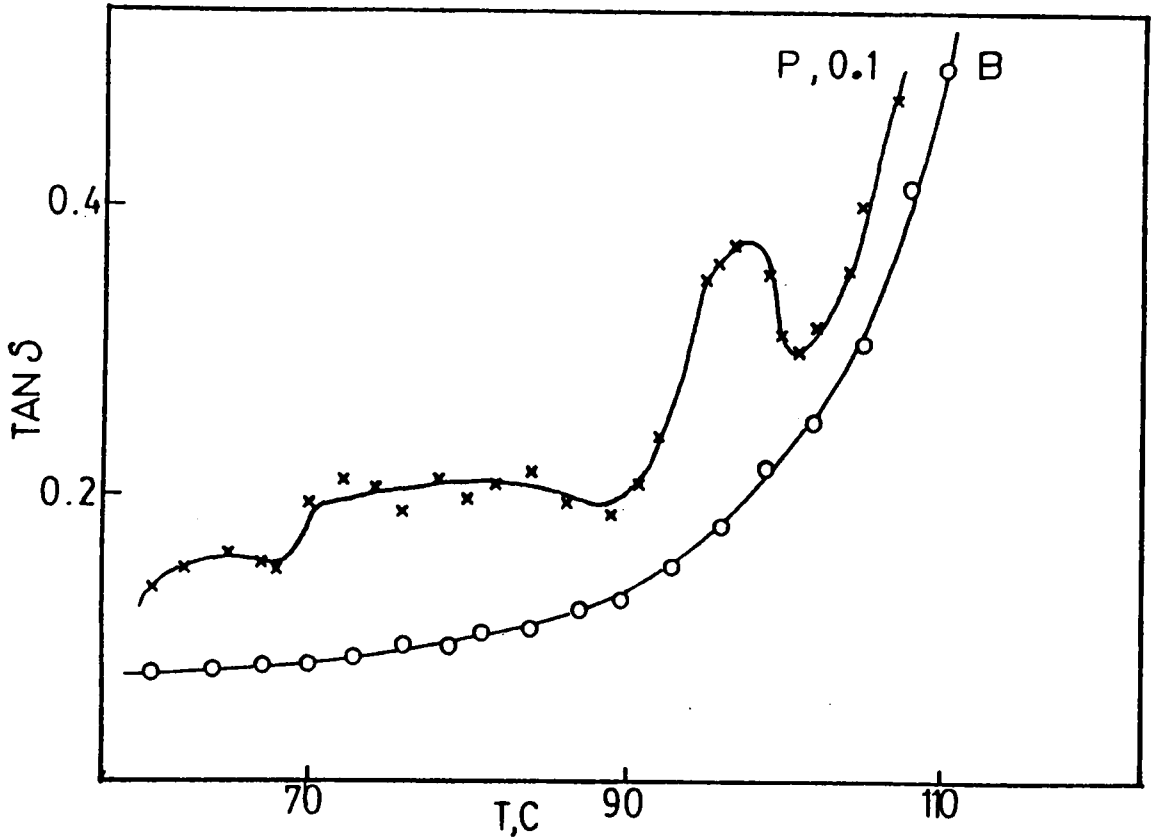


Figure 12. Dynamic mechanical damping of 50% styrene S/I/S free films, cooled with >5000 psi pressure. B = 0.6 mm, P,0.1 = 0.1 mm thick.

sample dimensions in each run almost the same with a thickness of 0.1 mm, preparation of the specimens differed only in that cooling was accomplished after molding with either >5000 psi pressure applied (P) or with no pressure (NP). The difference in $\tan \delta$ was dramatic again and parallels that found when a thick specimen (B) was used with pressurized cooling, Figure 12, instead of the thin one. Neither of the comparisons made in Figure 12 or Figure 13 causes a shift of the $\tan \delta$ curves to higher temperatures as was found when bonded joints were investigated.

DISCUSSION AND CONCLUSIONS

In both the thermosetting and thermoplastic adhesives there were always different $\tan \delta$ (at 110 Hz) functions of temperature when free and bonded films were compared at equal heating rates. Generally, the viscoelastic response of the composite joint occurred over a wider temperature range than that of the free film, again heating rates being equal. Substantially different magnitudes of the monitored relaxation events were observed in each case. Non-equilibrium effects in the testing procedure do not seem to be responsible for any of these observations, non-equilibrium states in the joints may be.

At this time no firm conclusions may be put forth concerning the origins of the variations in dynamic

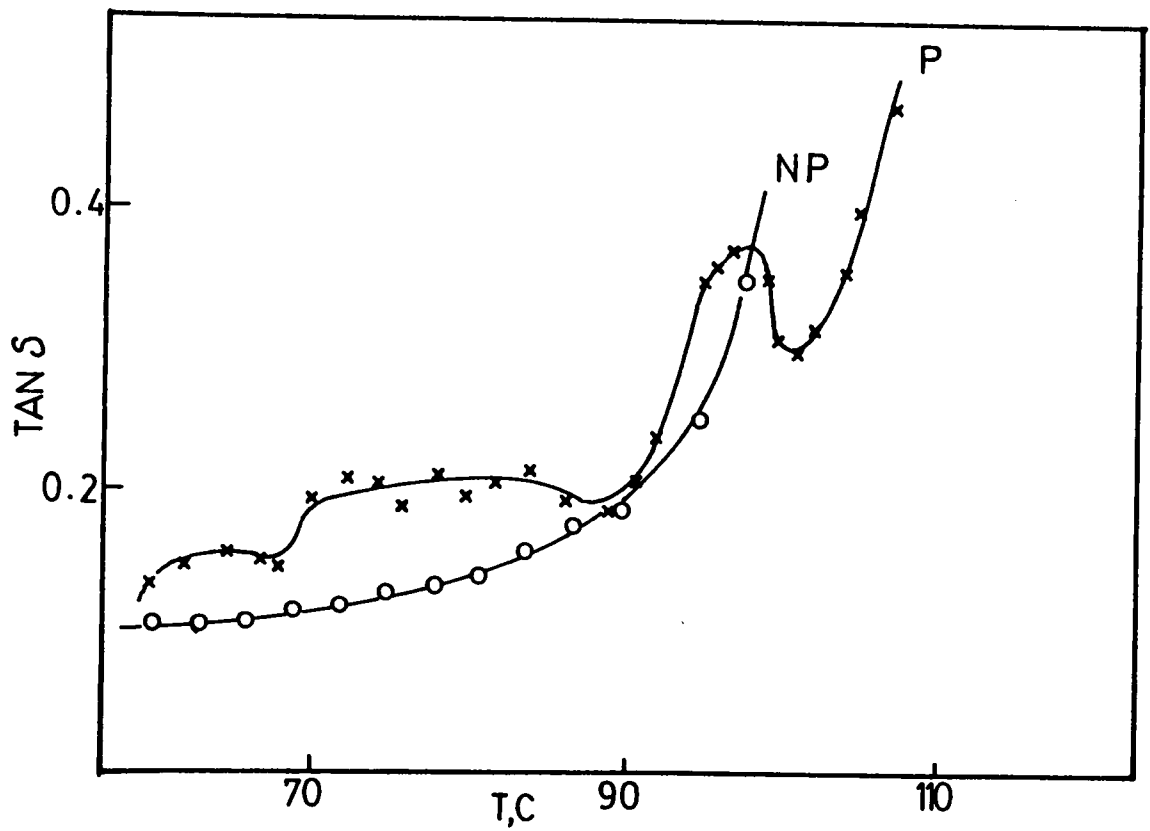


Figure 13. Dynamic mechanical damping of 50% styrene S/I/S free films of 0.1 mm thickness. P = cooled with >5000 psi pressure, NP = cooled without pressure.

mechanical properties with respect to free film vs. bonded lap shear joints; however, some facts are clear. In the thermoset materials and the polyester-polysulfone single phase block copolymer the differences in performance of bonded and free films are not as large and may reflect normal shifting due to the change in the monitored viscoelastic function in each case (tensile elongation vs. shear). Since simple shear is a constant volume process, and all other types of deformations require change in volume (Poisson's ratio = 0.5), a correct constitutive equation description of the polymer's response would predict different relaxation behavior at constant temperature, or different temperature profiles in isochronous experiments. In the investigations of the present paper this effect should be quite small, and difficult to calculate.

A second view of the difference in mechanical behavior of the free and bonded films would attribute the physical variations to frozen stresses (originating from shrinkage, non-equilibrium morphology and crosslinking). Certainly the results on the S/I/S block copolymers suggest that thermal history must not be ignored in evaluating damping in a polymerically bonded structure placed in oscillatory shear fields. As the bond thickness was decreased the magnitude of the changes in viscoelastic response usually increased, depending on the polymer. Further experimentation at other frequencies and under certain isothermal conditions where

stress release may be measured would be informative in clarifying the mechanism in this case.

With regard to long range polymer modulation (e.g. limitation of conformation isomers, damping of normal modes) by a highly rigid surface, the present experiments lead us to make no statement. The substrate surface area to volume of polymer ratio is so small that one finds it difficult to believe that any variation of dynamic mechanical relaxations of the overall bonded structure would manifest themselves in such simple experiments. Even in much more sensitive experiments on thin films, no mention is made of instrumentally induced limitation of molecular motion (27).

Finally, the series of investigations on the S/I/S block copolymers reveals some interesting conclusions vis-a-vis dynamic mechanical testing of compression molded heterophase polymers. It appears that either free films or bonded joints may be manufactured which will show a fine structure in the $\tan \delta$ vs. temperature experiment, prior to the actual maximum damping of the film or assembly. Cooling thin films with applied pressures greater than 5000 psi was required to produce these details. Using thick films, or thick bond lines, or cooling without pressure would completely remove these smaller damping peaks. Confirming our DSC work, there was always a "bump" in these curves in the region of 70°C. The presence of the substrates, furthermore, when a thin bond line was used, shifted the large $\tan \delta$ damping to

substantially higher temperatures, free films never showed this behavior.

Because of their nice model adhesive character, the S/I/S copolymers' behavior helped clarify the response observed in the other adhesives of this study. The generally broadened peaks of mechanical energy damping, occurring at higher temperatures, for these other samples may be manifestations of similar unrelaxed stress fields in the bonded joints. The caveat which was suggested on completion of this work reinforces the importance of sample preparation technique in systems where glass formation occurs during joint manufacture (such as is the case for structural adhesives).

REFERENCES

1. W. B. Jones, Jr., Organic Coatings and Applied Polymer Science Proceedings, 47, 247 (1982).
2. D. W. Dwight, E. Sancaktar and H. F. Brinson, in "Adhesion and Adsorption of Polymers", L. H. Lee, Editor, Part A, 141 Plenum Press, New York, 1980.
3. G. Dolev and O. Ishai, J. Adhesion, 12, 283 (1981).
4. L. R. F. Rose, J. Adhesion, 14, 93 (1982).
5. R. W. Hylands and E. H. Sidwell, J. Adhesion, 11, 203 (1980).
6. W. D. Bascom, R. L. Cottingham and C. O. Timmons, J. Appl. Polym. Sci., Appl. Polym. Symp., 32, 165 (1977).
7. D. L. Hunston, S. S. Wang, A. J. Kinloch, Organic Coatings and Applied Polymer Science Proceedings, 47, 408 (1982); also see J. T. Bitner, J. L. Rushford, W. S. Rose, D. L. Hunston and C. K. Riew, J. Adhesion, 13, 3 (1981).
8. V. F. Babich and Y. S. Lipatov, J. Appl. Polym. Sci., 27, 53 (1982).
9. Y. S. Lipatov, V. F. Rosovizky and V. V. Shifrin, J. Appl. Polym. Sci., 27, 455 (1982).
10. G. J. Howard and R. A. Shanks, J. Macromol. Sci.-Phys., B19 (2), 167 (1981).
11. P. Peyser, Polym - Plat. Technol. Engr., 10 (2), 117 (1978).
12. P. S. Theocaris and G. D. Spathis, J. Appl. Polym. Sci., 27, 3019 (1982).
13. D. J. Plazek, J. Polym. Sci., 20, 1533 (1982).
14. D. J. Plazek and G. F. Gu, J. Polym. Sci., 20, 1551 (1982).
15. M. Takayangi, in "Proceedings of the Fourth International Congress on Rheology," C. Klason and J. Kubat, Editors, Part I, p. 161, Swedish Soc. Rheo. Publisher, Gothenburg, 1965.

16. T. Murayama, *J. Appl. Polym. Sci.*, 19, 3221 (1975).
17. T. Murayama, in "Proceedings of the Seventh International Congress on Rheology," E. H. Lee and A. L. Copley, Editors, p. 402, Interscience, New York, 1977.
18. B. H. Shah and R. Darby, *Polym. Eng. Sci.*, 16, 46 (1976).
19. P. F. Erhardt, J. J. O'Malley and R. G. Crystal, *ACS Polym. Preprint*, 10(2), 812 (1969).
20. D. J. Massa, *J. Appl. Phys.*, 44, 2595 (1973); also A. R. Ramos, F. S. Bates, R. E. Cohen, *J. Polym. Sci., Polym. Phys. Ed.*, 16, 753 (1978).
21. S. Timoshenko, "Strength of Materials," Part I, Van Nostrand, Princeton, 1955.
22. Instruction Manual No. 68, Rheovibron Model DDV-II-C, Toyo Bladwin Co., Ltd. Tokyo (1973).
23. D. L. Kotzev, C. Konstantinov, P. Novabov, V. Kabaivanov, *Bulg. Pat. No.* 23321 (1977).
24. D. L. Kotzev, T. C. Ward, D. W. Dwight, *J. Appl. Polym. Sci.*, 26, 1941 (1981).
25. J. E. McGrath, Private Communication.
26. A. Wood, M.S. Thesis, Virginia Polytechnic Institute and State University, Blacksburg, Va. (1982).
27. J. D. Ferry, "Viscoelastic Properties of Polymers," 3rd Ed. Chapter 5, Wiley, New York, 1980.

CHAPTER III
BLOCK COPOLYMER ADHESIVE STUDIES

ABSTRACT

The thermal and dynamic mechanical behavior of triblock copolymers with a styrene/isoprene/styrene architecture were investigated in order to understand their adhesive properties. Both copolymer free films and films bonding together two titanium alloy plates were found to have thermal and mechanical response that was strongly dependent on joint preparation. Microphase separation in the melts of these triblock materials was felt to contribute to the observed phenomena; namely, the presence of residual stresses in thin films which had been cooled while under high pressure.

INTRODUCTION

It is well known that viscoelastic stress fields are developed in the flow of molten polymer. When such a flowing polymer is cooled, a molecular orientation process may lead to anisotropic mechanical properties. Studies relating residual stresses and impact failure behavior of ABS resins strongly point out the possible subtlety of structure-property relationships in oriented polymeric solids (1). Work in our laboratory has shown that styrene/isoprene/styrene triblock copolymers may also be prepared which show anisotropic behavior with respect to

fracture in adhesively bonded lap shear joints made with rigid substrates (2). Furthermore, extruded films of similar triblock materials used in the fracture study showed different free film storage moduli in the extruded and transverse directions (3).

Recent theories, (4,5) indicate that a sharp boundary does not exist in polystyrene-polydiene block copolymers, but rather, partial mixing exists in the interfacial region between the two thermodynamically incompatible phases. The thickness of the interface is temperature dependent. With increasing temperature, intermixing of the two phases increases at the expense of the pure phases, but the copolymers remain phase segregated. Indeed, structural changes continue to exist well into the melt, but the two phase structure of styrene-butadiene block copolymers persists to nearly 180°C (6). At a critical temperature T_c , complete mixing of both phases occurs; the system may be considered as thermodynamically homogeneous. Block copolymers, as a result of the existence of microphase separated morphologies in the melt, exhibit complex rheological properties. Sivashinsky, Moon, and Soong (7) have recently studied the time dependent stress growth and relaxation behavior of SBS systems as a function of casting solvent, temperature, and shear history. Their objective was to provide insight into the mechanism of structure breakdown and reformation in SBS melts. The underlying principal in

their investigation was that the rheology of SBS triblock copolymers is highly sensitive to the prevailing morphology. The morphology of the SBS systems, in turn, was found to be highly sensitive to many factors, such as casting solvent, temperature, shear history, and overall sample history. Therefore, rheological measurements may be very difficult to reproduce. Further complexities were found in studies of the stress relaxation behavior, where the morphology of the fluid evolves with time as stresses relax (7-9). Rheology work in our laboratories confirms their observations. Since molten adhesives of the microphase separated type flow into bonding positions and rapidly cool, variable morphologies may exist in almost identically prepared joints.

J. M. Widmaier and G. C. Meyer (10) have previously demonstrated that only SIS copolymers with a segregated structure exhibit notable shear adhesive strength. The joint strength was found to pass through a maximum on increase in temperature. Such behavior has been interpreted as depending on the morphology of the copolymers, as discussed above. The maximum corresponds to the temperature just below T_c (dependent on by the molecular weights and composition of the copolymers) where the morphology of the sample is favorable for strong bonding.

The morphology of the adhesive may be altered by kinetic effects; thus, different cooling conditions (i.e. quenched or annealed) result in bonds of differing lap shear strengths

(10). Studies on SIS copolymers in our laboratory also indicate that the presence or lack of pressure upon cooling of a bonded joint produces structures which exhibit different dynamic mechanical damping patterns as will be presented below. Clearly, the history of the adhesive was very important in determining its behavior, pressure included. Some background in this area is important.

Densified glasses, prepared by cooling amorphous polymers from the liquid state under elevated pressures, have been a topic of much investigation for the past decade. Currently, three types of properties are usually measured and available in the literature concerning densified glasses: specific volume data, density fluctuation as measured by SAXS, and enthalpy data from DSC measurements. Two different effects appear to result from the application of pressure during glass formation depending upon whether the formation pressure is above or below 1.5 kbar. For pressures less than 1.5 kbar all three of the above properties decrease with pressure, which is indicative of more efficient molecular packing. However, for pressures greater than 1.5 kbar a decrease in specific volume and a relatively constant fluctuation density is observed, accompanied by an increase in enthalpy. Weitz and Wunderlich (11) accounted for the increase in enthalpy at elevated pressures by noting that T_g increased with pressure; therefore, the glass prepared under elevated pressure contains chains of higher conformational

energy. Prest (12), studying PVC densified under different pressures, at constant temperature, observed an increase in enthalpy with pressure; however, he attributed the higher enthalpy of a pressure-densified glass not to high energy conformational states but rather to frozen in stored energy, either in terms of bond angle distortions or increased intermolecular potential energy. Curro and Roe (13), who have recently done SAXS studies of density fluctuation in pressure-densified polystyrene glasses, concur with Prest. They feel the results at higher pressures indicate that molecular packing can no longer be made more efficient, and any further volume reduction is obtained by forcing polymer segments into positions of local energy minimum, requiring distortion of chain bonds and higher overall energy.

Wunderlich (11) observed, by means of DSC studies on pressure densified PS glasses, an additional endothermic event at temperatures far below the glass transition temperature. This is consistent with the suggestion that strain energy is trapped in glasses prepared under elevated pressure. The strain energy, stored in the form of distorted chain bonds or unfavorable intersegmental interactions, could provide a driving force to overcome the local energy barriers; the chains, on a local level, could undergo cooperative rearrangements, even at temperatures well below the glass transition temperature. Also, as an interesting aside, there is preliminary evidence that such low

temperature rearrangements, occurring on a local scale, may lead to the formation of microcavities in such pressure densified glasses (13,15).

In our work presented below free and bonded films of variable thickness were investigated using triblock copolymers. We were interested in this because other workers have cited data to indicate that adhesive joints often do not perform as predicted from properties of the bulk polymer adhesive. However, some researchers (17) have reported good correlation between in situ and bulk properties. In our present investigation, the observations on different bonded and free, oriented polymer adhesives with (molecular) orientation both parallel and transverse to the testing direction are summarized in an effort to clarify the effect of a rigid substrate on bulk polymer properties. We want, additionally, to gain further insight into the role of molecular orientation of adhesive films in bonded joint properties.

Even though a "systems approach" has been utilized throughout our work, a specific set of measurements was necessary for analysis. Our exploration primarily involved the linear viscoelastic quantity $\tan \delta$, which is widely used by polymer researchers to characterize primary and secondary relaxations in bulk polymers, most notably the glass transition, T_g (3).

EXPERIMENTAL

The joint fracture experiments were conducted on a single lap shear joint with an overlap length of 1.27 cm, bond area of 3.22 cm^2 , and adhesive layer thickness averaging .038 cm. The adherends were titanium 6-4 alloy. The bonds were formed under conditions of minimal temperature, pressure, and time for retention of orientation within the adhesive. The oriented films were extruded on a CSI mini-max extruder and have been labeled "parallel" and "perpendicular" with respect to the machine direction of extrusion.

The joints were fractured at room temperature on an Instron Table Model 1130 with a cross-head speed of 1 cm/min. Joint strength was measured as the maximum stress applied, and the total fracture energy was obtained by integrating over the fracture curve.

DSC thermograms were collected on the Perkin-Elmer DSC-2. The heating rate was 10K/min.

The relaxation patterns for polymers in the bulk (free) form were obtained from experimentation conducted on a Rheovibron DDV-II-C in the usual Rheovibron tensile geometry. The heating rate was $1^\circ\text{C}/\text{min}$.

In the Rheovibron work on bonded films a test design which is shown in Figure 14 was developed. Each end of the joint is fitted into new clamps on the Rheovibron having slots offset as indicated in the figure. Shims were used to control bond thickness. The entire assembly is rigidly

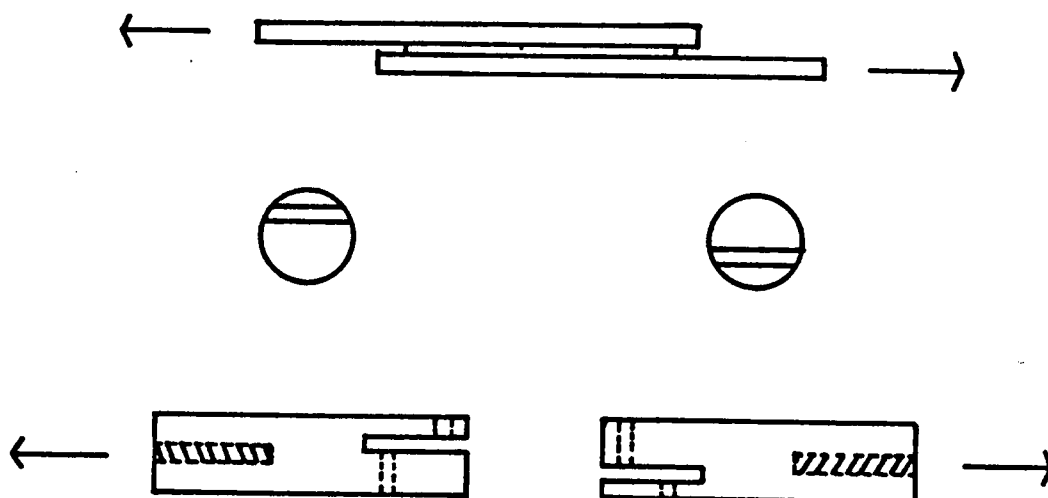


Figure 14. Modified lap shear assembly for mounting in Rheovibron. Middle and bottom views are of new clamps for Rheovibron (3).

screwed together. Titanium 6-4 alloy (phosphate fluoride etch) was used for the bonded substrates (3).

The weight percent styrene, and values of M_w/M_n and calculated number average molecular weights of the styrene and isoprene blocks of the SIS copolymers used in the studies are listed in Table 1.

RESULTS AND DISCUSSION

We have determined that S/I/S triblock copolymers may be prepared to show anisotropic behavior with respect to fracture in adhesively bonded lap shear joints made with rigid substrates. Table 2 summarizes joint strength and fracture energy data for lap shear joints prepared with the orientation (machine) direction of the adhesive layer either parallel or perpendicular to the fracture axis of the joint. The important comparison is that of the fracture energies of the different orientations for the 50% styrene S/I/S copolymer (E2) sample. The high fracture energy for the parallel orientation corresponded exclusively to ductile drawing failure, the perpendicular orientation produced only a brittle failure and low fracture energies (2).

Another important contribution to the orientation study came from the data on the elastic moduli for the two orthogonal orientations of triblock materials similar to those used in the fracture study. Figure 15 and Figure 16

Table 1. Materials (2).

Sample	Weight Percent Styrene	M_w/M_n (10^{-3})	S/I/S M_n (10^{-3})
C2	43	98/93	20/53/20
D3	50	65/63	16/31/16
E1	60	81/77	23/31/23
E2	59	64/61	18/25/18

Table 2. Orientation Study (2).

Sample	% Styrene	Fracture Axis Orientation	Average Joint Strength (N/cm ²)	Average Fracture Strength (J)
E2	59		430+70	3.9+0.8
		⊥	380+40	1.3+0.1
D3	50		290+40	3.0+1.0
		⊥	320+60	2.6+0.6
C2	43		210+40	2.6+0.7
		⊥	180+10	2.1+0.9

show different free film storage moduli in the parallel and perpendicular direction for a S/I/S triblock material and for a second triblock material also based on styrene hard blocks, respectively.

Results of experiments on S/I/S free films and on S/I/S bonded joints with the thermoplastic glue line thickness of 0.3, 0.5 and 0.7 mm appear together in Figure 17, as presented in Chapter II (3). All preparations were made with the 50% styrene content polymer. The preparation temperature was 150°C and at least 5000 psi was applied in the molding. Pressure was maintained during cooling in all cases. As the bond thickness increased the $\tan \delta$ behavior for joints approached that of the bulk, but was shifted to higher temperatures. Identical experiments on the 40% styrene copolymer gave essentially the same conclusions (not shown). The curves were quite reproducible.

Neither just pressure applied during cooling, nor the S/I/S being contained in a bonded joint were sufficient to produce the "fine structure" in the $\tan \delta$ vs. temperature experimental results shown in the figures. It was the combination of a thin bond, or free film, along with high pressure maintained during cooling that produced the details seen in Figure 17. This was confirmed by repeated experiments on free and bonded, thick and thin films, prepared with and without pressure. As an example, in Figure 18, two free films behave quite differently; both were

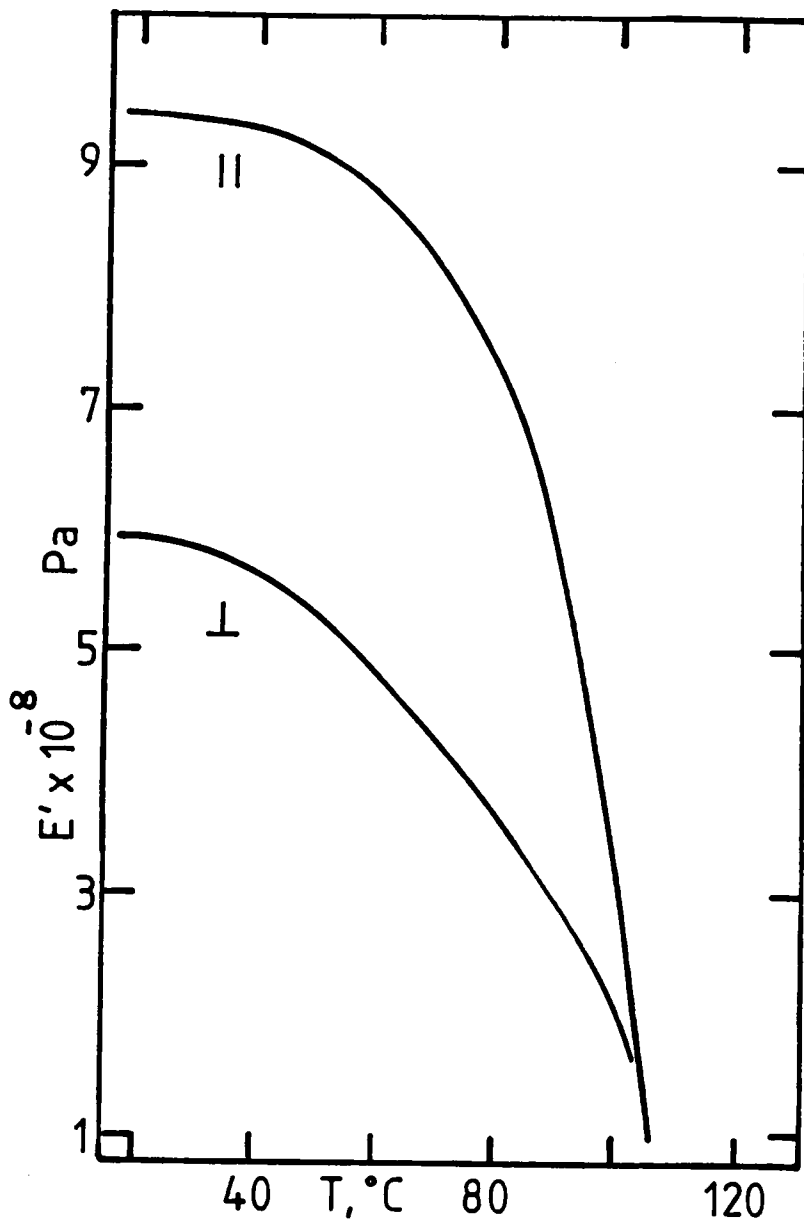


Figure 15. Dynamic mechanical storage modulus for S/I/S free films. with molecular orientation parallel (||) and perpendicular (⊥) to the testing direction (at 110 Hz).

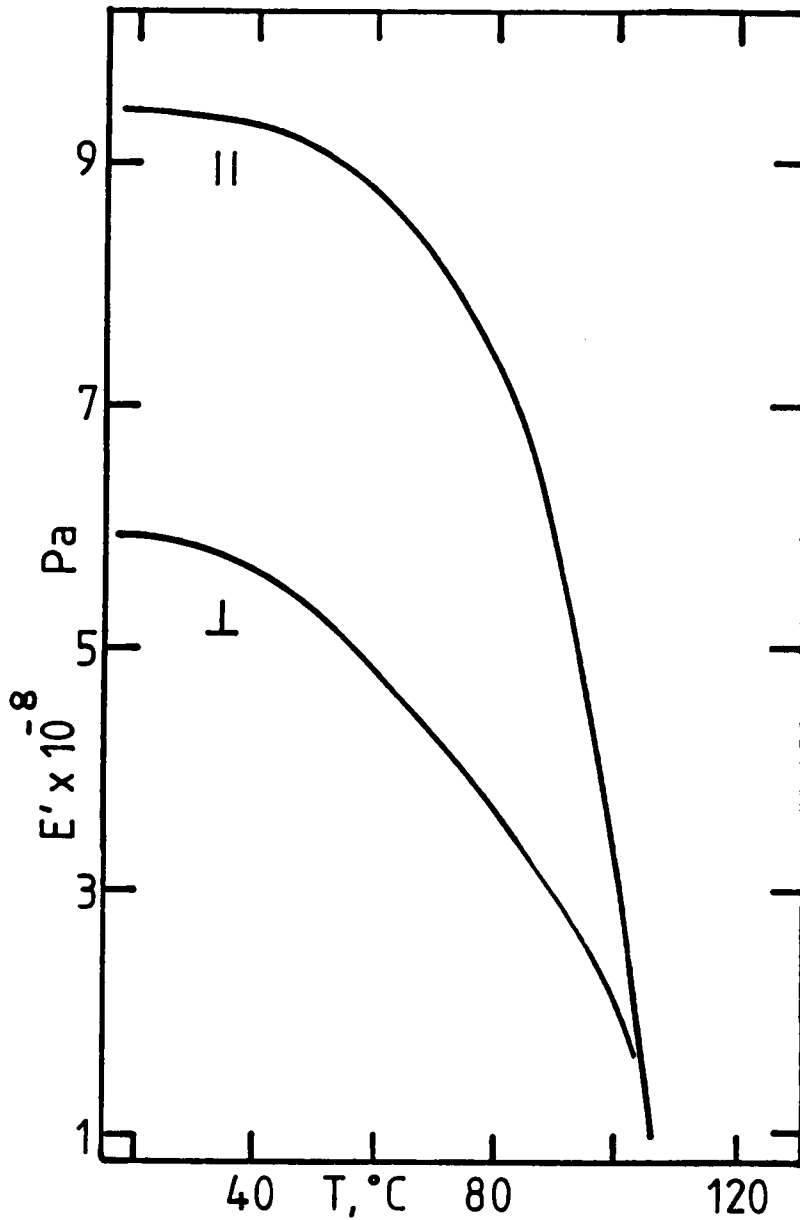


Figure 16. Dynamic mechanical storage modulus free film.: with molecular orientation parallel (||) and perpendicular (⊥) to the testing direction (at 110 Hz).

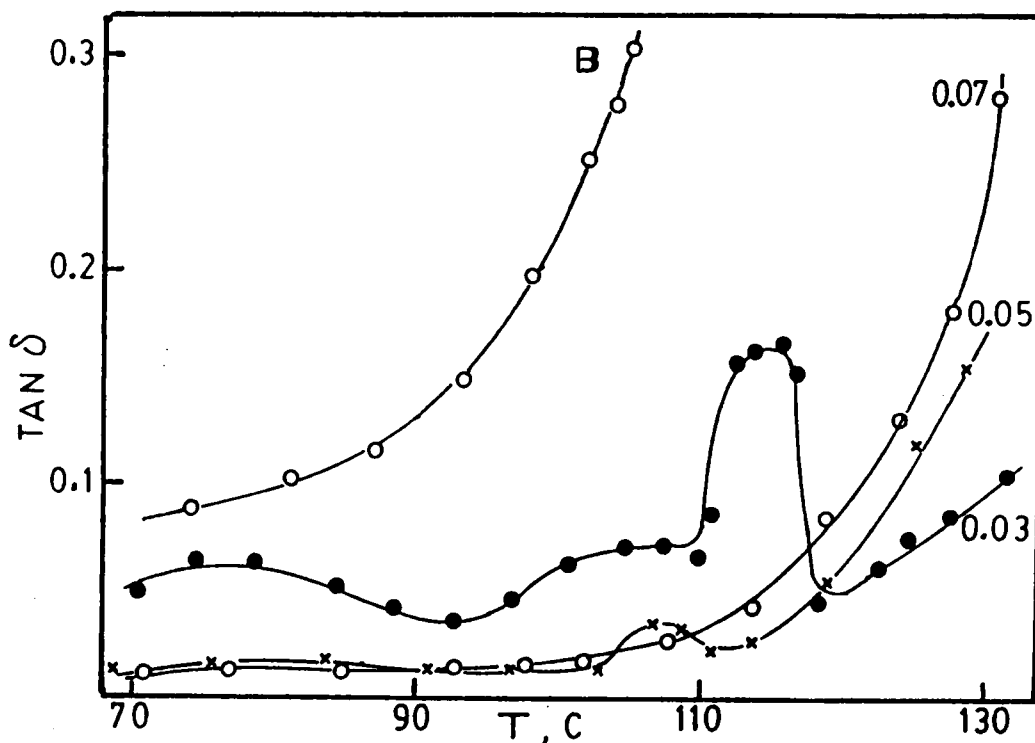


Figure 17. Dynamic mechanical damping of 50% styrene S/I/S bonded joint and free film at 110 Hz. Bond thicknesses shown on curves in cm for joints. Free film = B.

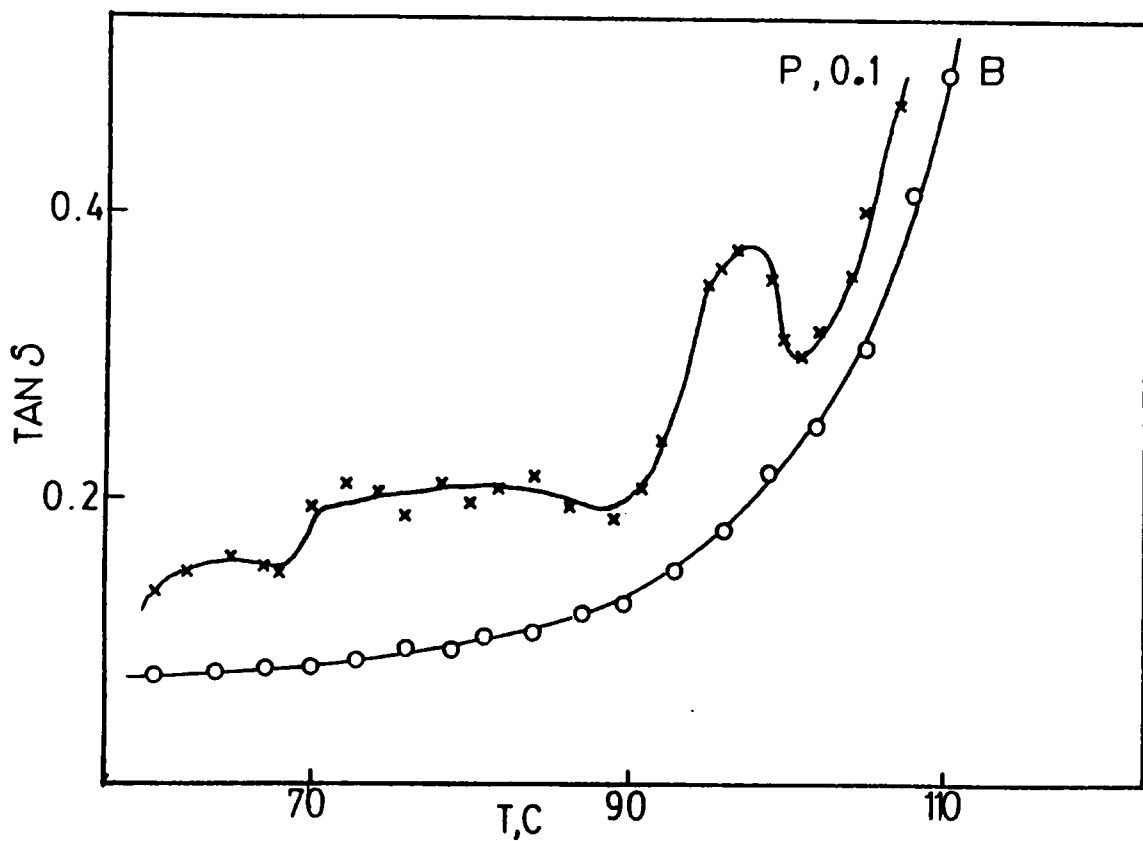


Figure 18. Dynamic mechanical damping of 50% styrene S/I/S (D3) free films, cooled with > 5000 PSI pressure. B = 0.6 mm; P = 0.1 mm thick (3).

cooled with pressure applied in the molding operation, however, one was 0.1 and the other 0.6 mm thick.

In a further exploration of the conclusions above we used the oriented films to prepared bonded joints, with thin bond lines, and cooled with pressure. The results are shown in Figure 19. While there are some similarities, the parallel and perpendicular (machine direction of film with respect to Rheovibron strain direction) responses are shifted from one another and not identical. These curves are reproducible in all major features.

Earlier studies conducted in our laboratory dealing with isotropic adhesive films demonstrated that differences in the compression molding operation could be associated with either the presence or the absence of stress release events.(2) Using DSC we sometimes noted unexpected thermal response of S/I/S copolymers about 20°C below the glass transition temperature which was attributed to a "stress release phenomena" (3). Figure 20 shows the DSC curves for a 60% styrene S/I/S copolymer (E1). Note that in curve II, for the compression molded film cooled under pressure, a baseline shift appears at about 70°C. This event was completely reproducible when similar thermal and pressure histories were established. No shift was observed on repeat runs on the same sample cooled from the melt in the DSC instrument.

In conclusion, we have followed a path of analysis which includes the following facts:

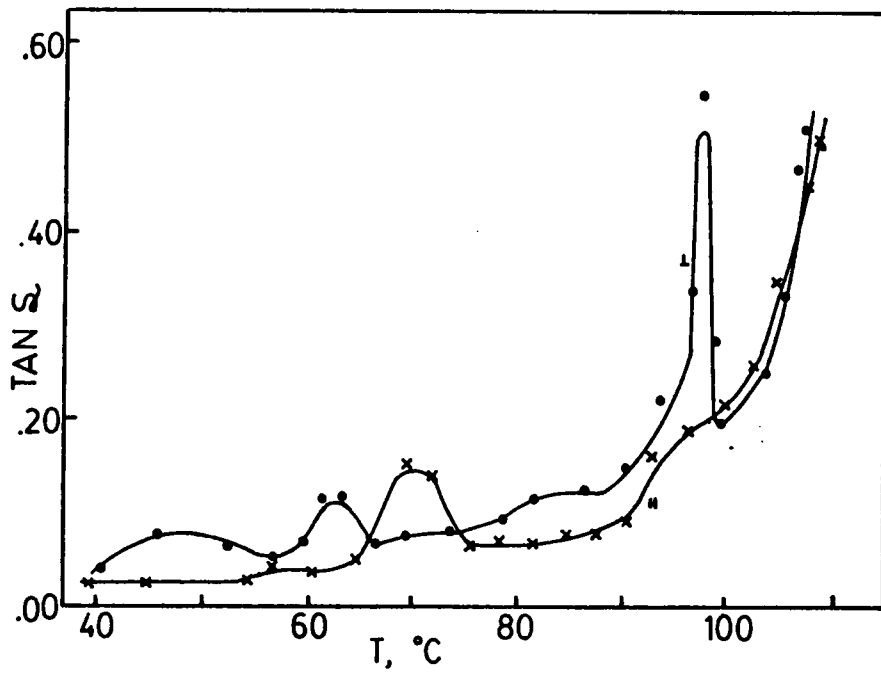


Figure 19. Dynamic mechanical damping of a block copolymer film. with molecular orientation parallel (||) and perpendicular (⊥) to the testing direction at 110 Hz.

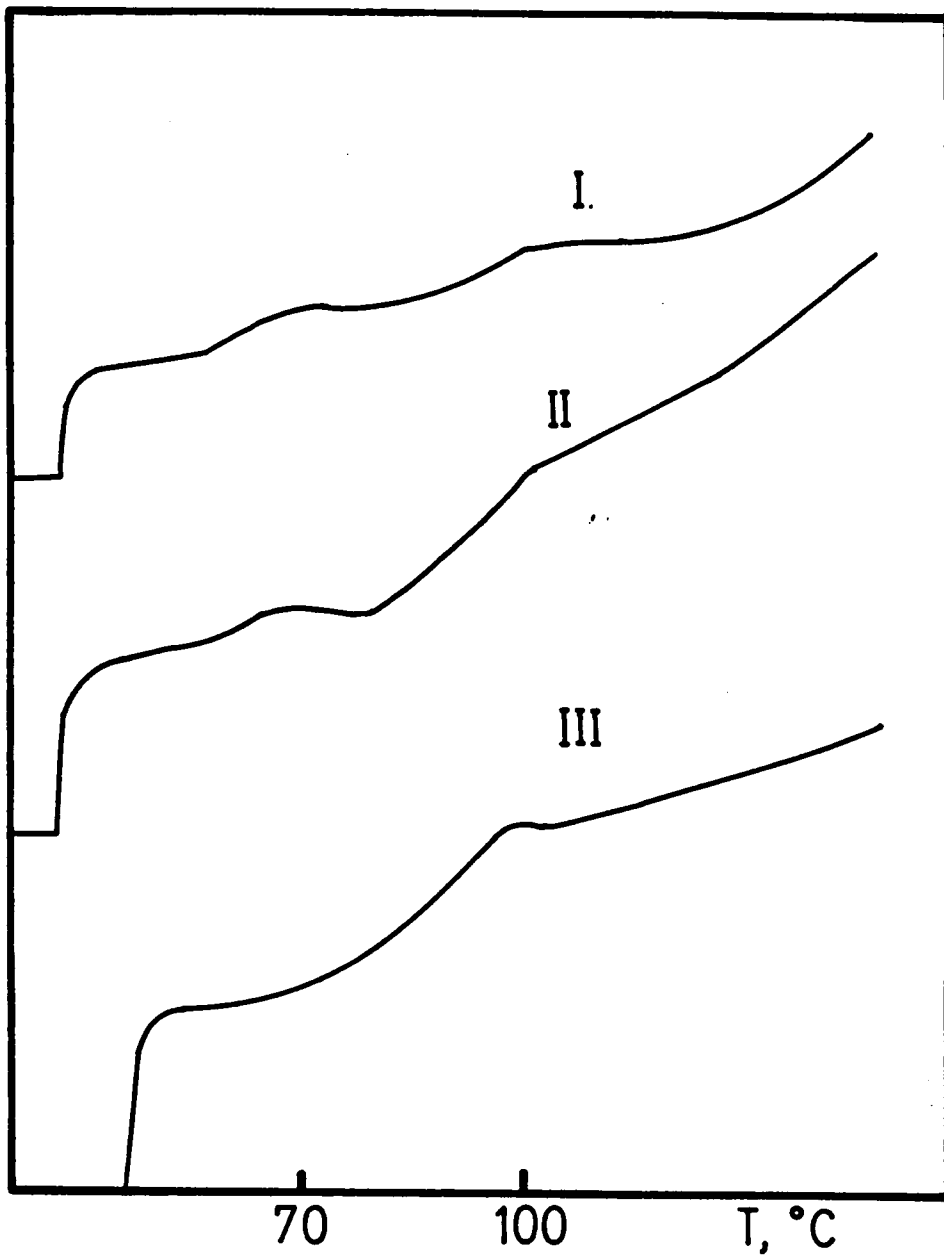


Figure 20. First run DSC curves for sample E1. (I) powder, (II) compression molded film cooled under pressure, (III) compression molded film cooled without pressure (2).

1. Microphase separated triblock thermoplastic materials have complex melt morphologies when flowing, which may be trapped by rapid cooling in a variety of states.
2. Cooling microphase separated triblock copolymer melts of S/I/S under pressure in situations where large amounts of flow occurs (thin bonds) and allowing them to solidify may produce behavior that is related to that observed in pressure densified homopolymer glasses. Thermal analysis supports this conclusion.
3. Compression molding produced thin films that were basically isotropic with respect to "frozen stress" release (as measured by $\tan \delta$) on heating. Extrusion, in contrast, could produce S/I/S polymer films which exhibited anisotropic mechanical response in free films and in bonded joints.

A summary of the importance of these reported conclusions would certainly emphasize extreme care that should be observed in measuring either ultimate (adhesive failure) or small displacement (linear viscoelastic) properties of block copolymers which have been extruded or molded.

REFERENCES

1. J. H. Daane and S. Matsuoka, *Polymer Engineering and Science*, 8(4), 246 (1968).
2. A. Wood, M.S. Thesis, Virginia Polytechnic Institute and State University, Blacksburg, Va. 24061 (1982).
3. T. C. Ward, Margaret Sheridan, D. L. Kotzev, "Nondestructive Evaluation of Some Bonded Joints," in "Adhesive Joints: Formation, Characteristics, and Testing," K.L. Mittal (ed.), Plenum Press, New York, August (1983).
4. D. J. Meier, *J. Polym. Sci., Part C*, 26, 81 (1969).
5. D. F. Leary and M. C. Williams, *J. Polym. Sci., Polym. Phys. Ed.*, 11, 345 (1973).
6. G. Kraus, T. Hashimoto, *J. Appl. Polym. Sci.*, 27, 1745 (1982).
7. N. Sivashinsky, T. J. Moon and D. S. Soong, *J. Macromol. Sci.-Phys.*, B22 (2), 213 (1983).
8. A. Ghijsels and J. Raadsen, *Pure Appl. Chem.*, 52, 1361 (1980).
9. J. Kelterborn and D. S. Soong, *Polym. Eng. Sci.*, 19, 1140 (1979).
10. J. M. Widmaier and G. C. Meyer, *J. Appl. Polym. Sci.*, 28, 1429-1437 (1983).
11. A. Weitz and B. Wunderlick, *J. Polym. Sci., Polym. Phys. Ed.*, 12, 2473 (1974).
12. W. M. Prest Jr. and F. J. Roberts Jr., *Structure and Mobility in Molecular and Atomic Glasses*, 371, 67 (1981).
13. J. J. Curro and R. J. Roe, *J. Polym. Sci., Polym. Phys. Ed.*, 21, 1785 (1983).
14. H. J. Oils and G. Rehage, *Macromolecules*, 10, 1036 (1977).
15. J. B. Yourtee and S. L. Cooper, *J. Appl. Polym. Sci.*, 18, 897 (1974).

16. D. W. Dwight, E. Sancaktar and H. F. Brinson, Adhesion and Adsorption of Polymers, Part A, 141, L. H. Lee (ed.), Plenum (New York), 1980.
17. G. Dolev and O. Ishai, J. Adhesionj, 12, 283 (1981).

CHAPTER IV
APPLICATION OF COMPRESSIVE CREEP COMPLIANCE MASTER CURVES
AS A PREDICTIVE TOOL IN THE EVALUATION OF PRESSURE SENSITIVE
ADHESIVES

ABSTRACT

One of the essential properties of a pressure sensitive adhesive (PSA) is tack. Pressure sensitive tack is the adhesive property closely related to initial bond formation with the surface of another material upon brief contact under light pressure. A criterion for the establishment of contact in a phenomenological sense was proposed by Dahlquist (1). According to this concept, the compressive creep compliance on the time scale of the bonding process (1 second) should be of the order of 10^{-7} cm²/dyne or larger; i.e.,

$$D(1s) \geq 10^{-7} \text{ cm}^2/\text{dyne} \quad (4.1)$$

When $D(1s)$ is substantially smaller than 10^{-7} cm²/dyne serious lack of tack will result from a limitation of the adhesive to conform intimately to the contours of the substrate.

The DMA-2, an accessory for the Perkin Elmer TMS-2 Thermomechanical Analyzer, allowed the evaluation of adhesive tack on a fundamental and wide ranging level. Compressive creep compliance measurements were made over four decades of

time at different temperatures. From this data, "master curves" were constructed, allowing one to predict compliance, and, hence, tack over a wide range of temperatures and times of applied pressure. This superposition technique was successfully applied to thermorheologically complex adhesives described in the next paragraph. Time-temperature superposition worked because of the domination of one dispersion mechanism in the temperatures spanned by the research.

A series of radial styrene (and substituted styrene) and isoprene block copolymers (25% weight styrene) were chosen in order to evaluate the compliance master curve concept for PSAs. This series included p-tert-butylstyrene and isoprene (TBS-I)*, p-methyl styrene and isoprene (PMS-I)*, and styrene and isoprene (S-I)* radial, or star, block copolymers. The polymers in this series varied in the degree of mixing of the component blocks in the interfacial region between the two microphases, as controlled by the styrenic block type. The role of the phase mixing phenomena had important practical implications for block polymers of this type which are used to formulate pressure sensitive adhesive compositions. The compatibility of the two components determined the overall behavior even though the polyisoprene contributed the most toward the compliance response.

INTRODUCTION

A. Pressure Sensitive Adhesives - Property of Tack

In the primary stage of adhesion, the bonding process begins with the wetting of the surface by adhesive. Pressure sensitive adhesives require a proper cohesive strength and viscoelastic nature so they can spread over the surface under conditions of light contact pressure and short contact time to make an adhesive bond (2).

Tack is a complex temperature and rate dependent property, involving a bonding and a debonding sequence carried out in fairly rapid succession. In the ideal bonding stage the objective would be that maximum contact on a molecular level would be established between the soft adhesive and the microscopically rough substrate. Subsequent debonding would require stresses and deformations, the outcome of which will depend on the intermolecular forces acting at the adhesive/substrate interface and the rheological properties of the adhesive layer (2-15). A criterion for the establishment of successful PSA contact in a measurable sense was proposed several years ago by Dahlquist (1). This principal emphasizes that the compressive creep compliance on the time scale of the bonding process (1 second) must be of the order of 10^{-7} cm²/dyne or larger,

$$D(1 \text{ sec}) \geq 10^{-7} \text{ cm}^2/\text{dyne} \quad (4.2)$$

When $D(1s)$ is substantially smaller than $10^{-7} \text{ cm}^2/\text{dyne}$, serious loss in tack will result due to incomplete establishment of intimate surface contact.

Testing the Dahlquist contact criterion in a wide variety of applications requires knowledge of the 1 second creep compliance at many temperatures. $D(1 \text{ sec})$ is not easily measured directly, even at room temperature, this time occurring too soon after the (hypothetical) instantaneous application of stress. The DMA-2, accessory of the Perkin Elmer TMS-2 Thermomechanical Analyzer, however, is capable of direct measurement of the compressive creep compliance at easily accessible and widely varying temperatures.

B. Time and Temperature Dependence in Polymeric Systems

Unlike more classical engineering materials where the mechanical properties depend essentially only on temperature, in polymeric systems time dependent behavior is also of great importance. Considerations of multiple relaxation phenomena which may occur in polymers adds additional complications; the value of a measured modulus or compliance depends on the exact manner (history) in which the experiment is carried out. The time dependence may be explored from experiments involving discontinuous stress or strain levels or by using oscillatory perturbations, in the latter case as is done when

investigating dynamic mechanical properties or dielectric relaxation in polymers (17-21).

An experimental "master curve" depicts the behavior of a polymeric system at any temperature over a broad expanse of time or frequency, usually about 15 decades. Reduced variables or viscoelastic corresponding state theory allows an analysis of the two principal variables of time and temperature on which the viscoelastic properties depend, expressing the properties in terms of a single function, a_T , whose form can be determined experimentally (22).

i. Temperature Dependence

The isochronal mechanical behavior of a polymer system may be most simply presented as a function of temperature. For a linear amorphous polymer four distinct regions of viscoelastic behavior are usually observed, and each of these regions may be related to specific types of molecular motion (17).

In Figure 21, a schematic representation of the modulus-temperature behavior which is common to linear amorphous polymers is presented. The curve shows the glassy region, characterized by a very high value of the modulus, the transition region from glassy to rubbery-like consistency, the rubbery plateau at much lower modulus values than those characteristic of glasses and, at high temperatures, a flow region (17).

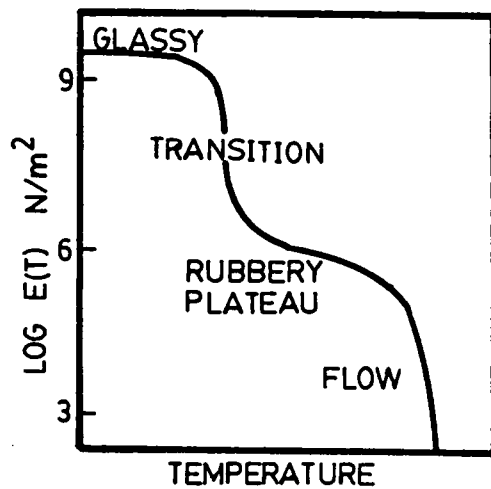


Figure 21. Schematic modulus-temperature curve showing the four regions of viscoelastic behavior (17).

The microscopic behavior of polymer molecules in each of these regions is very different. In the glassy domain the relatively low levels of thermal energy result in limited extents of molecular motion. Here, short range torsions, vibrations and oscillations of side chains on the polymer backbone or perhaps limited backbone motions involving short sequences of atoms take place. As the temperature increases, a situation is reached where substantial segments of individual polymer chains have enough energy to surmount local barriers which hinder molecular motion and these segments begin to move. In this range, cooperative motions on a scale of perhaps ten monomer units might occur. This is termed the transition zone. At higher temperatures still, even longer range motion involving larger segments and numbers of chains commence. However, due to the fact that long polymer molecules are entangled, translational motions of entire polymer chains are forbidden. This temperature is one leading to an interpretation of behavior at the onset of the rubbery plateau region. At even higher temperatures, molecular motion is so extensive that even chain entanglements are no longer effective in restricting flow of one molecule past another and a liquid-like regime is realized. Thus, with increasing temperature, the amplitude and character of molecular motion in polymeric systems increases yielding the four domains of viscoelastic behavior

discussed. With this simple interpretation of molecular behavior, it is possible to rationalize modulus-temperature curves for a variety of systems (17).

ii. Time Dependence

In addition to the temperature sensitivity of the mechanical properties of polymers, there is a marked property dependence on time; the value of a measured modulus or compliance will depend on the exact manner in which the experiment is carried out. In a creep experiment the sample is subjected to a constant stress, τ_0 , and its strain, $\gamma(t)$, is measured as a function of time. The shear creep compliance $J(t)$ is defined as

$$J(t) = \frac{\gamma(t)}{\tau_0} \quad (4.3)$$

whereas the tensile creep compliance, $D(t)$, in a similar fashion becomes

$$D(t) = \frac{\epsilon(t)}{\sigma_0} \quad (4.4)$$

where σ_0 is the constant tensile stress. In a stress relaxation experiment the strain is maintained constant and the stress is measured as a function of time. $E(t)$, the tensile relaxation modulus,

$$E(t) = \frac{\sigma(t)}{\epsilon_0} \quad (4.5)$$

with ϵ_0 being the constant tensile strain. A shear relaxation experiment would measure $G(t)$, the shear stress relaxation modulus,

$$G(t) = \frac{\tau(t)}{\gamma_0} \quad (4.6)$$

with γ_0 being the constant shear strain.

In terms of classical physics, the material parameters do not vary with time, the modulus and the compliance are always reciprocally related. Since polymers are viscoelastic, moduli and compliances are time-dependent functions; and, hence,

$$E(t) \neq \frac{1}{D(t)} \quad (4.7)$$

$$G(t) \neq \frac{1}{J(t)} \quad (4.8)$$

and where ω is the frequency in a dynamic mechanical experiment. The stress relaxation moduli may be measured directly only from constant strain experiments while the creep compliances may be measured directly only from constant

stress experiments even though, in theory, they may all be interconverted.

iii. Time-Temperature Superposition Principle

The method of reduced variables or viscoelastic corresponding states is a technique for expanding the effective time or frequency scale of data resulting from experimental measurements. It affords a valuable simplification by establishing the functionality between the two principal variables of time and temperature on which viscoelastic properties depend, expressing the overall behavior in terms of a single function, a_T , termed the shift factor, whose form can be determined experimentally (22). With the help of the time-temperature superposition principle, experimental data measured on accessible time scales at various temperatures can be used to prepare a "master curve" at a fixed temperature over a very broad time scale through application of the shift factors (22).

On the left of Figure 22, stress relaxation data is represented over the reasonably accessible time scale of three to four decades, at several temperatures, T . These curves were superposed by horizontal shifts along a logarithmic time scale to give a single curve covering a very large range of times (or frequencies). Such curves, referred to as master curves, use some arbitrary temperature, T_0 , as

a reference temperature, and predict response times outside the range easily accessible by practical experiments (18).

Mathematically these ideas may be expressed as

$$E(T_0, t) = E(T, t/a_T) \quad (4.9)$$

where the effect of changing temperature is the same as applying a multiplicative factor to the time scale; i.e., an additive factor to the log time scale (18).

Data measured at temperatures below the reference temperature are shifted to shorter times while data measured at temperatures above the reference temperature are shifted to longer times in constructing the master curve. The information contained in the horizontal shifts along the log time scale is expressed by a_T . If the glass transition temperature is chosen as the reference temperature, the temperature dependence of the shift factor can be expressed analytically in terms of the WLF equation

$$\log a_T = \frac{-C_1(T-T_g)}{C_2 + T-T_g} \quad (4.10)$$

where C_1 and C_2 are constants. It was originally thought that C_1 and C_2 were universal constants; in fact, they vary from polymer to polymer. The "universal" values for C_1 and C_2 were 17.4 and 51.6°, respectively (17). The shift factor

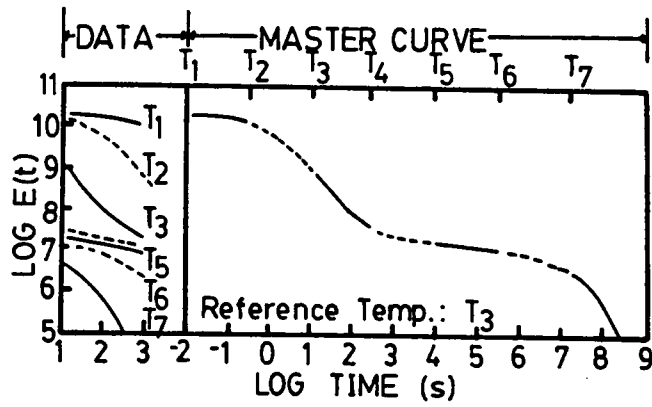


Figure 22. Preparation of a stress relaxation master curve from experimentally measured modulus-time curves at various temperatures (18).

a_T is idealized for purely viscoelastic phenomena as being related to the temperature coefficient of viscosity, η , or to a "characteristic relaxation time", τ , by the relationship

$$\log a_T = \log(\tau/\tau_0) = \log(\eta/\eta_0) \quad (22) \quad (4.11)$$

The master curve as described above uses horizontal shifts to compensate for a change in the time scale brought about by changing temperature. There is also, however, an inherent change in the modulus or compliance brought about by a change in temperature which is sometimes important. The modulus of a rubbery network, according to theory, is directly proportional to T , the absolute temperature. Thus, in applying a reduced variable procedure to make a master curve from individual isothermal experiments, not only must one take into account the time scale shift, one must also consider that there would be an expected slight vertical shift due to the temperature variation. Similarly, since the specific volume of a polymer is a function of temperature and the modulus, a corresponding density correction must be made in addition. These considerations lead one to write

$$\frac{E(T_0, t)}{\rho(T_0)T_0} = \frac{E(T, t/a_T)}{\rho(T) T} \quad (4.12)$$

Division by the temperature adjusts for the inherent dependence of modulus on temperature while division by the density corrects for the changing number of chains per unit volume with temperature variation. At the reference temperature T_0 , the modulus at any time t , is therefore given as

$$E(T_0, t) = \frac{\rho(T_0)T_0}{\rho(T)T} \times E(T, t/a_T) \quad (4.13)$$

If one is considering compliance functions, using $D(t)$ as an example,

$$\rho(T_0)T_0 \times D(T_0, t) = \rho(T)T \times D(T, t/a_T) \quad (4.14)$$

and

$$D(T_0, t) = \frac{\rho(T)T}{(\rho(T_0)T_0)} \times D(T, t/a_T) \quad (4.15)$$

An important test of the validity for applying the time-temperature superposition principle is that the shape of the original curves at different temperatures must match over a substantial range of frequencies or times. Two others are: a) the same values of a_T must superpose all the viscoelastic functions; and b) the temperature dependence of a_T must have a reasonable form consistent with experience.

For a simple amorphous polymer the method of reduced variables is appropriate for data treatment in the transition, plateau, and terminal zones of the time-temperature scale, with the provision that all contributions to the measured viscoelastic properties involve the same molecular mechanisms and, moreover, that the internal structure of the system does not change with changing temperature. These restrictions are inherent in the development of the method of reduced variables (22).

The method of time-temperature superposition was successfully applied to the (S-I)* and the (TBS-I)* radial block copolymer adhesives despite the fact that the adhesives are thermorheologically complex. The shapes of the original curves provided a reasonable match over the temperatures spanned by the research. In addition, the temperature dependence of a_T , for both polymers, obeyed the WLF equation. Horizontal shifts along the log time scale resulted in superposition of the original curves, only slight vertical shifts were required in a few cases to affect an accurate match. Examination of the original data curves, in Figure 23 and Figure 24, reveal that it is the curves constructed at temperatures intermediate to the glass transition temperatures of the constituent phases that do not result in direct overlap upon horizontal shifting alone. Such behavior was not unexpected, because it is in this

temperature range that molecular mechanisms of relaxation from both phases are exhibited.

The vertical shift correction, described earlier, was not applied to the original data curves because the vertical shifts required for accurate superposition were small (ca. $1 \times 10^{-7} \text{ cm}^2/\text{dyne}$). Also, because the required vertical shifts most probably resulted in part from an inherent change in the compliance brought about by a change in temperature, expected for rubbery networks, as well as from the polyphase character of the materials, resulting in multiple relaxation mechanisms having different temperature dependencies; and it would be difficult to separate their individual contributions to the applied shift.

Simple translation of the measured viscoelastic responses along the logarithmic time or frequency axis is valid for thermorheologically simple materials where all retardation or relaxation times are equally affected by a change in temperature. In thermorheologically complex systems, where two or more different classes of molecular motion with different temperature dependences are involved, such as block copolymers, physical blends, or semi-crystalline polymers, some modification in the treatment is necessary.

As previously mentioned, the method of time-temperature superposition, though only strictly valid for simple

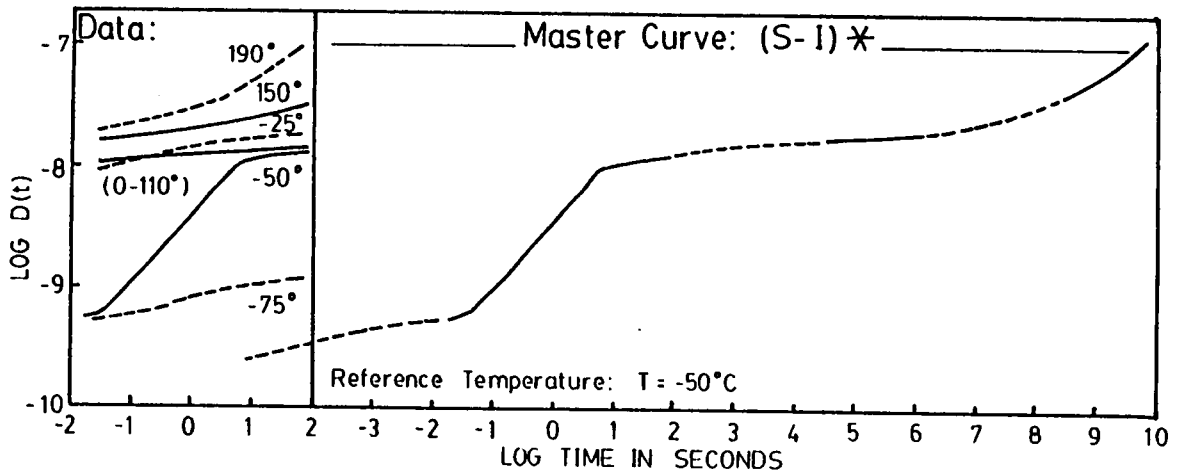


Figure 23. Compressive creep compliance data and master curve for styrene and isoprene radial block copolymer, (S-I)* as cast from cyclohexane.

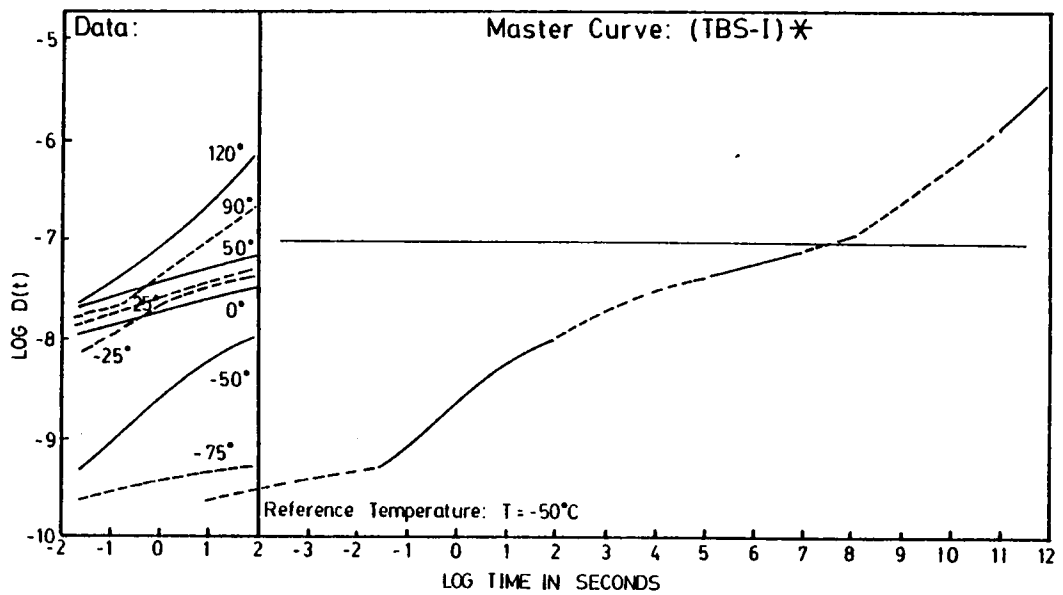


Figure 24. Compressive creep compliance data and master curve for the (TBS-I)* radial block copolymer as cast from cyclohexane.

amorphous polymers, was successfully applied to (S-I)* and (TBS-I)*. First, for (S-I)*, the apparent reason for the success of the application of time-temperature superposition was the dominance of the polyisoprene dispersion mechanism for the temperatures spanned by the experiment. Isochronal dynamic mechanical thermal analysis (DMTA) of (S-I)* supports this statement. The DMTA results, presented in Chapter VI, reveal a strong polyisoprene transition at lower temperatures with the polystyrene transition appearing only as a very weak dispersion superposed on the rapidly rising $\tan \delta$ baseline. Thus, the polyisoprene response dominates the overall behavior for nearly the entire temperature range. For (TBS-I)*, the two phases were so intimately mixed, as supported by DMTA (Chapter VI) and preliminary small angle x-ray scattering (SAXS) studies (Chapter IX), the material responded essentially as a homopolymer. As a result, the method of time-temperature superposition worked very nicely for (TBS-I)*.

Mechanical response curves obtained on thermorheologically complex materials at different temperatures cannot, in principle, be brought into superposition by a simple shift along the logarithmic time or frequency axis. The shift factors become functions of time or frequency in addition to temperature. For a complete analysis of isothermal data obtained on a thermorheologically complex material, contributions of various mechanisms to the

mechanical properties must be isolated by decomposition, and the time-temperature relationship must be determined separately for each contribution (24). Such complications have been dealt with in the past in order to account for the effect of β -mechanism in polymethacrylates (25), slippage in rubbery networks (23), and terminal flow viscosity in polystyrene (26).

A general treatment of time-temperature superposition in thermorheologically complex materials has been developed by Fesko and Tschoegl (24,27). For a two-phase material, incorporating a model proposed by Takayanagi, the amount of shift could be calculated which was necessary to bring a point on a mechanical response curve obtained at a given temperature and time or frequency into superposition at another temperature. The mechanical responses of the constituent homopolymers and their temperature functions must be known. For the tensile storage compliance, the change in the shift factor with respect to temperature at constant time was given by

$$\left[\frac{\delta \log a_T(t)}{\delta T} \right]_t = - \left[\frac{\delta D(T)}{\delta T} \right]_t \left[\frac{\delta D[t/a_T(t)]}{\delta \log t/a_T(t)} \right]_{T_0}^{-1} \quad (4.16)$$

i.e., a_T depends on the change in the compliance with respect to temperature at any time as well as on the change in the compliance with respect to logarithmic time at the reference

temperature T_0 . Similar equations can be written for other monotonically increasing or decreasing viscoelastic response functions such as the relaxation modulus and the storage modulus (24,27).

Equation 4.16 cannot easily be applied in practice, therefore, Fesko and Tschoegl introduced a different approach based on a model which combined the contributions of the individual phases. For a polystyrene 1,4-polybutadiene polystyrene triblock copolymer in which the polystyrene phase is dispersed in a rubbery polybutadiene matrix, a model assuming additivity of the strains (or the compliances) in the individual phases described the observed behavior. The total compliance was

$$D = \frac{\epsilon}{\sigma_0} = w_B D_B + w_S D_S \quad (4.17)$$

where the weighting factors, w_B and w_S , were to be proportional to the amount of each phase present. An interlayer could be regarded, where appropriate, as a third component which contributes to the overall compliance independently (24,27).

The resulting equation derived from the combination of equation 4.16 with the model was

$$\left[\frac{\delta \log a_T(t)}{\delta T} \right]_t = N_B(t) \frac{\delta \log a_{T_B}}{\delta T} + N_S(t) \frac{\delta \log a_{T_S}}{\delta T} \quad (4.18)$$

where

$$N_B(t) = \left[\frac{w_B L_{1B}(\tau)}{w_B L_{1B}[\tau/a_{TB}(t)] + w_S L_{1S}[\tau/a_{TS}(t)]} \right]_{t=\tau} \quad (4.19)$$

and

$$N_S(t) = \left[\frac{w_S L_{1S}(\tau)}{w_B L_{1B}[\tau/a_{TB}(t)] + w_S L_{1S}[\tau/a_{TS}(t)]} \right]_{t=\tau} \quad (4.20)$$

where $L_1(\tau)$ is the first approximation to the retardation spectrum for each appropriate homopolymer. This analysis indicates, as one would expect, that the contribution of each phase to the total shift should be proportional to the amount of that phase, its a_T temperature function, and some rate of change of its mechanical response with time. The time dependence enters the relationship through the coefficients N_B and N_S . The time scale of the experiment will determine at which temperature the dominance by the polybutadiene phase, to the total viscoelastic response of the copolymer, shifts to dominance by the polystyrene phase, thereby shifting the major weight from the first term to the second (24,27).

In order to apply Equation 4.18 to multiple component systems, the compliances and the temperature dependencies of the constituent homopolymers must be known. Shift factors

are then derived from the assumption that the compliances are additive. Based on this assumption, a reference master curve of the compliance at any reference temperature can be constructed. Similar short response curves are also generated for the temperatures and times at which data are available. Then, by comparing the time t , at which a given compliance appears at temperature T , to the time $t/a_T(t)$, at which the same compliance appears on the reference master curve, and taking the difference, one obtains the shift factor, $\log a_T(t)$, for that time and temperature. Thus, an appropriate set of shifts is generated for the superposition.

EXPERIMENTAL

A. Synthesis (28)

Radial or "star" topology block copolymers were anionically prepared beginning with isoprene and continuing with either of the monomers of styrene (S), p-methyl styrene (PMS), or p-tert-butylstyrene (TBS). "Living" diblock copolymers having polydienyllithium chain ends were then linked with divinyl benzene (DVB) to produce the desired radial architecture. The reaction was carried out at 60°C in cyclohexane, and terminated with methanol. Size exclusion chromatography and molecular weight determinations indicate 8-10 arms on average per chain with essentially no diblock residue.

Overall the composition of the p-tert-butylstyrene, p-methylstyrene, and styrene and isoprene radial block polymers was 25% (weight) of the styrenic block and 75% of the hydrocarbon block, with the former block number average molecular weight, $\langle M_n \rangle$, of about 25,000 g/mole. From size exclusion chromatography analysis, these materials were found to contain only 2-3% residual diblock.

The number average molecular weight of the styrenic block for each polymer studied and the calculated average number of arms per "star", as determined by size exclusion chromatography analysis, are listed in Table 3. The polymers are identical to those investigated in Chapter VI.

B. Sample Preparation

Creep compliance measurements were made on the styrene and isoprene and t-butylstyrene and isoprene radial block copolymers. The polymer films were solution cast from 20% weight solutions in cyclohexane onto teflon trays and allowed to slowly dry at room conditions for 72 hours. During this 72 hour period, the films were partially covered with a watch glass to protect them from dust and to allow for slow evaporation of the solvent. In the final stage, the films were vacuum dried at 60°C for 48-72 hours to assure total evaporation of the solvent. The film thickness was between 0.4 and 0.6 mm.

Table 3. Characterization of Radial Block Copolymers.

	$\langle M_N \rangle$ of hard block	Arms	δ (cal/cm ³) ^{1/2} hard block
(S-I)*	24,100	8-10	9.2
(PMS-I)*	23,500	8-10	8.8
(TBS-I)*	23,700	8-10	8.12

C. Instrumentation

Thermomechanical analysis (TMA) is a technique in which the deformation of a material is measured under a constant stress as a function of temperature as the material is subjected to a controlled temperature program. The Perkin Elmer TMS-2 is shown schematically in Figure 25. In the penetration mode, the sample is mounted horizontally as a film on the platform of a quartz sample tube. A quartz probe is connected to the armature of a linear variable differential transformer (LVDT) and any change in the position of the armature results in an output voltage from the transformer which is then recorded. The probe assembly includes a weight tray which permits a choice of applied stresses on the sample surface. Instrument specifications include: sensitivity of 0.01 mm full scale (100 mm), noise level of 5×10^{-5} mm, and temperature range of -150° to 325°C using a standard furnace (29).

The DMA-2 accessory for the Perkin Elmer TMS-2 is designed for the evaluation of mechanical data of films of 2.5 mm thick or less either from experiments involving discontinuous stress levels (step-function experiments), or using oscillatory perturbations as in dynamic mechanical experiments. The DMA-2 is constructed to permit the following parameters to be selected (30):

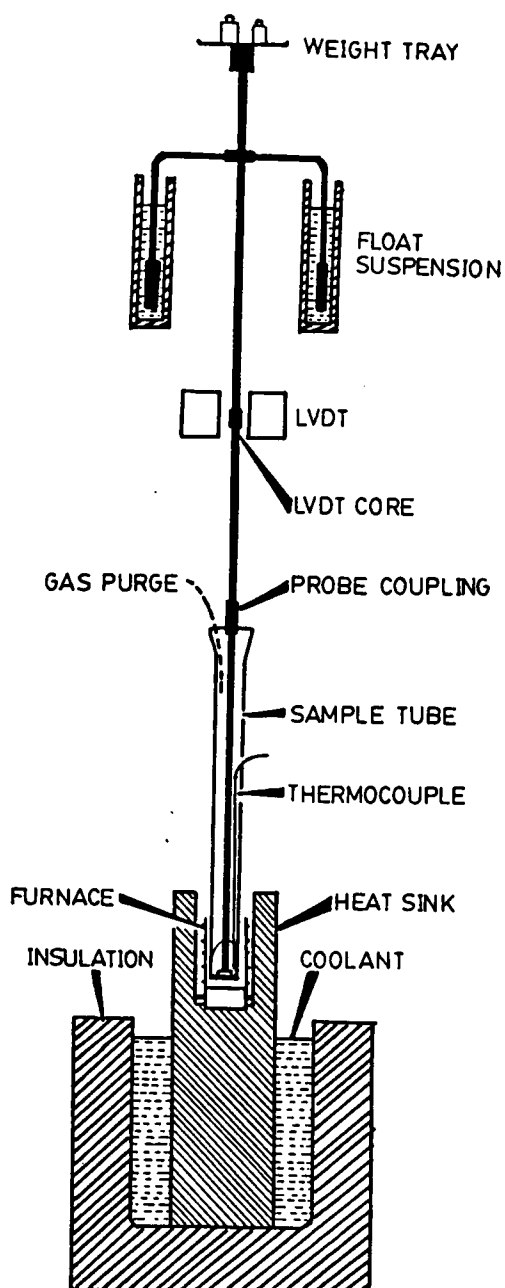


Figure 25. Perkin Elmer TMS-2 (28).

1. Temperature: -150° to 325°C , isothermal or dynamic
2. Frequency: 0.01 Hz to 10 Hz in steps of 0.01 Hz
3. Force: 5mN to 195mN in steps of 5mN
4. Loading curve form:
 - a. constant without load
 - b. constant with preselected load
 - c. square wave form with preselected load
 - d. sine wave form with preselected load

With the DMA-2, direct evaluation of the compressive creep compliance $D_c(t)$ of polymer films is possible. In the compressive creep experiment, the response of the material to a constant stress was determined as a function of time at constant temperature. Compressive creep compliance measurements were made using a flat tip penetration probe (area = 0.0062 cm^2) applying the square wave loading curve form with a preselected load of 50mN. Measurements were made over four decades of time at a number of different temperatures ranging from -75° to 190°C by selecting various frequencies, ω and setting creep time, t , equal to $1/2\pi\omega$. The creep time is equal to the amount of time the probe is in actual contact with the sample.

It is important to point out that the actual experiment is not a pure compressive creep test. Due to the fact that the surface area of the film sample is larger than the surface area of the penetration probe, when the probe is

applied to the film there are shear forces acting at the edges of the probe. Whereas, the compressive response most surely dominates over the majority of the temperatures and the times spanned in the testing, at the higher temperatures and the longer times, where there is high strain, the shear component of the overall polymer response may be significant. However, the magnitude of this shear component was not evaluated.

In a mechanical creep experiment a stress σ_0 is applied to the specimen rapidly at zero time and then held constant until some time later, t_1 , when it is removed. The strain is commonly found by experiment to increase with time. After removal of the stress the strain recovers slowly with time. When the strain does not return ultimately to zero, under conditions of high strain or high temperature, the specimen is said to exhibit permanent set. Such a step function experiment, for the measurement of $D_c(t)$, is outlined in Figure 26. The polymer response curve is drawn from data for the p-tert-butylstyrene and isoprene radial block copolymer, (TBS-I)*, at 50°C and a creep time, t , of 16.7 seconds (freq. = 0.03Hz).

From the polymer DMA-2 response curve the compressive creep compliance was calculated as,

$$D_c(t) = \frac{\text{strain}}{\text{stress}} = \frac{\Delta L/L_0}{\text{Force/Area}} \quad (4.21)$$

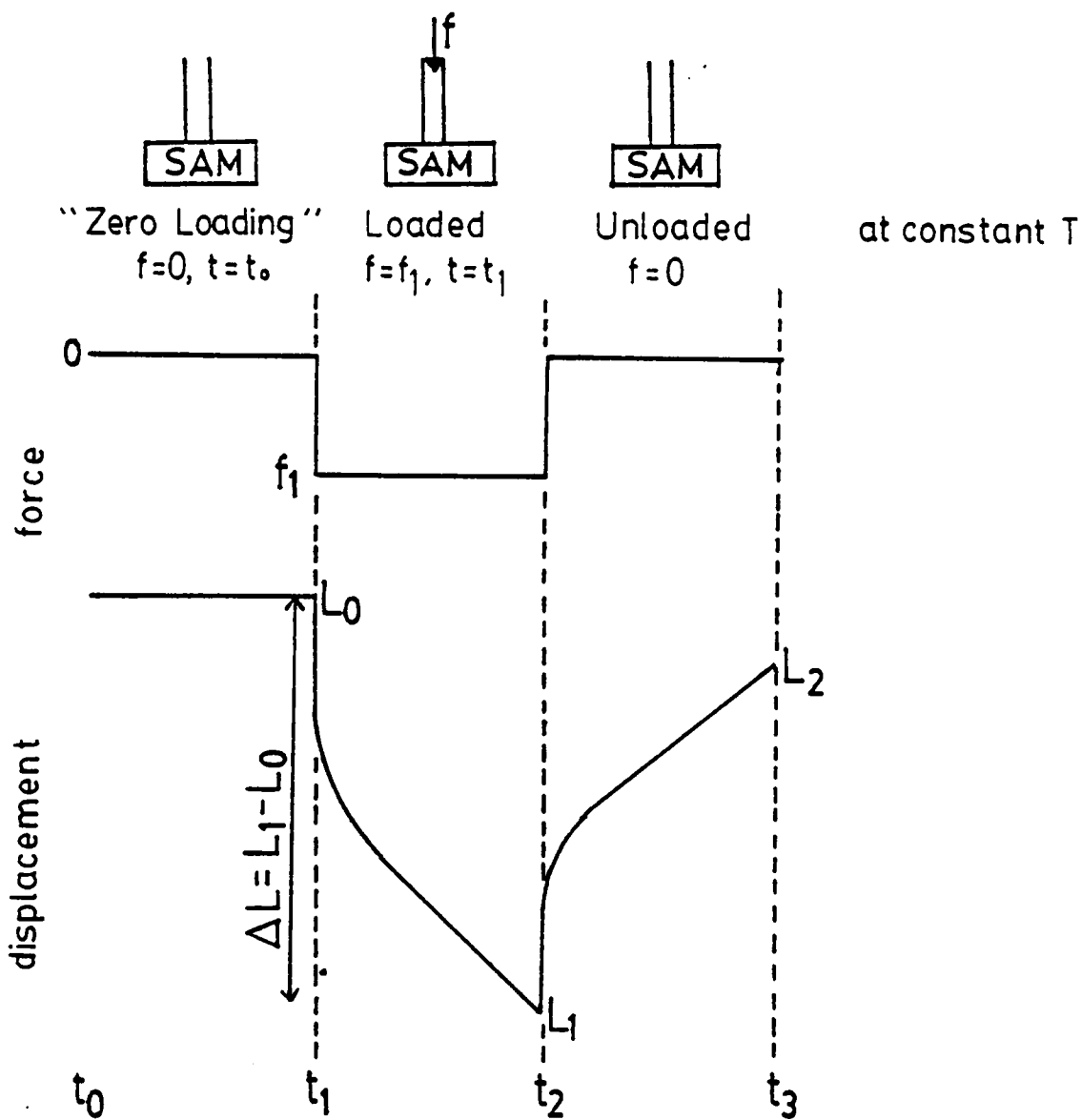


Figure 26. Schematic representation of compressive creep compliance experiment. The polymer response curve is drawn from data for (TBS-I)* at 50°C and $t_1=16.7$ seconds ($f=0.03$ Hz).

where,

$\Delta L = L_1 - L_0$, total probe penetration

L_0 = initial sample thickness

Force = preselected force (50mN = 5×10^3 dynes)

Area = probe area (0.0062 cm²)

For (TBS-I)* at 50°C and a creep time of 16.7 seconds the experimental data in Figure 26 may be analyzed in a sample calculation as follows:

$\Delta L = 0.0225\text{mm}$

$L_0 = 0.60\text{mm}$

Force = 50mN = 5×10^3 dynes

Area = 0.0062 cm²

giving,

$$\log D_c(16.7s)_{50^\circ\text{C}} = -7.33\text{cm}^2/\text{dyne}.$$

RESULTS

A. Creep Compliance Measurements

Figure 23 and Figure 24 show the compressive creep compliance curves at various temperatures for two of the block copolymers. The styrene and isoprene radial copolymer, (S-I)*, clearly shows two dominant creep processes, one at about -50°C and another in the range of 150°C. The low temperature process can be attributed to the microbrownian motion of the polyisoprene phase, while the high temperature transition of this polymer is interpreted as the temperature

marking the transition from the well-formed domain structure to a more homogeneous molten state through a series of successive states of increased interdomain mixing. The domain structure of (S-I)* survived heating beyond the upper (polystyrenic) glass transition temperature as evidenced by the retained compliance of the radial polymer in the temperature range of 150° to 190°C. In the plateau zone, above -50°C, the compliance does not change much with temperature, indicating that a relatively sharp interfacial boundary exists between the two microphases.

Typically, for systems having a two phase structure, two relaxation processes attributed to the microbrownian motion of the two phases are evident. However, the creep compliance curves for (S-I)* do not show strong evidence for the upper (polystyrene) glass transition temperature. This can be attributed to the crosslinked structure in the isoprene phase, as well as a high degree of association within the polystyrene domains and the well known phenomena of a two phase melt structure exhibited by block copolymers.

On the other hand, the p-tert-butylstyrene and isoprene copolymer, (TBS-I)*, compliance curves indicate a much broader low temperature transition than was the case for (S-I)*, and a second broad transition at about 90°C. In addition, the mechanical response between the two transitions is highly temperature dependent. In this region, the compliance continually increases with temperature. The

homopolymers of isoprene and p-tert-butylstyrene, of comparable molecular weight and microstructure to that incorporated into the copolymer, have glass transition temperatures of -50° and 155°C as determined by dynamic mechanical testing at 1 Hz. Therefore, the creep compliance data for the (TBS-I)* indicates that the blocks of p-tert-butylstyrene and isoprene form a reasonably compatible pair of components.

B. Master Curve Construction

Two-phase polymeric materials, such as the block copolymers of this study, are thermorheologically complex. Mechanical response curves obtained on such materials at different temperatures cannot, in principle, be brought into superposition by a simple shift along the logarithmic time axis. The shift factors become functions of time in addition to temperature.

The isothermal compressive creep compliance curves shown in Figure 23 and Figure 24 were superposed by horizontal shifts along a logarithmic time scale. The reference temperature was chosen as -50°C for both cases. A vertical shift factor was also required in order to give a satisfactory single creep curve covering a very large range of times. The vertical shift resulted in part from the inherent change in modulus brought about by a change in temperature, and from the polyphase character of the

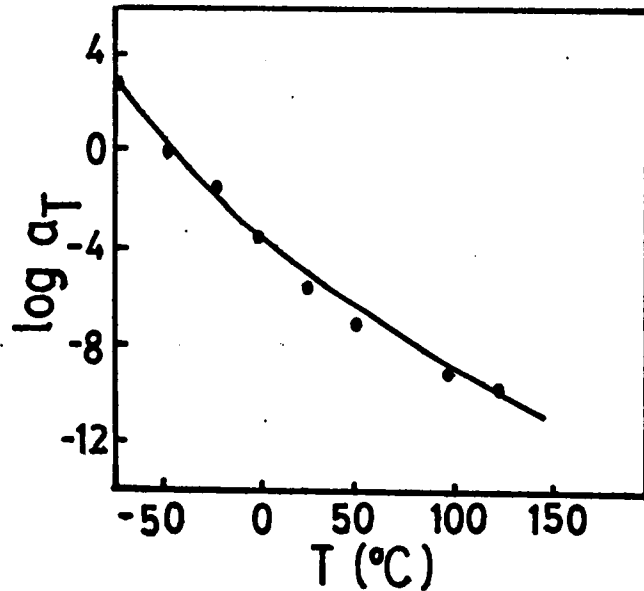
materials. In these multiple component, multiple phase polymers, there are domains of different chemical composition resulting in multiple relaxation mechanisms having different temperature dependencies. This result was most significant for the mechanical response of the p-tert-butylstyrene and isoprene radial block copolymer where the boundary between the poly(p-tert-butylstyrene) and the polyisoprene domains was diffuse. The effect was much diminished for the mechanical response of the styrene and isoprene radial block polymer, where the boundary between the polystyrene and the polyisoprene domains was a much sharper one.

Despite the difficulties raised by the thermorheological complexity of block copolymers, satisfactory master curves were obtained. A large part of the reason why the procedure was successful was due to the morphology of the polymers. The high degree of miscibility of the p-tert-butylstyrene and isoprene microphases in the (TBS-I)* block polymer resulted in polymer response typical of a structurally homogeneous material in the sense that the temperature dependence of the shift factors follows WLF type behavior throughout the entire temperature range (Figure 27). In the styrene and isoprene radial block polymer, the isoprene containing phase was continuous and thus dominated the viscoelastic response up to high temperatures. Even the (S-I)* shift factors tend to largely follow the expected WLF shape over most temperatures.

Table 4. WLF Parameters.

Polymer	T_o	C_1	C_2
(S-I)*	-50°C	9.0	85.0°
(TBS-I)*	-50°C	15.9	152.7°

(TBS-I)* / Cyclohexane:



(S-I)* / Cyclohexane:

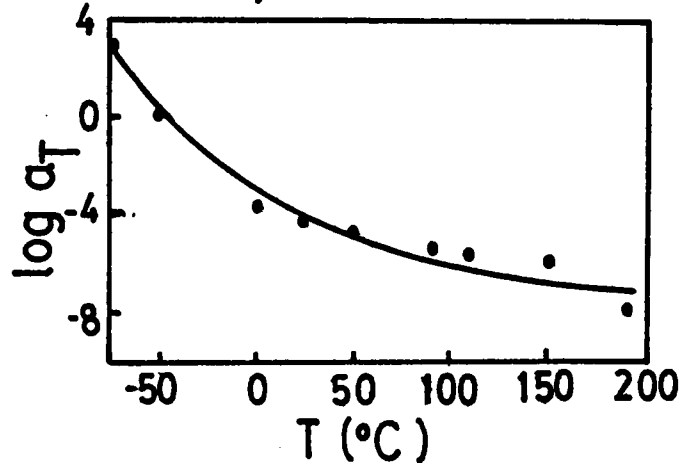


Figure 27. Experimental shift factor plots for styrene and isoprene, (S-I)*, and p-tert-butylstyrene and isoprene, (TBS-I)*, radial block copolymers as cast from cyclohexane. (The lines represent the best fit lines to the experimental data points.)

DISCUSSION

The principle of time-temperature superposition allowed compressive creep compliance data, measured on an accessible time scale at various temperatures, to be extrapolated into a master curve at a fixed temperature covering a very broad time scale. The superposition technique was successfully applied to the thermoheologically complex adhesives. Time-temperature superposition worked for the (S-I)* radial block copolymer because of the dominance of the polyisoprene dispersion mechanism in the temperatures spanned by the research. Time-temperature superposition was also successfully applied to the (TBS-I)* copolymer because the two microphases were so highly compatible that the material responded essentially as a homopolymer.

Using the master curve, and the temperature dependence of a_T , predictions can be made regarding the temperatures and times at which a material will have suitable application as a pressure sensitive adhesive. The compressive nature of the experiment is the key to the predictive capabilities of the master curve combined with the shift factor plot because compression is the form of application of typical PSAs.

Of immediate interest is $D(1s)$ at room temperature. The creep compliance master curve for (S-I)*, upon shifting the predicted four decades of time to the left, corresponding to

25°C, clearly shows that $D(1s)$ at room temperature is substantially smaller, by an order of magnitude, than 10^{-7} cm^2/dyne . Therefore, based on the Dahlquist criterion for the establishment of contact, serious lack of tack would be experienced from limitation of contact on a microscopic scale. In the plateau region of the compressive creep compliance curve, the mechanical response of (S-I)* is invariant with time; the compliance value of 10^{-8} cm^2/dyne is retained over nearly eight decades of time. Only when the (S-I)* compliance curve is shifted 10 decades of time to the left, corresponding to very high temperatures (not of practical use) is $D(1s)$ on the order of 10^{-7} cm^2/dyne .

On the other hand, the creep compliance master curve for (TBS-I)* indicates that under appropriate conditions of time and temperature (TBS-I)* is compliant enough such that it would be possible to establish contact on a microscopic scale with the bonding substrate sufficient to produce high tack. The mechanical response of (TBS-I)* is highly temperature dependent; the compliance continually increases with temperature. A small change along the time scale results in a significant change in the compliance of the (TBS-I)* copolymer.

In addition to the evaluation of adhesive tack on a fundamental and wide ranging level, which was indeed the principal aim of this work, evaluation of the adhesive response, from the compressive creep compliance master curve,

can also be made at very short times (ca. 0.01s), on the time scale of the debonding process, and at very long times. The precise time of the debonding process is dependent upon the pull rate. From the master curve, one could possibly make a prediction as to whether bond failure would be adhesive or cohesive at a specified pull rate. However, in order to predict the mode of bond failure, from the master curve, information is needed on the intermolecular forces acting at the adhesive/adherend interface. Furthermore, long term stability of an adhesive can be evaluated based on the material's response at long times. Overall, using the compressive creep compliance master curve combined with the temperature dependence of a_T , the prediction of a materials application as a PSA in terms of peel, tack and long-term stability can be made over a full range of times and temperatures. This approach is discussed in greater detail in Chapter VI.

REFERENCES

1. C. A. Dahlquist, "Tack, Adhesion, Fundamentals and Practice," London: McLaren and Sons, Ltd. (1966).
2. F. H. Hammond, Jr., "Tack," in "Handbook of Pressure Sensitive Adhesive Technology," D. Satas (ed.), Van Nostrand and Reinhold Co.
3. P. J. C. Counsell and R. S. Whitehouse, "Tack and Morphology of Pressure Sensitive Adhesives," Chapter 4, p. 99. Inc., N.Y. (1982).
4. J. J. Bikerman, J. Coll. Sci., 2, 163 (1947).
5. G. J. Crocker, Rub. Chem. and Tech., 42, 30 (1969).
6. J. R. Dann, J. Coll. and Inter. Sci., 32(2), 302 (1970).
7. J. R. Huntsberger, Chem. and Eng. News, 82 (1964).
8. Y. Iyengar and D. E. Erickson, J. Appl. Polym. Sci., 11, 2311 (1967).
9. M. Toyama, T. Ho, H. Moriguchi, J. Appl. Polym. Sci., 14, 2295 (1970).
10. F. Wetzel, Characterization of Pressure-Sensitive Adhesives. ASTM Bulletin No. 221, 64 (1957).
11. G. Kraus and K. W. Rollmann, J. Appl. Polym. Sci., 21, 3311 (1977).
12. J. L. Gordon, J. Phys. Chem., 67, 1935 (1962).
13. F. H. Hammond Jr., Polyken Probe Tack Tester, ASTM Spec. Pub. 360 (1963).
14. M. Toyama, T. Ho, and H. Horiguchi, J. Appl. Polym. Sci., 14, 2039 (1970).
15. C. A. Dahlquist, "Creep," in "Handbook of Pressure Sensitive Adhesive Technology," D. Satas (ed.), Van Nostrand and Reinhold Co. Inc., N.Y. (1982).
16. I. M. Ward, Mechanical Properties of Solid Polymers, Wiley-Interscience, New York (1971).
17. J. J. Aklonis, Journal of Chemical Education, 58, 892 (1981).

18. J. J. Aklonis, W. J. MacKnight and M. Shen, Introduction to Polymer Viscoelasticity, Wiley-Interscience, New York (1972).
19. A. V. Tobolsky, Properties and Structure of Polymers, John Wiley and Sons, New York (1960).
20. Lawrence E. Nielsen, Mechanical Properties of Polymers and Composites, Vol. 1, Marcel Dekker, New York (1974).
21. J. J. Aklonis and W. J. MacKnight, Introduction to Polymer Viscoelasticity, 2nd ed., Wiley-Interscience, New York (1983).
22. J. D. Ferry, Viscoelastic Properties of Polymers, 3rd ed., John Wiley and Sons, New York (1980).
23. J. D. Ferry, Viscoelastic Properties of Polymers, 2nd ed., John Wiley and Sons, New York (1970).
24. D. G. Fesko and N. W. Tschoegl, Intern. J. Polymeric Mater., 3, 51 (1974).
25. W. C. Child, Jr. and J. D. Ferry, J. Colloid Sci., 12, 327 (1957).
26. D. J. Plazek and V. M. O'Rourke, J. Polym. Sci., 9A2, 209 (1971).
27. D. G. Fesko and N. W. Tschoegl, J. Polymer Sci., C, 35, 41 (1971).
28. Polymer synthesis and molecular characterizations were carried out by Mr. Jim Hoover, a Ph.D. candidate in the Materials, Engineering and Science program at VPI&SU, under the guidance of Drs. James E. McGrath and Thomas C. Ward.
29. Perkin Elmer Model TMS-2 Thermomechanical Analysis System Manual, The Perkin Elmer Corporation, USA, 1979.
30. The Perkin Elmer DMA-2 Supplement to the Perkin Elmer TMS-2 manual.

CHAPTER V

ROLE OF MICROPHASE SEPARATION IN ADHESION, I

ABSTRACT

Surface chemical and bulk physical characterization studies of a series of radial styrene (and substituted styrene) and isoprene block copolymers (25% weight styrene) were conducted in order to evaluate the mechanisms of their adhesive performance. The series included polymers based on t-butylstyrene and isoprene, p-methylstyrene and isoprene, and finally styrene and isoprene. A sharp interfacial boundary does not necessarily exist in this series of radial block copolymers; rather, partial mixing of the component blocks may be possible in the interfacial region between the two thermodynamically incompatible microphases. This series is an excellent model system to study in terms of microphase separation - property response. Based on solubility parameter arguments, and supported by dynamic mechanical and thermal mechanical analysis, the polymers based on t-butylstyrene and isoprene, (TBS-I)*, were the most intermixed of the three systems, while the styrene and isoprene radial block copolymer, (S-I)*, had the highest degree of phase separation, and the p-methylstyrene and isoprene radial block copolymer, (PMS-I)*, fell between these limits in terms of sharpness of delineation of morphology.

The goal of this study was to investigate the above polymer series, characterizing those aspects which played major roles in adhesion, and to model the role of microphase separation in adhesive performance. The polymers in this research could also vary in their degrees of microphase separation by the choice of casting solvent for film production, prior to adhesive bonding. Data interpretation was guided with consideration to the physical properties of the respective hard segments. Furthermore, the hard segment polymer chain lengths differed in some cases which aided the modeling.

The uniqueness of this set of investigated polymers lies in the combination of their tack and holding power, both necessary for pressure sensitive adhesives, which partially derived from the light crosslinked structure in the isoprene phase, deriving from the radial topology, as well as the microphase separation variation.

BACKGROUND

Triblock copolymers, ABA, composed of non-crystallizable A and B block sequences typically form a two phase, or a pseudo two phase, structure in the solid state in which domains of one component are dispersed in a medium of the other component on a microscopic scale (1,2). Generally, there exists an interfacial region of a certain thickness in which the incompatible sequences of A and B are

intermixed and separating the regions of pure A and B segments. The morphology and the arrangement of the two microphases are known to depend upon thermodynamic and molecular parameters (3-21) both of which strongly affect the microphase separation which results. Specifically, the chemical nature of the phases, the fraction of A and B segments, the preparation conditions of the solids, the molecular weight of each block copolymer, and experimental conditions such as the temperature are involved in influencing the final structure.

Several studies of the mechanical properties of block copolymers have proposed existence of the interphase (22-26). The interphase plays an important role in the mechanical properties of block copolymers used as thermoplastic elastomers (in terms of Young's modulus and its time and temperature dependencies, and flow behaviors, etc.); the same is equally true of adhesive compositions formulated from such materials. The design of block polymers for use as pressure sensitive adhesives is centered on the morphological uniqueness of these materials in which the domain formation was used to give a balance of tack, peel adhesion and holding power.

A. Block Copolymers

Numerous studies (1,27-51) have been conducted on ABA block copolymers where A was polystyrene and B was

polybutadiene or polyisoprene. These investigations probed characteristic structural properties (e.g. organization into spheres, cylinders, or lamellae), as well as the amounts of miscibility between the component blocks as functions of composition, preparation conditions of the films, molecular weight, and temperature.

Few investigations (52-54,95,96) have addressed the morphological questions that result from modifications of the chemical nature of the styrene and diene phases, either by replacement of the polystyrene with a ring substituted styrenic polymer such as poly(p-tert-butylstyrene), or by partial or full hydrogenation of the polydiene. The role of the morphology on the mechanical properties of these "modified" copolymers was a major theme of this research.

i. Composition

In general, five basic morphologies have been observed in styrene-diene (butadiene or isoprene) block copolymers, the perfection of which is very much dependent on the method of sample preparation (27,36,48). Up to about 20% by weight of styrene in the system, spheres of polystyrene are dispersed in a continuum of polydiene. As the styrene content is increased, the spherical domains develop an increasing degree of connectivity; in the range of 20-35% styrene a cylindrical or rod-like morphology is favored. In the composition range of 35-65% styrene alternating lamellae

are formed. At still higher styrene contents, the polystyrene phase becomes continuous while the polydiene forms discrete domains, either rod-like in the range 65-80% styrene, or as spheres of polydiene when the styrene content is above 80% (27). The typical composition limits mentioned are subject to considerable variation depending on sample history, particularly in films prepared by solution casting from different solvents (27,31).

ii. Sample Preparation

There are several ways in which the morphology can be changed. One method is to cast the polymer from different solvents. Selective solvation of one type of block causes its chains to expand in solution but leaves the chains from the other block in a collapsed state. This promotes the continuity of the block that is more highly solvated while casting, even though that block may be the minor component of the copolymer. It should be recalled that the morphology of a solvent cast film is not a true thermodynamic equilibrium morphology. In particular, the film morphology is established at some time during the evaporation process thus having some features of solution morphology.

Heat and pressure can be used to form test specimens of ABA block copolymers. The morphology of block polymers that have been melted and compression molded tends toward a more

random arrangement, while subsequent annealing brings about a more ordered morphology (27).

iii. Molecular Weight

The principal effect of molecular weight, in polystyrene-polydiene block copolymers, is on the polystyrene domain glass transition temperature. Kraus and Rollmann (59) have shown that a styrene block molecular weight of 20,000 g/mole is the approximate minimum value above which the position of the polystyrene domain glass transition temperature becomes constant, regardless of polymer composition and architecture (ABA and $(AB)_x$ for $x < 4$). When the styrene block molecular weight falls below 20,000 g/mole, there is a shift of the polystyrene domain glass transition temperature to lower temperatures as a result of intermixing of polydiene and polystyrene blocks.

iv. Temperature

It has been established that the domain structure of styrene and butadiene, and styrene and isoprene block polymers survives heating beyond the upper (polystyrene) glass transition temperature and that there exists a critical temperature, T_c , usually well above the polystyrene glass transition, at which these polymers become homogeneous melts. Evidence for a transition from a microheterogeneous state to a homogeneous one has come forth from rheological

measurements (44,46,49,50,51,55,56) and confirmed by small angle x-ray scattering (SAXS) studies (41,50,57,58).

The temperature T_c strongly depends on the molecular weight and chemical composition of the block polymer. T_c also depends on the degree of incompatibility between the component blocks; the greater the repulsive interaction the higher the T_c . Thus, in the case of block polymers composed of block chains having large molecular weights and a high repulsive interaction, the microphase-separated structure may not necessarily evolve into a homogeneous mixture on heating before the onset of thermal degradation (60).

v. Chemical Nature of the Phase

A study involving the replacement of polystyrene with poly(p-tert-butylstyrene) (PTBS) in linear ABA block copolymers was undertaken by Fetters, et. al (52). The work examined the effect of block compatibility upon the mechanical behavior of these copolymers, especially in view of the favorable high glass transition temperature of poly(p-tert-butylstyrene), relative to polystyrene. The solubility parameters for this styrenic end block (52, 61-63) and the polydiene center segment indicate that there is some possibility of compatibility between the prospective blocks. The calculated solubility parameter (61) for poly(p-tert-butylstyrene) is $8.12 \text{ (cal/cm}^3)^{\frac{1}{2}}$. The reported literature values (64) for polybutadiene, PB, and

polyisoprene, PI, fall within the range of 8.1-8.6 and 7.9-8.35 (cal/cm³)^{1/2}, respectively. The extent of compatibility was found to affect the degree of microphase separation and hence the integrity of the domains.

The linear poly(p-tert-butylstyrene) and polyisoprene triblock copolymers studied by Fetters and coworkers were tacky and found to flow with time at ambient temperature. They did not appear to differ appreciably from uncrosslinked polyisoprene of equivalent molecular weight. Virtually no tensile strength was obtained for these triblocks containing as much as 40% (weight) poly(p-tert-butylstyrene) and having end block molecular weights as high as 30,000 g/mole. The polyisoprene series exhibited significant tensile strengths only when the block polymers contained greater than 50% weight poly(p-tert-butylstyrene) with an end block molecular weight of 36,000 g/mole or greater. In order to achieve measurable values for the engineering stress, sufficient phase separation was found to be essential. Therefore, the tensile properties of these triblock copolymers demonstrated that poly (p-tert-butylstyrene) and polyisoprene are, to a large extent, mutually compatible. Hoover, et. al (53) have studied the dynamic mechanical behavior of two types of PTBS-PI radial block copolymers. Thermoplastic elastomers containing 15 to 25% weight PTBS and rubber modified thermoplastics containing 60 to 75% weight PTBS were investigated. The dynamic mechanical thermal analysis data

for a star block elastomer containing 25% weight poly(TBS) of 25,000 g/mole showed a broad low temperature transition and a low plateau modulus value, and also lacked a distinct high temperature transition corresponding to the poly(p-tert-butylstyrene) phase. Both observations are characteristic of a highly phase mixed system. In the case of a star block copolymer containing 60% weight poly(TBS) of 60,000 g/mole two distinct transitions were present, a broad low temperature damping and a relatively low (64°C) damping peak presumably for the poly(TBS) phase, indicative of some degree of phase separation, most probably coupled with a change in morphology. These results support the observations of Fetters, et. al for the stress-strain properties of these types of materials.

When butadiene was used instead of isoprene in these polymerizations by Fetters and coworkers (52), a series of triblocks exhibiting significant tensile strengths was obtained. However, relative to the reported tensile strengths for SBS copolymers, TBS-B-TBS triblock materials having both larger overall molecular weights and/or end segments were required in order to obtain comparable values for the engineering stress at given strains. The minimum critical molecular weight of poly(p-tert-butylstyrene) for apparent domain formation is about $1.5-2.0 \times 10^4$ g/mole. The existence of some phase blending was confirmed by an

examination of the block copolymer morphology via x-ray scattering and electron microscopy in their investigations.

Although poly(p-tert-butylstyrene) has a favorable, high, glass transition temperature relative to styrene ($\sim 145^{\circ}\text{C}$), the higher degree of compatibility of the TBS blocks with those of PI and PB affects the mechanical properties, lowering them in some cases. Thus, in order to achieve significant tensile strength, it was necessary to synthesize triblocks of either higher overall molecular weight or to increase the amounts of TBS overall.

vi. Radial vs. Linear Topology

Investigations of the effect of chain geometry on the morphology and rheology of polystyrene-polydiene block copolymers indicate that the effects of branching are minor, for A-B to $(\text{A-B})_4$, when the polymers are compared at equal lengths of the terminal block. In an investigation by Price, et. al (65), where the overall composition of the polymers studied was 25% by weight of polystyrene, results indicated that within experimental error the cylindrical radii and interdomain distances are independent of the change in chain geometry from A-B to $(\text{A-B})_4$ provided the polystyrene end-block lengths and overall composition remained constant. Steady flow and dynamic viscosities determined for symmetric linear and star-branched block copolymers, up to $(\text{A-B})_4$, of styrene and butadiene, above their upper (polystyrene) glass

transition, by G. Kraus and colleagues (66), showed that the length of the terminal blocks, not the total molecular weight, dominates the viscoelastic behavior of these polymers.

B. Block Copolymer Based Pressure Sensitive Adhesives

The design of block copolymers for use in pressure-sensitive adhesives requires compromises between tack, peel adhesion and holding power. Polystyrene domain connectivity leads to diminished tack in block polymers, a result of decreased creep compliance on the time scale of the bonding process and failure to achieve full contact with the substrate. Holding power (shear resistance) increases with polymer styrene content and molecular weight; this being a consequence of the polystyrene domain structure effectively inhibiting viscous flow at temperatures sufficiently below T_g of the styrene block. The important trade-off exists between tack and holding power. Peel strength is closely related to the evaluation of tack in the present context (67,68).

i. Shear Holding Power

The outstanding feature of styrene-diene block polymers in pressure sensitive adhesive formulations is their excellent resistance to adhesive creep (67). Shear holding power increases with polymer styrene content and molecular

weight, as discussed above (68). It is anticipated that additional factors are involved such as structure developed by varying solvents in cast films, and orientation as developed from rapid extrusion or molding as discussed in Chapter II of this thesis.

ii. Tack

The other essential property of a pressure sensitive adhesive is tack (71). In the broadest sense, tack is the ability of the adhesive to bond rapidly under conditions of light contact pressure and short contact time. Tack of an adhesive is both a surface thermodynamic and a rheology related property. Pressure sensitive tack, and bond formation in general, ultimately involves molecular interactions at the adhesive/adherend interface. A major driving force towards bond formation is the widely used "work of adhesion," which is related to the surface energies of the adhesive and adherend. A pressure sensitive adhesive must also possess viscoelasticity, that is, the adhesive must be able to conform to micro and macroscopic surface roughnesses to achieve the desired adhesive bonding while maintaining a degree of nonflowing physical integrity (70-85).

Surface Chemistry and Tack: To have good pressure sensitive tack, an adhesive should have low surface energy. This contributes to an overall lowering of the Gibbs free energy on bonding. Zisman's concept (83) of critical surface

tension for a solid provides a basis for estimating the surface energy of an adhesive and understanding why low surface energy adhesives are desirable. According to this method small drops of liquids in a homologous series chemically are placed on solid surfaces and make characteristic angles of contact with the solid that depend on the liquid's surface tension. Plots of observed contact angle versus liquid surface tension are extrapolated to zero contact angle in order to give the critical surface tension for wetting, γ_c . Zisman suggested correctly that the liquid surface tensions obtained in this way are characteristic of the solid surface. Gordon (80) showed how critical surface tensions may be related to the solid's chemical composition through Hildebrand's solubility parameter and cohesive energy density. The critical surface energies of pressure sensitive adhesives and adherends can be measured following the methods of Zisman and coworkers. Care must be used in selecting test liquids to avoid complications of solubility, specific chemical reactions, and time dependency of contact angle (74).

The extent of contact between adhesive and an adherend can depend on their relative surface energies (81,82). A simple liquid with a surface tension less than the critical surface tension will make a zero contact angle and spontaneously wet and spread over a solid's surface. Adhesives with surface tensions less than the adherend's

critical surface tension are also expected to wet and spread, but this requires some period of time because of the adhesive viscosity. Sharpe and Schonhorn (86,87) first recognized the significance to strong bond formation of the adhesive having a lower surface energy than the adherend. Adhesives of hydrocarbon composition, having low surface energy, generally exhibit good tack to the widest variety of adherends.

The surface chemistry that gives the greatest tack may not always have a critical surface tension less than the adherend but may be some higher value. Zisman pointed out the maximum "work of adhesion" between simple liquids and solids was for liquids with surface tensions greater than the solid's critical surface tension. This circumstance should be true of practical adhesives and adherends as well. Huntsberger (75,88-90) has shown that complete wetting of solid surfaces does not require zero contact angles but can occur for liquids making contact angles up to 90 degrees. Huntsburger also reasoned the greatest rate of wetting would be achieved by adhesives having surface tensions somewhat greater than the solid's critical surface tension. Toyama (82) and others have observed experimentally a maximum in probe tack when the surface energy of the adhesive was slightly greater than that by the adherend.

Rheology and Tack: While adhesive and adherend surface chemistries determine interaction energy at the molecular level, their bulk physical properties also determine the rate

and extent of contact and bond strength between them (91). Pressure sensitive adhesives differ from other materials primarily because of the unique rheological properties they possess. Rheological properties are the major factors in the phenomenon of pressure sensitive tack. These are difficult to separate from "viscoelastic" behavior and in the context of the time scales involved the semantic difference should be ignored.

For good pressure sensitive tack and rapid bond formation, the adhesive should be easily deformed in the time frame of the bonding process. Dahlquist (92) found that the 1 second compressive creep compliance of a pressure sensitive adhesive having good tack needed to be greater than or equal to 10^{-7} cm²/dyne. When the creep compliance is much less than 10^{-7} cm²/dyne, the degree of conformability to solid surfaces is not sufficient to effect the desired adhesive bonding (27,79,93,94). This criterion applies to pressure sensitive adhesives in general, including those formulated from block copolymers.

Kraus (48) has developed a criterion similar to Dahlquist's for block copolymer adhesives, based on the shear storage modulus at 25°C and 35 Hz. Reasonable estimates had to be made in the transformation due to the fact that the block polymer based adhesives are thermorheologically complex.

A compressive creep compliance of 10^{-7} cm²/dyne is equivalent to a shear creep compliance of 3×10^{-7} cm²/dyne for rubbery materials of Poisson's ratio 1/2. According to Riande and Markovitz (69)

$$|J(t)| \approx |J^*(\omega)| \quad \omega = 1/t \quad (5.1)$$

where $|J^*(\omega)|$ is the absolute magnitude of the complex dynamic shear compliance. If $\tan \delta$ is not large (say, < 0.35),

$$|J^*(\omega)| \approx 1/G'(\omega) \quad (5.2)$$

is a good approximation. For 35 Hz, $\omega = 220$ rad/sec and $t = 0.0045$ seconds, so that,

$$J(1) > J(.0045) \approx 1/G'(35 \text{ Hz}) \quad (5.3)$$

At 25°C, the requirement that $J(1) \geq 3 \times 10^{-7}$ cm²/dyne will be met conservatively if (48):

$$G'(35 \text{ Hz}) \leq 3.3 \times 10^6 \text{ dynes/cm}^2 \quad (5.4)$$

For good tack, the adhesive deformation in the bonding stage should be in a large part viscous. Energy absorbing fluidlike flow is desirable to relax the stress put on the adhesive as it is made to conform to the irregularities of the adherend. If bonding deformation were only elastic, the recoverable stored stress would assist external stress in the rupture of the bond. Pressure sensitive adhesive tack is favored by a high ratio of viscous to elastic properties at time spans comparable to bonding times (71).

INTRODUCTION

In the course of work on the relationship between the morphology of ABA poly(styrene-b-isoprene) block copolymers (SIS) and their properties as heat activated films adhering to glass, Widmaier and Meyer observed the very important role played by the activation temperature on the shear resistance of joints: for each SIS, resistance to break was maximal for a well defined activation temperature . They attributed this effect to an evolution of morphology towards phase miscibility increasing with activation temperature rather than to a simple decrease of copolymer viscosity favoring wetting (97).

In order to gain further insight into the influence of the overall compatibility of the component blocks of ABA poly(styrene-b-isoprene) block copolymers on adhesive performance, a study was undertaken at Virginia Tech and featured the replacement of polystyrene with poly(p-methylstyrene) and poly(p-tert-butylstyrene) in radial $(AB)_x$ block polymers.

The solubility parameter for the poly(p-tert-butylstyrene) end block and the polyisoprene center segment indicate possible compatibility between the prospective blocks. The calculated solubility parameter (61) for poly(p-tert-butylstyrene) is $8.12 \text{ (cal/cm}^3)^{\frac{1}{2}}$. The reported literatures values for polyisoprene fall within the range of $7.9\text{-}8.35 \text{ (cal/cm}^3)^{\frac{1}{2}}$. This proximity suggests the

possible compatibility of poly(p-tert-butylstyrene) with polyisoprene, particularly at lower molecular weights. The reported literature value of the solubility parameter (102) or polystyrene is 9.2 to 9.3 $(\text{cal}/\text{cm}^3)^{\frac{1}{2}}$. Numerous studies (1-51) of polystyrene-polyisoprene block copolymers indicate that a high degree of microphase separation exists between the component blocks. While the poly(p-methylstyrene) - polyisoprene block copolymer is expected to fall between these limits with its morphology, the literature value of the solubility parameter (102) for poly(p-methylstyrene) is 8.8 $(\text{cal}/\text{cm}^3)^{\frac{1}{2}}$.

Therefore, by modifying the chemistry of the end block, all other parameters held constant, one might be able to vary the degree of compatibility of the component blocks of this series of block copolymers. The extent of compatibility affects the degree of microphase separation and hence the integrity of the domains. The goal of this study was to translate the effect of block compatibility into the adhesive performance of the copolymers, against high surface energy, rigid, reproducible substrates. A view of the surface chemistry and bulk physical properties of the materials would contribute to the interpretation.

EXPERIMENTAL

A. Synthesis and Characterization (1)

The radial or "star" topology block copolymers were anionically prepared (53) from isoprene and then separately with each of the three styrenic monomers: styrene (S), p-methyl styrene (PMS), and t-butyl styrene (TBS). "Living" diblock copolymers having polydienyllithium chain ends were subsequently linked with divinyl benzene (DVB) to produce the desired radial architecture. The reaction was carried out at 60°C in cyclohexane, and terminated with methanol. Size exclusion chromatography and molecular weight determinations indicate 3-6 arms.

Molecular weight determinations of each of the three styrenic monomers were conducted by means of size exclusion chromatography, GPC, prior to the subsequent addition of isoprene to produce the "living" diblock copolymer. Molecular weights were calculated based upon polystyrene standards with appropriate correction factors being applied for the poly(p-tert-butylstyrene) (1.1) and the poly(p-methylstyrene) (1.02) homopolymers.

The number of arms per radial polymer was calculated by dividing the peak molecular weight of the radial polymer by the peak molecular weight of its respective diblock copolymer. All molecular weights were determined by GPC based upon polystyrene standards with appropriate corrections

applied. The calculated number of arms is approximate and it represents the minimum value. The radial polymers are highly branched molecules and the apparent molecular weight as determined by GPC, which separates based upon hydrodynamic volume, is lower than the true molecular weight of the radial polymers. A more appropriate method for determination of the molecular weights is membrane osmometry which gives a true number average molecular weight.

The percent residual diblock present in the final radial block copolymer was calculated from the gel permeation chromatogram by the ratio of the peak area of the diblock polymer to the peak area of the radial block copolymer. Figure 28 shows a gel permeation chromatogram of a radial block polymer prepared by the reaction of divinylbenzene with dienyllithium chain ends. It is readily seen that the radial block polymers possess a bimodal molecular weight distribution and contain ca. 20-30 weight % diblock polymer.

FTIR and FT proton NMR analysis indicate that the polydiene microstructure consisted of 72% cis-1,4, 22% trans-1,4 and 5% 3,4 polyisoprene.

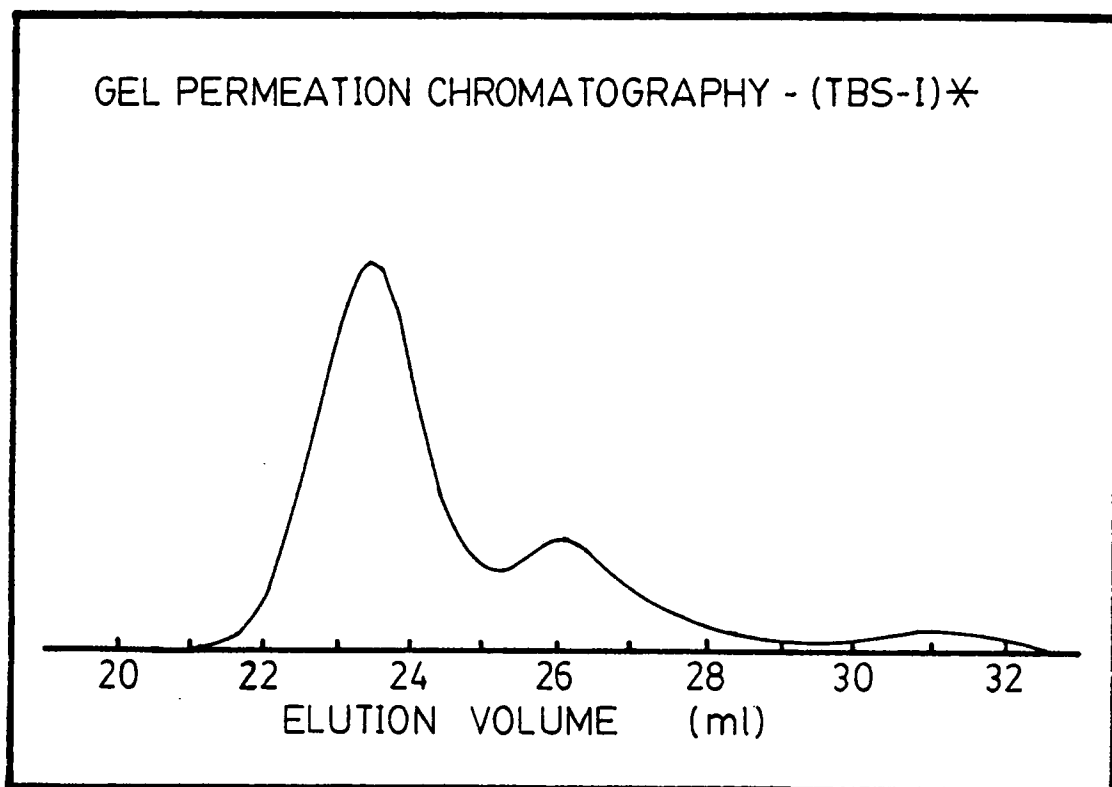


Figure 28. GPC trace of p-tert-butylstyrene and isoprene radial block copolymer (1).

B. Characterization of Bulk Polymer Properties

i. Dynamic Mechanical Thermal Analysis

Isochronal dynamic mechanical measurements were made in the shear mode with a Polymer Laboratory Dynamic Mechanical Thermal Analyzer (PL-DMTA). Measurement frequency was 1 Hz and the heating rate was 5°C/minute. Typical sample dimensions of .5 mm thickness, 1 mm length and 15 mm width were used (98,99).

PL-DMTA Theory (98,99) - The sample in the PL-DMTA is subjected to a sinusoidal force F in phase with the current applied to the vibrator drive. The sample stiffness (kE^*) is measured in parallel with the instrument spring stiffness (S^*).

Under these conditions, the equation of motion of the clamp/drive/sample system is:

$$F_p \sin \omega t = Mx + \frac{S''}{(\eta + \omega)} + \frac{kE''}{\omega}x + (S' + kE')x \quad (5.5)$$

where x is the displacement, M the moving mass and $\omega (=2\pi f)$ is the angular frequency of the applied force. The DMTA evaluates the storage (kE') and loss (kE'') components of stiffness via the solutions of the equation of motion as:

$$kE' = K \cos \beta + M\omega^2 - S' \quad (5.6)$$

$$kE'' = K \sin \beta - S'' - \omega\eta \quad (5.7)$$

where K is (Peak Force)/(Peak Displacement). Now S' is the storage part of the spring stiffness of the instrument with no sample present and S'' the corresponding loss term.

Normally the term $\omega\eta$ in these equations, due to air damping, is small and $M\omega^2$ the inertia term is small at low frequencies (less than 10Hz).

Thus, for most measurements:

$$kE' = K \cos \beta - S' \quad (5.8)$$

$$kE'' = K \sin \beta - S'' \quad (5.9)$$

and $\tan \delta = \text{Eq}(5.9)/\text{Eq}(5.8)$.

ii. Thermal Mechanical Analysis

Thermal mechanical measurements were made in the penetration mode as a function of temperature, with a Perkin Elmer Thermomechanical Analyzer System (TMS-2). The heating rate was 10°C/minute. The sample thickness was on the order of .5 mm.

Polymer films for mechanical measurement were solution cast from 20 weight % solutions in cyclohexane. Solutions were poured into teflon trays and evaporated slowly at ambient temperature. After films were visibly dry, approximately 72 hours, they were vacuum dried at 60°C for 48-72 hours.

C. Surface Characterization

The critical surface tensions of the polymers were determined by the empirical method first reported by Zisman and described above. The Zisman liquid series includes: water, glycerol, formamide, methylene iodide, 1-bromonaphthalene and the alkane series: hexadecane, decane, octane and hexane.

Contact angles were measured in a Rame-Hart 100-00 contact angle goniometer. To obtain the advancing contact angle, a $2\mu\text{l}$ drop of the liquid was deposited on the polymer substrate. The procedure was repeated until a constant angle was reached. The reading was taken as soon as possible after each additional increment to insure that minimal evaporation occurred and the true advancing angle was obtained. To determine the receding angle, the liquid was withdrawn in $2\mu\text{l}$ increments and the angle read until all the liquid was recovered. Critical surface tensions for each polymer were determined by extrapolation of $\cos \theta_A$ (θ_A = measured advancing contact angle) versus the surface energy of the spreading liquid to $\cos \theta_A$ equal to 1.00. The corresponding surface energy is equal to the critical surface tension of the polymer.

Polymer films for contact angle measurements were spin coated from 2 weight % polymer solutions in cyclohexane onto 1" square ferro-type plates. The polymer films were ca. 1000

Å thick, measured by interferometry, and of uniform thickness.

D. Adhesive Performance Testing

A 180° peel test, in close agreement with an ASTM test (100), was conducted on an Instron Model 1122. The peel test was done at room temperature and a pull rate of 11.8 inches/minute (300 mm/min). Polymer solutions of 5 weight % were cast onto a 1" wide mylar flexible backing, and evaporated slowly at ambient temperatures for 72 hours, then vacuum dried at 60°C for 48 hours. This consistently produced a visibly smooth adhesive film of 0.004-0.005 mm. The thickness of the mylar backing was 0.01 mm. The adherend was a Ti 6-4 (Al-V) alloy which was pretreated by a chromic acid anodization. The purpose of the anodization process was to give a reproducible "clean" surface. Bonding immediately followed the anodization process to avoid contamination of the "clean" metal surface. Bonding was conducted upon an application pressure of 1000 psi for one minute. The bond area was 1" (width) by 2.5" (length).

The three radial polymers were each cast separately from each of three different solvents: cyclohexane, toluene and dichloroethane, and evaluated as pressure sensitive adhesives. When pressure sensitive adhesive films are cast from solution, the resulting polymer morphology and hence the

adhesive properties, will in general, depend upon the solvent (27,31).

Details of the pretreatment of the mylar and the Ti 6-4 adherend, and the bonding procedure are given below.

Mylar Pretreatment: The mylar flexible backing was wiped with acetone prior to the casting of the polymer solutions onto the mylar, to rid the surface of any contamination. There was no visible evidence of solvent induced crystallization of the mylar as a result of the wiping with acetone. However, a closer examination, by scanning electron microscopy, showed evidence for small amounts of crystallization, induced by the acetone wipe.

Chromic Acid Anodization of Ti 6-4 (2): The chromic acid anodization (CAA) pretreatment of the Ti 6-4 adherend is detailed below.

1. Wipe with methyl ethyl ketone (MEK).
2. Soak in sodium hydroxide solution (13g/250ml) at 70°C for 5 minutes.
3. Rinse three times in deionized water.
4. Immerse in pickle solution (15 ml conc. HNO_3 , 3 ml 49%w/w HF, 82 ml H_2O) at room temperature for 5 minutes.
5. Rinse three times in deionized water.

6. Anodize at room temperature for 20 minutes at 10 volts, 26.9 amp sq.m (2.5 amp/sq. ft.) in a chromic acid solution (50 g CrO₃/1000 ml) with a Ti 6-4 coupon as the cathode. 49% w/w HF is added to attain the desired current density.
7. Rinse three times in deionized water.
8. Blow dry with prepurified N₂ gas until visibly dry.

Bonding Procedure: Details of the application of the adhesive tape, prepared as described previously, to the pretreated Ti 6-4 adherend are described below.

1. Gently match the adhesive tape to the pretreated bond area of the Ti 6-4 coupon (Refer to Figure 29).
2. Place a 1/4" thick felt backing over the flexible adhesive backing (Refer to Figure 29).
3. Place the specimen between hydraulic press plates.
4. Apply 2500 psi for 1 minute.
5. Release the pressure after 1 minute and remove the specimen from the press and remove the felt backing.

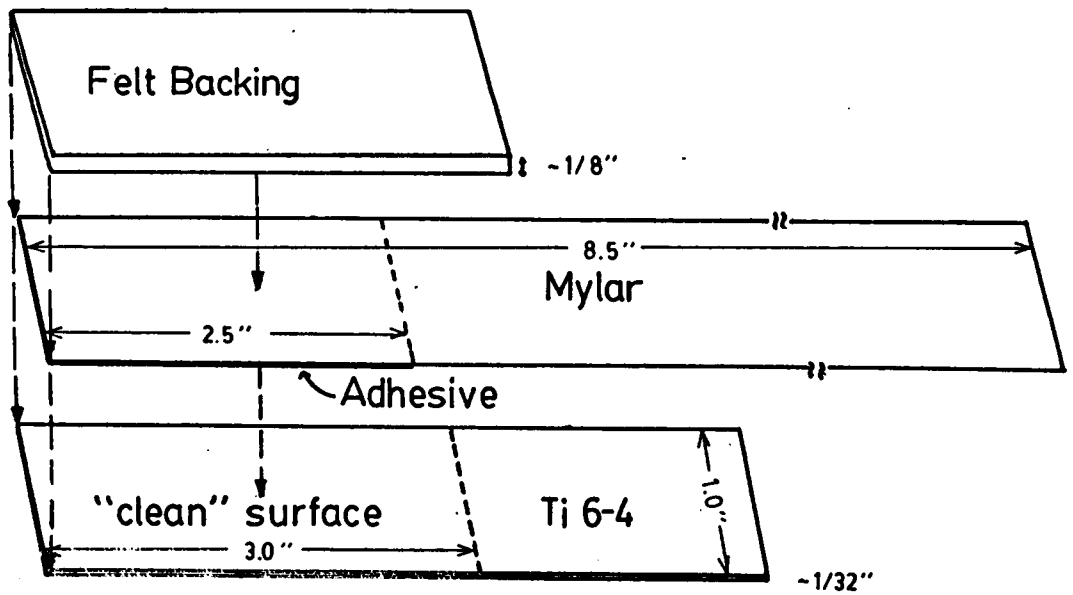


Figure 29. Schematic representation of the construction of the 180° peel specimen.

RESULTS AND DISCUSSION

A. Polymer Characterization (1)

The number average molecular weight $\langle M_n \rangle$ of the styrenic block for each polymer studied and the calculated average number of arms per "star", as determined by GPC analysis, are listed in Table 5. The t-butyl styrene, p-methyl styrene, and styrene and isoprene radial block polymers are 25% (weight) styrenic block - 75% hydrocarbon block, with hard block $\langle M_n \rangle$ of around 25,000 g/mole. Each of these three polymers was found to contain about 20-30% by weight diblock on analysis. The overall compositions of the radial block polymers are such that the polymers have application as pressure sensitive adhesives, including natural tack caused by the diblock.

B. Microphase Separation

From the dynamic mechanical (Figure 30) and thermal mechanical analysis (Figure 31) of the series of styrene (and substituted styrene) and isoprene radial block copolymers the relative degree of microphase separation is suggested by the breadth and position of the $\tan \delta$ dispersion for the isoprene segment, greater peak width at higher temperatures indicating higher degree of phase mixing, and the temperature range over which the plateau in modulus is retained.

Table 5. Characterization of Radial Block Copolymers (1).

	<u><Mn> of Hard Block</u>	<u><*Arms></u>	<u>δ (cal/cm³)^{1/2} Hard Block</u>
(S-I)*	27,300	4	9.2
(PMS-I)*	26,700	2-3	8.8
(TBS-I)*	23,300	6	8.1

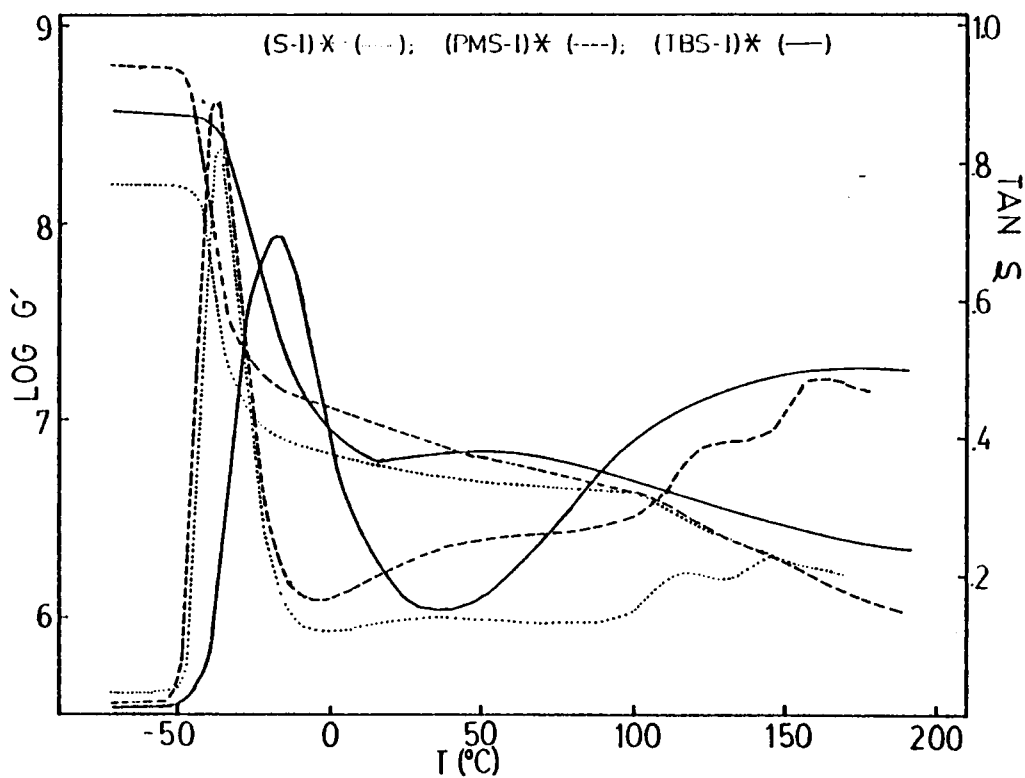


Figure 30. Viscoelastic properties of styrene, p-methylstyrene and p-tert-butylstyrene and isoprene radial block copolymers (1 Hz).

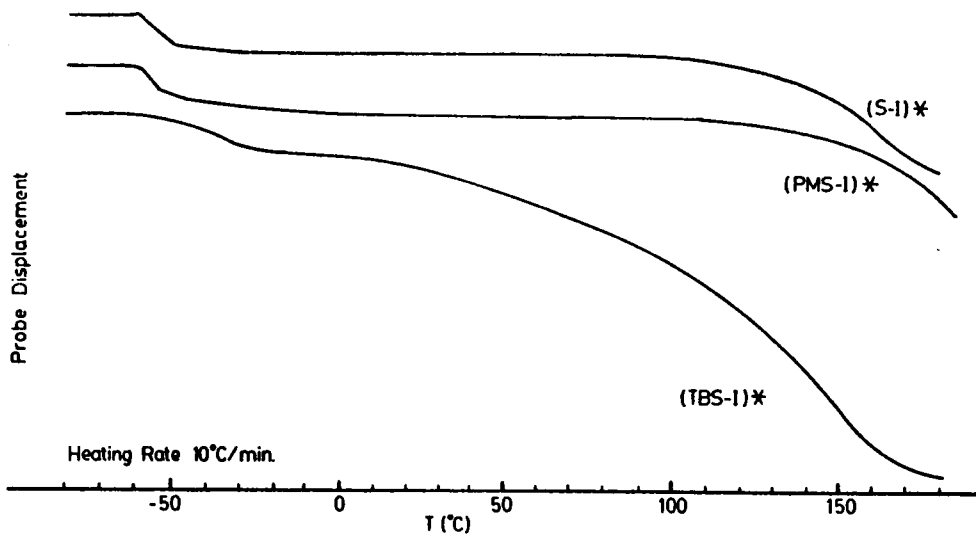


Figure 31. Thermal mechanical analysis of styrene, p-methylstyrene and p-tert-butylstyrene and isoprene radial block copolymers.

Figure 30 shows the shear storage modulus (G') and $\tan \delta$ as a function of temperature at 1Hz for the series of radial block polymers. The styrene and isoprene, and p-methylstyrene and isoprene radial block polymers show two primary dispersions associated with the microbrownian motion of the polyisoprene and polystyrenic phases, in the respective phase-separated domains. The temperature of each primary dispersion is very near that of the respective homopolymer (Table 6). The lower (polyisoprene) transition is fairly sharp; it is slightly broader for the p-methylstyrene and isoprene radial block polymer. The upper (polystyrenic) transition is not well resolved in either block copolymer; a peak of much diminished height is superimposed on a rising $\tan \delta$ approaching the melt region. On the other hand, the p-tert-butylstyrene and isoprene radial block copolymer exhibits essentially a single broad primary dispersion at -20°C , followed by a rising $\tan \delta$ approaching the melt region. The breadth and position of the low temperature transition and the lack of a distinct high temperature transition corresponding to the poly(p-tert-butylstyrene) phase, are characteristic of a highly phase mixed system.

The thermal mechanical analysis (Figure 31) of the styrene and isoprene, p-methylstyrene and isoprene, and p-tert-butylstyrene and isoprene radial block copolymers

Table 6. Glass Transitions of Homopolymers (DMTA, 1 Hz).

Polystyrene	2.5×10^4 g/mole	--
Poly (p-methylstyrene)	2.5×10^4 g/mole	115°C
Poly (p-tert-butylstyrene)	2.5×10^4 g/mole	157°C
Polyisoprene	7.5×10^4 g/mole	-45°C

compliment the dynamic mechanical analysis. The styrene and isoprene, and p-methylstyrene and isoprene radial block polymers show a sharp low temperature transition very near that of the polyisoprene homopolymer and retention of the plateau modulus over a temperature range covering 150° to 200°C. Whereas the poly(p-tert-butylstyrene) and isoprene polymer exhibits a broad low temperature transition followed by a continual decrease in modulus.

Therefore, based on solubility parameter arguments and supported by dynamic mechanical and thermal mechanical analysis, the t-butylstyrene and isoprene based radial block copolymer, (TBS-I)*, was the most intermixed of the three systems, while the styrene and isoprene based radial block copolymer, (S-I)*, had the highest degree of phase separation, while the p-methylstyrene and isoprene based radial block copolymer, (PMS-I)*, fell between these limits with its morphology.

C. Surface and Bulk Polymer Properties

Surface chemistry and bulk physical properties of adhesives are of major importance in ultimate adhesive performance (1). Adhesive surface chemistry plays a major role in bond formation, since bond formation ultimately involves interactions at the adhesive/adherend interface. The physical properties of the adhesive also determine the rate and extent of contact, and the adhesive bond strength.

i. Surface Characterization

To have good pressure sensitive tack, an adhesive should have low surface energy. Zisman's (10) concept of critical surface tension for a solid provides a basis for estimating when surface energies are low. The values for the critical surface tension of the radial polymers were measured following the methods of Zisman and coworkers; the values are listed in Table 7. The radial polymers are of hydrocarbon compositions, therefore, they naturally have low surface energies. Although, taking into consideration data scatter, the values are similar, significant trends are present.

1. For a given liquid, the angle of contact made with the polymer surfaces was consistently larger on the (TBS-I)* surface than on the (PMS-I)* surface, which was larger than the angle of contact made on the (S-I)* surface (Figure 32).
2. When measuring the contact angle of the liquids of higher surface tension on the (TBS-I)* polymer surface, the liquid would initially have a high contact angle, then spread and have a lower contact angle. This behavior did not occur on the (PMS-I)* and (S-I)* surfaces.

Table 7. Critical Surface Tensions.

	γ_c (dynes/cm)
(TBS-I)*	27.2
(PMS-I)*	31.4
(S-I)*	34.0

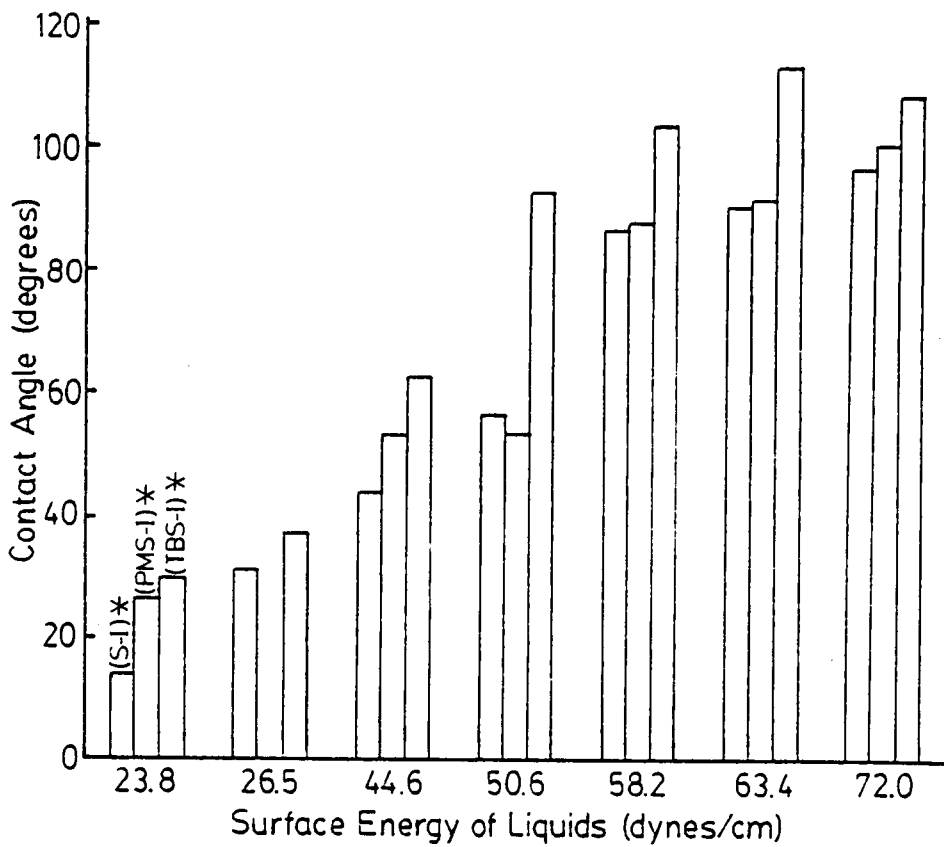


Figure 32. Contact angle measurements for styrene, p-methylstyrene and p-tert-butylstyrene and isoprene radial copolymers.

The extent of contact between adhesive and an adherend can depend on their relative surface energies (81,82). Adhesives with surface tensions less than the adherend's critical surface tension are expected to wet and spread, but this requires some period of time because of the adhesive viscosity. Sharpe and Schonhorn (86,87) first recognized the significance to strong bond formation of the adhesive having a lower surface energy than the adherend. The radial polymers having low surface energies are expected to exhibit good tack to a wide variety of adherends, including the Ti 6-4 alloy of this study which is a high energy surface.

ii. Bulk Polymer Characterization

While adhesive and adherend surface chemistries determine interaction energy at the molecular level, the bulk physical properties of the adhesive can be related to the rate and extent of contact (91). For good pressure sensitive tack and rapid bond formation, the adhesive should be easily deformed in the time frame of the bonding process (92); this is generally assured if the 1-second compressive creep compliance is ca. 10^{-7} cm²/dyne or more.

Repeating, Kraus et al. (48) have modified this criterion in reports on block copolymer adhesives based on the shear storage modulus G' at 25°C and 35 Hz. For satisfactory pressure sensitive adhesives (PSA) they

determined that $G'(35 \text{ Hz}) \leq 4 \times 10^6 \text{ dynes/cm}^2$ to achieve satisfactory adhesive bonding. All three radial polymers have a shear storage modulus G' value less than 10^7 dynes/cm^2 from a temperature range of 0° to 100°C as measured at 1 Hz. Thus, the radial block systems are within range of meeting the contact criterion.

D. Adhesive Performance

Peel adhesion (101) is one of the important characteristics of PSAs. This property is evaluated by measuring the tensional force required to remove the adhesive tape. The peel force depends on the adhesion, but it also depends strongly on the viscoelasticity of the adhesive, as well as many other factors: stiffness of the adherend, adhesive thickness, flexible backing, rate of separation, temperature, etc. For block copolymer based PSAs, it is the morphological uniqueness of these materials in terms of domain formation and the extent of compatibility of the component blocks that strongly influences the overall adhesive performance.

Based on the results obtained in the present work, and for the copolymers of this chapter containing some diblock material, maximum peel strength resulted in those systems where there was the greatest mismatch in solubility parameter between the polymer styrenic block and the casting solvent. Table 8 summarizes the data and reveals that the styrene and

isoprene radial polymer with cyclohexane and the p-methylstyrene and isoprene radial polymer with cyclohexane are the strongest systems. Selective solvation of the polyisoprene block causes those chains to expand in solution and leaves the chains from the polystyrene and poly(p-methylstyrene) blocks in a collapsed state. This promotes the continuity of the polyisoprene phase and the polystyrene and poly(p-methylstyrene) blocks exist as better defined domains within the polyisoprene matrix than do the poly(t-butylstyrene) blocks. The continuous polyisoprene phase gives rise to appreciable tack, as does the diblock material, whereas sufficient phase separation is essential to achieve measurable values for the peel strength. Low values of peel strength resulted in those systems where there was a close match of the solubility parameters of the polymer styrenic block and the casting solvent, i.e. (S-I)* cast from DCE and (PMS-I)* cast from DCE. Polystyrene and poly(p-methylstyrene) tended to be less well defined phases when the solvent was relatively better for polystyrene and poly(p-methylstyrene) than polyisoprene, even though they are the minor components of the respective copolymers. Connectivity of the polystyrenic domains greatly decreases the compliance in the temperature-time region of interest, resulting in failure to meet the contact criterion.

Table 8. Peel Force (lbs/in)¹

Solvent [δ (cal/cm ³) ^{1/2}]	Dichloroethane ($\delta = 9.2$)	Toluene ($\delta = 8.9$)	Cyclohexane
<u>Polymer</u> [δ (cal/cm ³) ^{1/2}]			
$\frac{(TBS-I)^*}{(\delta_{PTBS} = 8.1)}$	6.4 + .7	6.8 + .9	7.5 + .4
$\frac{(PMS-I)^*}{(\delta_{PMS} = 8.8)}$	2.9 + .2	7.1 + .1	8.6 + .4
$\frac{(S-I)^*}{(\delta_{PS} = 9.2)}$	4.0 + .4	6.4 + .4	11.9 + 1.1

¹ Application Pressure = 1000 psi; Rate = 11.8 in/min;
Temperature = 23°C

Furthermore, the (TBS-I)* morphology was virtually unaffected by choice of casting solvent as revealed by these experiments. The measured peel strengths for (TBS-I)* as cast from the three solvents are, within experimental error, the same. This is a result of the compatibility of the poly(p-tert-butylstyrene and polyisoprene phases. Fetters, et al. (52) studied the mechanical properties of linear poly(p-tert-butylstyrene)-polyisoprene triblock copolymers, of varying composition and molecular weight. The materials were tacky and found to flow with time at ambient temperature. Virtually no tensile strength was obtained for those materials having molecular weights as high as 10^5 g/mole and greater than 40% weight poly(p-tert-butylstyrene). Thus, demonstrating that poly(p-tert-butylstyrene) and polyisoprene are to a large extent mutually compatible.

The (S-I)* morphology was most affected by the choice of casting solvent, due to the incompatibility of the polystyrene and polyisoprene microphases. Dichloroethane preferentially solvates polystyrene; this promotes connectivity of the polystyrene domains and leads to a loss in tack, reflected in the lower values of peel strength, but high shear resistance. On the other hand, cyclohexane selectively solvates polyisoprene; this promotes a rubber continuous morphology of the polymer and development of tack, reflected in the higher values of peel strength, but a decrease in shear resistance.

Overall, the measured peel strengths were well near the maximum of observed performance of industrial PSAs of similar formulation. However, typical block polymers generally require the addition of a sufficient quantity of a polydiene compatible tackifier to meet the contact criterion and to perform well as a PSA. Recall, the styrene (and substituted styrene) and isoprene radial block polymers studied contained 20-30% by weight residual diblock. This diblock material served to "plasticize" the compositions and cause G' (35 Hz) to exceed the minimum requirement, in most cases. Therefore, as a result of the plasticizing effect of the residual diblock, in general, these materials were inherently "high" tack and "low" shear resistant adhesives; the highest peel strengths resulted in those systems whose morphology contained well defined hard segment domains within the rubber matrix.

REFERENCES

1. G. E. Molau, "Block Polymers," pp. 79-106, S. L. Aggarwal, ed., Plenum Press, New York (1970).
2. E. Vanzo, J. Polym. Sci., A-1, 4, 1727 (1966).
3. T. Inoue, T. Soen, H. Kawai, M. Fukatsu and M. Kurata, J. Polym. Sci., B, 6, 75 (1968).
4. T. Inoue, T. Soen, T. Hashimoto and H. Kawai, J. Polym. Sci., A-2, 7, 1283 (1969).
5. T. Inoue, T. Soen, T. Hashimoto and H. Kawai, Macromolecules, 3, 87 (1970).
6. T. Soen, T. Inoue, K. Miyoshi and H. Kawai, J. Polym. Sci., A-2, 10, 1757 (1972).
7. D. J. Meier, J. Polym. Sci., C26, 81 (1969).
8. D. J. Meier, Polym. Prepr.; ACS, Div. Polym. Chem., 11, 400 (1970).
9. D. J. Meier, "Block and Graft Copolymers," pp. 105-139, J. J. Burke and V. Weiss, ed., Syracuse University Press, N.Y. (1973).
10. D. J. Meier, Polym. Prepr., ACS, Div. Polym. Chem., 15, 171 (1974).
11. E. Helfand, Polym. Prepr., ACS, Div. Polym. Chem., 15, 970 (1973).
12. E. Helfand, "Recent Advances in Blends, Grafts and Blocks," L. H. Sperling, ed., Plenum Press, New York (1974).
13. E. Helfand, Macromolecules, 8, 552 (1975)
14. E. Helfand and Z. R. Wasserman, Macromolecules, 9, 879 (1976).
15. D. F. Leary and M. C. Williams, J. Polym. Sci., Polym. Phys. Ed., 11, 345 (1973); 12, 265 (1974).
16. W. R. Krigbaum, S. Yazyan and W. R. Talbert, J. Polym. Sci., Polym. Phys. Ed., 11, 511 (1973).
17. R. E. Boehm and W. R. Krigbaum, J. Polym. Sci., C54, 153 (1976).

18. S. Kraus, J. Polym. Sci., A-2, 7, 249 (1969).
19. S. Kraus, Macromolecules, 3, 84 (1970).
20. U. Bianchi, E. Pedemonte and A. Turturro, Polymer, 11, 268 (1978).
21. L. Marker, Polym. Prepr., ACS Div. Polym. Chem., 10, 524 (1969).
22. S. L. Aggarwal, R. A. Livigni, L. F. Marker and T. J. Dudek, "Block and Graft Copolymers," pp. 157-194, J. J. Burke and V. Weiss, ed., Syracuse University Press, N.Y. (1973).
23. M. Shen and D. H. Kaelble, J. Polym. Sci., B8, 149 (1970).
24. D. G. Fesko and N. W. Tschoegl, Intern. J. Polymeric Mater., 3, 51 (1974).
25. T. Soen, M. Shimomura, T. Uchida and H. Kawai, Colloid and Polym. Sci., 252, 933 (1974).
26. G. Kraus and K. W. Rollman, J. Polym. Sci., Polym. Phys. Ed. 14, 1133 (1976).
27. G. Kraus, F. B. Jones, O. L. Marrs and K. W. Rollmann, J. Adhesion, 6, 235 (1977).
28. R. P. Zelinski and C. W. Childers, Rubb. Chem. Technol., 41(1), 161 (1968).
29. R. J. Ceresa, ed., "Block and Graft Copolymerization," John Wiley and Sons, N.Y. (1973).
30. M. Matsuo, et al., Polymer, 9, 425 (1968).
31. G. Kraus, K. W. Rollmann and J. O. Gardner, J. Polym. Sci., Physics Ed., 10, 2061 (1972).
32. T. Uchida, et al., J. Polym. Sci. A-2, 10, 101 (1972).
33. T. Hashimoto, et al., Macromolecules, 7, 362 (1974).
34. B. Gallot, Pure and Applied Chem., 38(4), 1 (1974).
35. E. Campos-Lopez, D. McIntyre and L. J. Fetters, Macromolecules, 6, 415 (1973).

36. J. C. Kelterborn and D. S. Soong, *Polym. Eng. Sci.*, 22(11), 654 (1982).
37. A. Todo, Hiroyukiuno, K. Miyoshi, T. Hashimoto and Hiromichikawai, *Polym. Eng. Sci.*, 17(8), 587 (1977).
38. T. Hashimoto, Y. Tsukahara and H. Kawai, *Polymer J.*, 15(10), 699 (1983).
39. E. J. Amix, O. J. Glinka, . C. Han, H. Hasegawa, T. Hashimoto, T. P. Lodge and Y. Matsushita, *Polym. Prepr. (ACS, Div. Polym. Chem.)*, 24(2), 215 (1983).
40. H. Hashimoto, M. Fujimura, T. Hashimoto and H. Kawai, *Macromolecules*, 14, 844 (1984).
41. T. Hashimoto, Y. Tsukahara and H. Kawai, *Macromolecules*, 14, 708 (1981).
42. C. I. Chung, H. L. Griesbach and L. Young, *J. Polym. Sci., Polym. Phys. Ed.*, 18, 1237 (1980).
43. C. I. Chung and J. C. Gale, *J. Polym. Sci., Polym. Phys. Ed.*, 14, 1149 (1976).
44. C. I. Chung and M. I. Lin, *J. Polym. Sci., Polym. Phys. Ed.*, 16, 545 (1978).
45. T. Hashimoto, M. Fujimura and H. Kawai, *Macromolecules*, 13, 1660 (1980).
46. E. V. Gouinlock and R. S. Porter, *Polym. Eng. Sci.*, 17, 535 (1977).
47. A. Ghijsels and J. Raadsen, *Pure Appl. Chem.*, 52, 1361 (1980).
48. G. Kraus and K. W. Rollmann, *J. Appl. Polym. Sci.*, 21, 3311 (1977).
49. G. Kraus and T. Hashimoto, *J. Appl. Polym. Sci.*, 27, 1745 (1982).
50. J. M. Widmaier and G. C. Meyer, *J. Polym. Sci., Polym. Phys. Ed.*, 18, 2217 (1980).
51. N. Sivashinsky, T. J. Moon and D. S. Soong, *J. Macromol. Sci. - Phys.*, 822(2), 213 (1983).
52. L. J. Fetters, E. M. Firer and M. Dafauti, *Macromolecules*, 10, 1200 (1977).

53. J. M. Hoover, T. C. Ward and J. E. McGrath, Polym. Prepr. (ACS, Div. Polym. Chem.), 25(1), 253 (1985).
54. W. P. Gergen, Kautsch Gummi, Kunstst., 37(4), 284 (1984).
55. E. R. Pico and M.C. Williams, Polym. Eng. Sci., 17, 573 (1977).
56. O. J. Chung, H. L. Griesbach and L. Young, J. Polym. Sci. Phys. Ed., 18, 1237 (1980).
57. T. Hashimoto, Y. Tsukahara and H. Kawai, J. Polym. Sci., Polym. Letters Ed., 18, 585 (1980).
58. Y. Tsukshara, N. Nakamura, T. Hashimoto, H. Kawai, T. Nagaya, Y. Sugiura and S. Tsuge, Polymer J., 12(7), 455 (1980).
59. G. Kraus and K. W. Rollmann, J. Polym. Sci., Polym. Phys. Ed., 14, 1133 (1976).
60. D. J. Meier (ed.), "Block Copolymers: Science and Technology," MMI Press Symposium Series Vol. 3, Hardwood Academic Publishers (1983).
61. P. A. Small, J. Appl. Chem., 3, 71 (1953).
62. A. E. Rheineck and K. F. Lin, J. Point Technol., 40, 611 (1968).
63. R. F. Fedors, Polym. Eng. Sci., 14, 147, 472 (1974).
64. J. Brandrup and E. H. Immergut, ed., "Polymer Handbook," Interscience, New York, N.Y., 1967.
65. C. Price, A. G. Watson and M. T. Chow, Polymer, 13, 333 (1972).
66. G. Kraus, F. E. Naylor and K. W. Rollmann, J. Polym. Sci., Part A-2, 9, 1839 (1971).
67. G. Kraus, in "Block Copolymers: Science and Technology," D. J. Meier (ed.), MMI Press Symposium Series Vol. 3, Hardwood Academic Publishers (1983).
68. G. Kraus, R. B. Jones, O. L. Marrs and K. W. Rollmann, J. Adhesion, 8, 235 (1977).
69. E. Riande and H. Markovitz, J. Polym. Sci. Phys. Ed., 13, 947 (1975).

70. P. J. C. Counsell and R. S. Whitehouse, "Tack and Morphology of Pressure Sensitive Adhesives," Ch. 4, p. 99.
71. F. H. Hammond, Jr., "Tack," in "Handbook of Pressure-Sensitive Adhesive Technology," D. Satas (ed.), Van Nostrand and Reinhold Co. Inc., N.Y. (1982).
72. J. J. Bikerman, J. Coll. Sci., 2, 163 (1947).
73. G. J. Crocker, Rub. Chem. and Tech., 42, 30 (1969).
74. J. R. Dann, J. Coll. and Inter. Sci., 32 (2), 302 (1970).
75. J. R. Huntsberger, Chem. and Eng. News, 82 (1964).
76. Y. Iyengar and D. E. Erickson, J. Appl. Polym. Sci., 11, 2311 (1967).
77. M. Toyama, T. Ho and H. Moriguchi, J. Appl. Polym. Sci., 14, 2295 (1970).
78. F. Wetzel, Characterization of Pressure-Sensitive Adhesives. ASTM Bulletin No. 221, 64 (1957).
79. G. Kraus and K. W. Rollmann, J. Appl. Polym. Sci., 21, 3311 (1977).
80. J. L. Gordon, J. Phys. Chem., 67, 1935 (1962).
81. F. H. Hammond Jr., Polyken Probe Tack Tester, ASTM Spec. Pub., 360 (1963).
82. M. Toyama, T. Ho and H. Moriguchi, J. Appl. Polym. Sci., 14, 2039 (1970).
83. W. A. Zisman, in "Contact Angle, Wettability and Adhesion," ACS Advances in Chemistry Series, (1964).
84. M. Toyama and T. Ho, Polym.-Plast. Technol. Eng., 2(2), 161 (1973).
85. C. A. Dahlquist, "Tack, Adhesion, Fundamentals and Practice," London: McLaren and Sons, Ltd. (1966).
86. L. H. Sharpe and H. Schonhorn, International Science and Technology, p. 26 (1964).
87. L. H. Sharpe and H. Schonhorn, in "Contact Angle, Wettability and Adhesion," ACS Advances in Chemistry Series No. 43 (1964).

88. J. R. Huntsberger, *Adhesives Age*, 21, 23 (Dec. 1978).
89. J. R. Huntsberger, *J. Adhesion*, 7, 289 (1976).
90. D. H. Kaelble, *Rub. Chem. and Tech.*, 45, 1604 (1972).
91. C. A. Dahlquist, "Tack, Adhesion, Fundamentals and Practice," London: McLaren and Sons, Ltd., 1966.
92. H. Kambe and K. Kamagata, *J. Appl. Polym. Sci.*, 13, 493 (1969).
93. G. Kraus, K. W. Rollmann and R. A. Gray, *J. Adhesion*, 10, 221 (1979).
94. Refer to Chapter V.
95. Refer to Chapter VII.
96. J. M. Widmaier and G. C. Meyer, *Polymer*, 18, 587, 1977.
97. Polymer Laboratories' Dynamic Mechanical Thermal Analyzer Instruction Manual, Polymer Laboratories Ltd., England (1982).
98. Dr. Ray Wetton, "Basic Theory and Applications of the PL-DMTA," paper presented at PL-DMTA Users Meeting in Philadelphia, Pennsylvania, Polymer Laboratories (1984).
99. ASTM Designation: D903-49, Standard Test Method for Peel or Stripping Strength of Adhesive Bonds, Volume 15.06, 29 (1984).
100. D. Satas, "Peel," in "Handbook of Pressure-Sensitive Adhesive Technology," D. Satas (ed.), Van Nostrand and Reinhold Co. Inc., N.Y. (1982).
101. J. Brandrup and E. H. Immergut, eds., *Polymer Handbook*, 2nd Ed., Wiley-Interscience, New York (1975).
102. J. J. Bikerman, *The Science of Adhesive Joints*, 2nd ed., N.Y.: Academic Press (1968).
103. Polymer synthesis and molecular characterization were carried out by Mr. Jim Hoover, a Ph.D. candidate in the Materials, Engineering and Science program at VPI & SU, under the guidance of Drs. James E. McGrath and Thomas C. Ward.
104. J. A. Filbey and J. P. Wightman, Annual Report Prepared for the Office of Naval Research, "The Surface Chemistry

of Adherends: The Characterization of Ti-6-4 Surfaces
Before and After Bonding with FM-300," October, 1984.

CHAPTER VI

ROLE OF MICROPHASE SEPARATION IN ADHESION, II

ABSTRACT

Surface chemistry and physical characterization studies covering a series of radial styrene (or substituted styrene) and isoprene block copolymers (25% by weight styrene) were conducted in order to interpret their performance as adhesives. The materials produced included the monomer combinations of p-tert-butylstyrene and isoprene, p-methylstyrene and isoprene, as well as styrene and isoprene. Radial, or star, block copolymer, topologies were generated using divinyl benzene monomer in the final stage of the polymerization. A sharp interfacial boundary between microphases does not necessarily exist in this series of radial block copolymers; rather, partial mixing of the component blocks may be possible in the interfacial region between the two thermodynamically incompatible microphases. This series is an excellent model system to study in terms of microphase separation - property response. Based on solubility parameter arguments and supported by dynamic mechanical and thermal mechanical analysis, p-tert-butylstyrene and isoprene, (TBS-I)*, was the most intermixed of the three systems, while the styrene and isoprene radial block copolymer, (S-I)*, had the highest degree of phase separation, while the p-methylstyrene and

isoprene radial block copolymer, (PMS-I)*, fell between these limits with its morphology.

The goal of this study was to investigate the above polymer series, characterizing the aspects which play major roles in adhesion, and relate this to the role of microphase separation in adhesive performance. The polymers in the series could vary in the degree of microphase separation as controlled by casting solvent in addition to reasons described above. Consideration was also given to the physical properties of the respective hard segments; furthermore, the hard segment polymer chain lengths differed.

The uniqueness of all investigated polymers lies in the combination of their tack and holding power, both necessary for pressure sensitive adhesives, PSAs, partially derived from the light crosslinked structure in the isoprene phase, as well as the systematic variation of the microphase separation.

BACKGROUND ON PRESSURE SENSITIVE ADHESIVES

Pressure sensitive adhesives (1-14) require a rather specialized and characteristic set of rheological properties; a PSA must adhere when brought into contact with a surface under light pressure and have sufficient cohesiveness that it can be peeled away from the surface without leaving a residue. It must have sufficient compliance to conform to surface rugosity, and it must undergo relaxation so that the

stored energy due to elastic forces will be dissipated before they can overcome the forces of adhesion. On the other hand, the PSA must exhibit an elastic cohesiveness and a resistance to flow under stress.

In a broad sense, the entire stress-strain behavior of a PSA can be treated as a creep phenomenon (14). The creep compliance of a pressure sensitive adhesive is significant with respect to tack, adhesion, peel and to resistance to failure in loading. Both retarded elastic processes and steady-flow viscosity play important roles, the former in tack, bonding and peel (short-term response), the latter in long-term creep. In some circumstances, the non-Newtonian viscosity of pressure sensitive adhesives must be taken into account. Much of the art of formulating or synthesizing PSAs is centered on juggling physical properties to give a balance of tack, peel adhesion, and cohesive strength (shear creep resistance). Each of these three topics (which often present conflicting requirements) is discussed below in more detail.

A. Tack

In the broadest sense, tack is the ability of the adhesive to bond rapidly under conditions of light contact pressure and relatively short contact times. Tack of an adhesive is both a surface chemistry and a rheologically related property. Pressure sensitive tack, and bond formation in general, ultimately involves molecular

interactions at the adhesive/adherend interface. A major driving force towards bond formation is the "work of adhesion," which is related to the surface energies of the adhesive and adherend. A PSA must also possess viscoelasticity so that the adhesive is able to conform to micro and macroscopic surface roughnesses to achieve the desired adhesive bonding (1-14).

While adhesive and adherend surface chemistries determine interaction energy at the molecular level, their bulk physical properties also determine the rate and extent of contact and ultimate bond strength developed (15). Pressure sensitive adhesives differ from other materials primarily because of the unique bulk rheological properties they possess. Rheological properties are the major factors in the phenomenon of pressure sensitive tack.

For good pressure sensitive tack and rapid bond formation, the adhesive should be easily deformed in the time frame of the bonding process. Dahlquist (16) found the 1-second compressive creep compliance of a pressure sensitive adhesive having good tack to be greater than or equal to 10^{-7} cm²/dyne. When the creep compliance is much less than 10^{-7} cm²/dyne, the degree of conformability to solid surfaces in reasonable times is not sufficient to effect the desired adhesive bonding (10,17-19). Toyama, Kraus and others (10,17,18,20,21) found comparable values for this 1-second compliance.

For good tack, the adhesive deformation in the bonding stage should be largely viscous in character. Energy absorbing fluid-like flow is desirable in order to relax the stress put on the adhesive as it is made to conform to the irregularities of the adherend. PSA tack is favored by a high ratio of viscous to elastic properties in time spans comparable to bonding times. Tack is actually measured as the force, or energy, to break a bond at a certain deformation. Good PSAs should also have a high modulus, or low compliance, at the temperatures and the strain rates and magnitudes imposed on them during rupture of the bond (2). Thus, the conflicting demands on a PSA are apparent and are closely related to the time scales of deformation.

While typical block polymers generally do not meet the compliance contact criterion (22), the addition of a sufficient quantity of a polydiene compatible tackifier plasticizes the composition and can cause D (1s) to exceed the minimum requirement (Figure 33). Effective tackifiers invariably are resins of relatively high T_g and so raise the T_g of the polydiene/tackifier phase; in isothermal creep data this manifests itself as a shift of the transition zone to longer times. The strain rate of the debonding step in typical tack measurements is of the order of 0.01s; on this time scale the compliance of the tackified polymer is much less than that of the pure polymer and energy dissipation is increased (14). The tackify resin acts as a plasticizer on

the time scale of the bonding process, and as a stiffening agent on the time scale of the debonding process. The PSA is more compliant than the rubber in the time scale of bond making, but less compliant in the time scale of bond breaking.

B. Peel

Peel adhesion is one of the important characteristics of pressure sensitive adhesives. This property is evaluated by measuring the tensional force required to remove the adhesive tape at a steady strain rate. The peel force depends on the adhesion, but it also depends on many other factors: viscoelastic properties of the adhesive, stiffness of the adherend, rate of separation, temperature, etc. (23).

Peel strengths for pressure sensitive adhesives depend strongly upon the rate of detachment and test temperature because these materials are viscoelastic in character. The mechanical properties of simple elastomers depend upon the rate of deformation and upon temperature in a well known way. In peeling rupture of adhesive joints, changes in the energy dissipated upon deformation are mainly responsible for the rate and temperature dependence of the observed strength (24).

Many PSAs exhibit a transition from cohesive to adhesive failure at low peel rates or at elevated temperatures. In

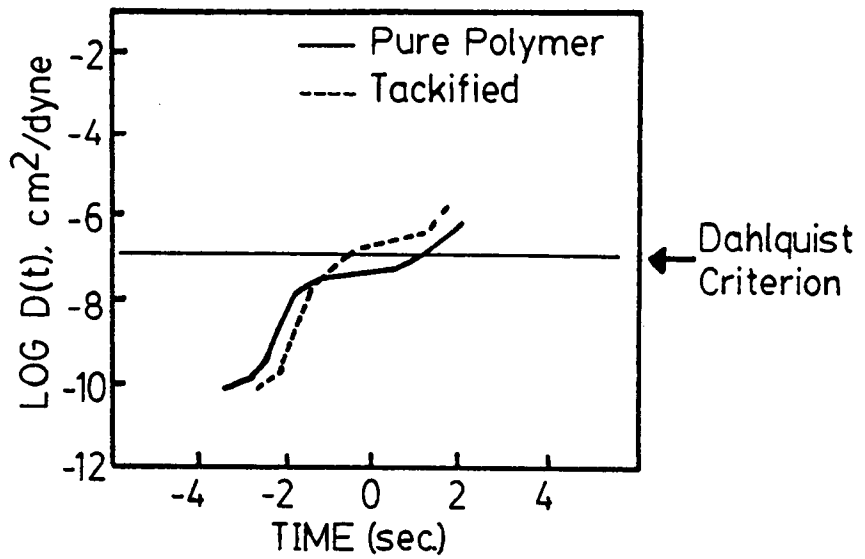


Figure 33. Creep response of a styrene-diene block copolymer, untackified (-) and tackified (--).

addition, a failure transition from a relatively steady to an oscillating peel force is observed at higher peel rates. Figure 34 (23) shows a generalized peel force versus peel rate curve. The dotted line at low peel rates represents the cohesive failure, the solid line to adhesive failure and the striped line at high peel rates represents the region of oscillating peel force. The peel force shows a decrease immediately after the transition to adhesive failure, then a steady increase with increasing peel rate and again a gradual decrease just before the onset of oscillations. The oscillations of peel force are of a nonrandom nature, and are generally referred to as "stick-slip" peel (23).

i. Transition from Cohesive to Adhesive Failure:

The response of the PSA to a stress has a strong viscoelastic nature. At low rates of force application or at elevated temperatures, the response is predominately viscous and the result is a cohesive failure. At higher rates of force application, the response becomes predominately elastic and failure becomes adhesive, or at least appears to take place at the adhesive/adherend interface.

The transition from cohesive to adhesive failure has been discussed by many researchers. McLaren and Seiler (25) have shown that low molecular weight polyvinyl acetate

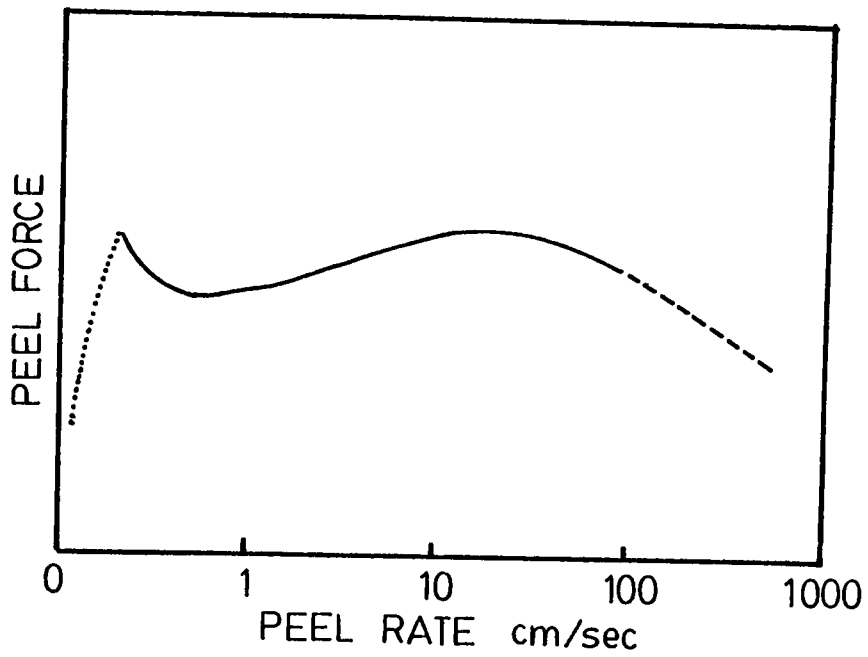


Figure 34. Generalized peel force versus peel rate behavior (23).

adhesives fail cohesively in a peel test, while higher molecular weight materials exhibit adhesive failure. Similar behavior was also observed at elevated temperatures. The peel force showed a continuous increase with increasing temperature. Huntsberger (26) has shown similar data for poly(n-butylmethacrylate) adhesives. When the temperature decreases, the relaxation rate becomes slower than the rate of force application, and the stress concentration occurs at the edges, resulting in an interfacial failure. Further lowering of temperature causes a decrease in peel force, because of a higher stress concentration.

The most cited author describing this transition from cohesive to adhesive failure in PSAs is Bright (23). Figure 35 (23) shows some of his data. Segment C of the curve represents clean adhesive failure. Segment B represents the transitional period which takes place in a narrow temperature range, and segment A represents a cohesive failure within the adhesive mass.

The connection between the peel rate and temperature in pressure sensitive adhesive tapes has been discussed by many authors (27,28). Hendricks and Dahlquist (27) show a construction of a master curve for a given temperature which allows prediction of the force versus time relation over a wide time range for measurements obtained at a convenient time range and at several temperatures.

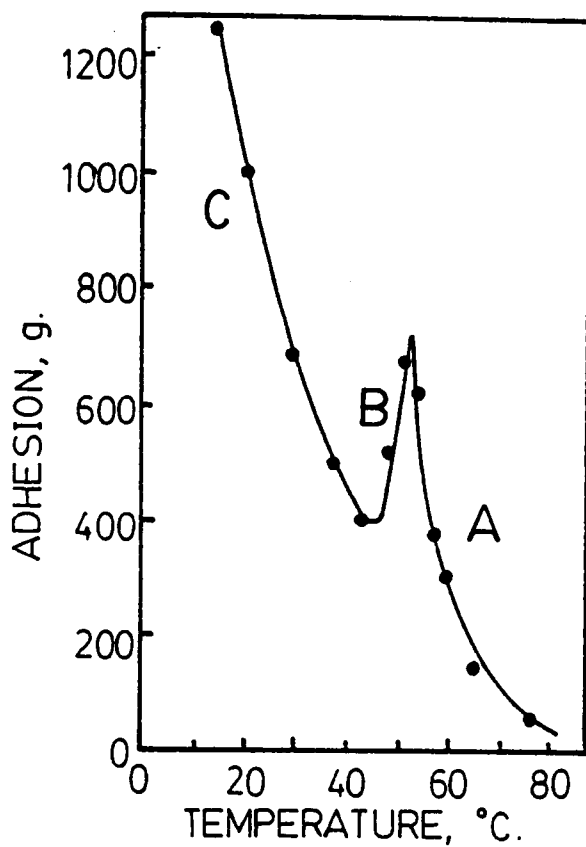


Figure 35. The dependence of peel force on temperature showing the transition from adhesive to cohesive failure (23).

It is generally agreed that the transition from cohesive to adhesive failure is associated with the transition from liquid-like (viscous) to rubber-like (elastic) behavior (29,30). Other possible mechanisms have been discussed by Gent and Petrich (30). That the failure mode transition is due to a change from a viscous to an elastic response is supported by the fact that crosslinked adhesives, which do not exhibit liquid flow, do not fail cohesively at low peel rates. Gent and Petrich also point out that the change from cohesive to adhesive failure is not an inevitable feature of this transition at low peel rates. The liquid response is not absolutely necessary.

Gent and Petrich (23,30) discuss the quantitative treatment of peel at low peel rates. The peeling force P , depends on the deformation energy of the polymer up to the point at which the tension stress is large enough either to cause the adhesive to fail cohesively or separate from the substrate. The value of P is given by:

$$P = h \int_0^{\sigma_m} \sigma dE \quad (6.1)$$

where:

h = thickness of adhesive

E = strain in adhesive, normal to substrate

σ = stress in adhesive

σ_m = maximum stress obtained

Equation 6.1 is based on two assumptions: the substrate film is completely flexible, and the elements of the adhesive can be treated as independent.

ii. Transition to Oscillating Failure (28)

At high peel rates, a second transition is observed from a smooth adhesive failure to a failure in which the peel force is oscillating in a nonrandom manner. The peel force versus peel rate curve has a negative slope in that area.

This behavior has been observed and discussed by many researchers. In pressure sensitive adhesives, it has been discussed by Hendricks and Dahlquist (27). This transition has been attributed to a change from elastic to glassy response, to localized plastic yielding (31), or to storage of elastic energy in the adhesive or in the substrate. Oscillations are generally connected with energy storage and the non-randomly oscillating peel force is explained as a result of storage of energy elastically until it is released by a sudden failure (32,33).

PSAs are viscoelastic materials, the viscous component decreases at higher rates of deformation. Therefore, it is expected that less elastic adhesives should exhibit the transition to nonrandomly oscillating peel force at higher peel rates than crosslinked or more elastic materials.

During the peeling of an adhesive tape from a rigid substrate, the force necessary and the mode of separation are strongly dependent on the bulk viscoelastic response of the adhesive. However, two other important contributions include: the effect of the backing material, and thermodynamic surface energy, arising from dispersion forces or chemical bonds acting across the interface (34).

The energy dissipated within the adhesive and the energy dissipated within the stripping member upon peeling of an adhesive tape from a rigid substrate are not wholly independent; and they are directly connected with the thermodynamic surface energy. The greater the true surface energy of adhesion, the greater the deformations generated in the adhering materials and the greater the dissipation of mechanical energy within them (13).

In addition, there are numerous other physical and chemical factors that affect the peel forces for elastomers adhering to rigid substrates. They include: the thickness of the adhesive layer (13,35-40) and of the adhering backing (41), the presence of chemical bonds between elastomer and the substrate, contact time (42,43), temperature (43-45), peel angle (46,47), etc.

C. Long-Term Creep - Shear Creep Resistance (14)

When shearing stresses are small and the rate of creep is very slow, the creep rate depends primarily upon the

steady-flow, zero shear rate viscosity, η_0 , of the PSA. If the shearing stresses are high and the rate of shear correspondingly high, the viscosity may vary as the shear rate changes (non-Newtonian viscosity). Factors that determine η_0 are generally the same in PSAs as in polymers in bulk form.

The steady flow zero shear rate viscosity of a polymer is strongly dependent on the molecular weight. Measurements on series of monodisperse homopolymers have shown that η_0 varies as the 3.4 power of the molecular weight if one is above a critical value of about 15,000 g/mole. Thus, a small increase in molecular weight can produce a significant improvement in capacity to support a load. Since the ability of a pressure sensitive adhesive to sustain loads for long times is directly proportional to its steady-flow viscosity, the significance of molecular weight is readily apparent. A small fraction of high molecular weight material can make a substantial contribution to creep resistance, markedly increasing the steady-flow viscosity and the creep resistance. The steady-flow viscosity is highly dependent upon molecular weight. Consequently, long-term creep can be greatly reduced by crosslinking, both chemical and physical.

i. Chemical Crosslinks

An obvious way to raise the steady-flow zero shear rate viscosity and increase the creep resistance of a PSA is to

take advantage of crosslinking. However, chemical crosslinking must be done under controlled conditions, because "overcure" can result in a loss of tack and adhesion.

ii. Physical Crosslinks

The concept of entanglement molecular weight has been introduced into the theory of long-term compliance and steady-flow viscosity of polymers. Long, linear, flexible polymers are believed to become entangled in interlinked loops which behave as pseudo-crosslinks, which, though they will eventually disentangle under stress, contribute long retardation times and high steady-flow viscosities. The contribution to high steady-flow viscosity and creep resistance will depend upon the number of entanglements per molecule.

Copolymerization of monomers having bulky aliphatic ether or ester group with monomers which provide hydrogen bonding, ionic bonding, or acid-base exchange has an effect on compliance similar to that of increasing the prevalence of chain entanglement, thereby raising the holding power of PSAs. The groups that enhance chain interaction generally raise the glass transition temperature. This will shift the whole mechanical spectrum such that the compliance is reduced at all time intervals of stress application. This can result in insufficient tack at room temperature, and poor peel

adhesion, if the introduction of the strongly interacting groups is not done in a controlled manner.

The ABA type of block copolymers provide physical crosslinking and control of polymer structure and molecular weight. The perfection of the network structure and the high level of chain anchoring provided by the complete incorporation of A blocks into separate glassy domains within the rubbery B matrix, gives rise to high shear resistance; generally at the expense of tack and adhesion (14,22).

The outstanding feature of styrene-diene block polymers in PSA formulations is their excellent resistance to adhesive creep. Shear holding power increases with polymer styrene content and molecular weight, the polystyrene domain structure effectively inhibits viscous flow at temperatures sufficiently below T_g of the styrene blocks (22).

INTRODUCTION

In contrast to the styrene (and substituted styrene) and isoprene radial block copolymer series investigated in Chapter V (48), the materials studied in the present investigation were, in general, inherently "low" tack and "high" shear resistant adhesives. The star block copolymers were virtually free of diblock impurities as shown by GPC and possessed a well-defined number of branches. The chain anchoring provided by the incorporation of polystyrenic blocks into separate glassy domains within the rubbery

polyisoprene matrix led to an increase in the creep resistance of the radial polymer series at the expense of tack and adhesion.

The present investigation consists of two parts. Part I deals with the evaluation of the role of microphase separation in fundamental adhesive performance, in terms of surface and bulk polymer properties, similar to the treatment in Chapter V (48). Part II addresses the evaluation and treatment of the overall adhesive performance, tack, peel and shear creep resistance, as a creep phenomenon, based on the characteristic time responses of the materials.

EXPERIMENTAL

A. Synthesis and Characterization (51)

The styrene (and substituted styrene) and isoprene radial block copolymer series was prepared by the method described in Chapter V (49). The star block copolymers were virtually free of diblock impurities (2-3% by weight) and possessed a well-defined number of branches. Size exclusion chromatography, GPC, and molecular weight determinations indicate 8-10 arms. Figure 36 is a GPC chromatogram of the p-tert-butylstyrene and isoprene radial block copolymer possessing an average number of arms of 8-10 and 2-3% by weight of residual diblock. Details on the determination of the molecular weight, the calculation of the number of arms

per radial polymer, and the calculation of the percent of residual diblock present after the coupling reaction to produce the radial topology are described in Chapter V (49).

B. Characterization of Bulk Polymer Properties

Isochronal dynamic mechanical measurements were made in the tensile mode with a Polymer Laboratory Dynamic Mechanical Thermal Analyzer (PL-DMTA). The measurement frequency was 1 Hz and the heating rate was 5°C/minute (48).

C. Surface Characterization

Surface characterization included the measurement and evaluation of the critical surface tension of the polymers as described in Chapter V (48). Take-off angle dependent ESCA studies to check surface homogeneity were also utilized. These studies were conducted using a Kratos XSAM 800 x-ray photoelectron spectrometer with a MgK x-ray source. The take-off angle was varied from 10° to 30° to 90°. Polymer films used for surface characterization were spin coated from 2 weight % polymer solutions. The polymer films were ca. 1000 Å thick, as measured by interferometry, and of uniform thickness.

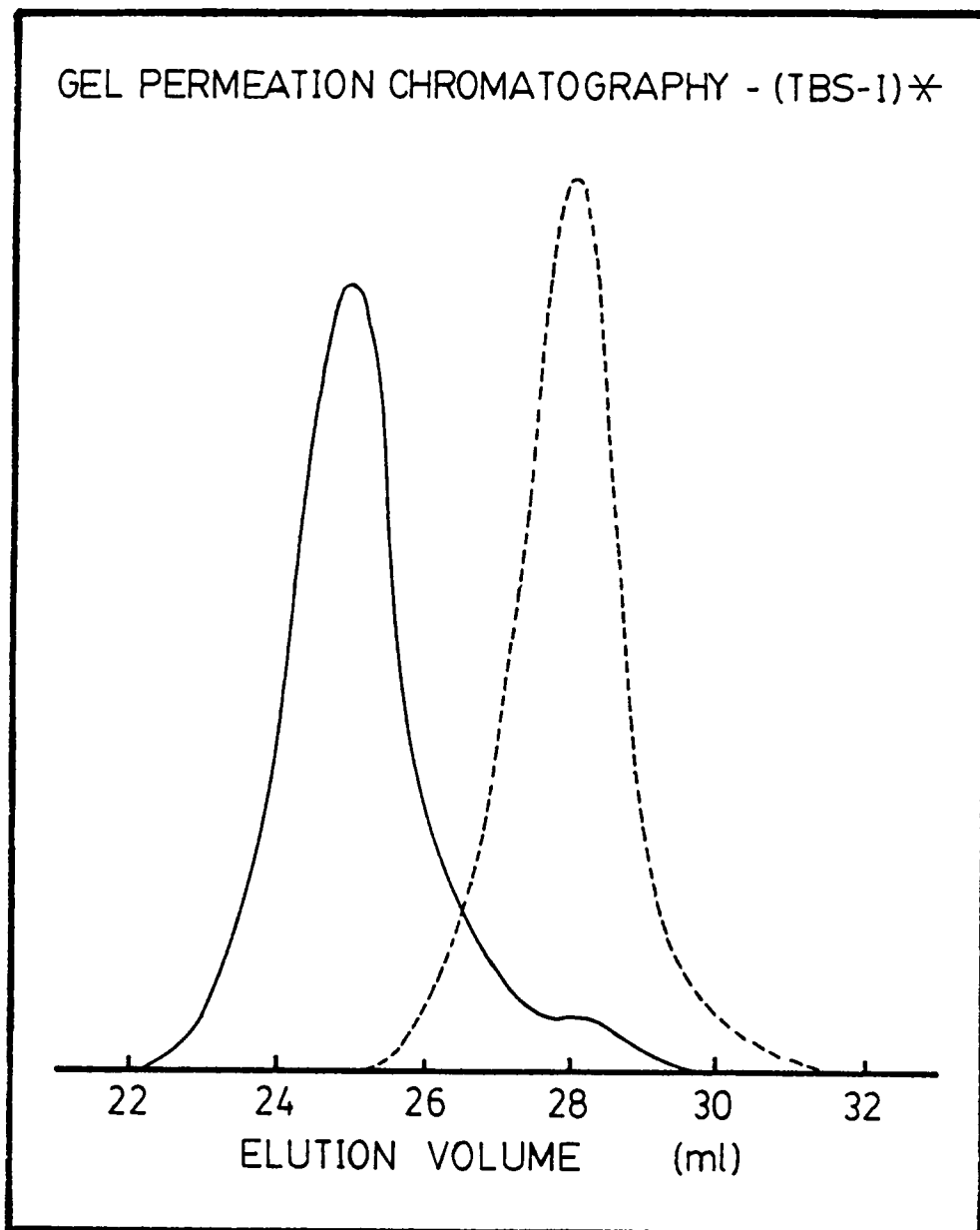


Figure 36. GPC trace of p-tert-butylstyrene and isoprene block copolymer. Diblock copolymer (...) prior to linking with DVB and radial block copolymer (—) after linking reaction (51).

D. Adhesive Performance Testing

A 180° peel test, in close agreement with an ASTM test (49) was conducted. The peel test was done at room temperature at peel rates ranging from 0.05 mm/minute to 1000 mm/minute. The details of adhesive preparation the adherend pretreatment and the bonding procedure are described in Chapter V (48). For the studies presented in the current chapter, two different application pressures were used: 8 psi and 1000 psi. Where the application pressure was 8 psi, the application of the adhesive tape to the Ti 6-4 adherend was carried out as described below.

1. Gently match the previously prepared adhesive tape to the pretreated bond area of the Ti 6-4 coupon.
2. Apply a rubber layer, weighted by a 2 kg weight, over the bond area at a rate of 1 cm/second.
3. Repeat step 2 three times for each bonded specimen.

RESULTS AND DISCUSSION

A. Polymer Characterization

Table 9 contains the characterization data of the star block copolymers synthesized for this work. The p-tert-butylstyrene, p-methylstyrene, and styrene and isoprene radial block polymers are 25% (weight) styrenic

block - 75% hydrocarbon block, with a hard block $\langle M_n \rangle$ of around 25,000 g/mole. The linking reaction was sufficiently effective so as to lead to virtually complete coupling. The star block copolymers were virtually free of diblock impurities and possessed a well-defined number of branches.

B. Part I: Surface and Bulk Polymer Characterization Related to Adhesive Performance

Surface chemistry and bulk physical properties of adhesives are of major importance in ultimate adhesive performance (40). Adhesive surface chemistry plays a large role in bond formation, since bond formation ultimately involves interactions at the adhesive/adherend interface; the physical properties of the adhesive also determine the rate and extent of contact, and the adhesive bond strength.

The styrene (and substituted styrene) and isoprene radial block copolymers investigated in Chapter V were, in general, inherently "high" tack and "low" shear creep resistant materials. The polymers contained 20-30% by weight residual diblock as an impurity, which served to "plasticize" the compositions, and possessed, on the average, 3-6 branches per star polymer. Results of investigations in Chapter V showed that high peel strengths resulted when the styrene (and substituted styrene) and isoprene radial block copolymers were solution cast from cyclohexane, due to the

Table 9. Characterization of Series C Radial Block Copolymers.

	<u><Mn> of Hard Block</u>	<u><# Arms></u>	<u>δ (cal/cm³)^{1/2} Hard Block</u>
(S-I)*	24100	8-10	9.2
(PMS-I)*	23500	8-10	8.8
(TBS-I)*	23700	8-10	8.12

preferential solvation of polyisoprene. The study also indicated that of the three polymers the styrene and isoprene radial block copolymer morphology was most affected by the choice of casting solvent, due to the incompatibility of the polystyrene and polyisoprene microphases. Guided by the above results, the present study focused on the following five polymer/solvent pairs: (TBS-I)* as cast from cyclohexane, (PMS-I)* as cast from cyclohexane, (S-I)* as cast from cyclohexane, (S-I)* as cast from toluene and (S-I)* as cast from dichloroethane. In the present study, the star block copolymers were virtually free of residual diblock material and possessed a well-defined number of branches.

i. Surface Characterization

The critical surface tension, γ_c , was measured for the styrene and isoprene radial block copolymer films cast from each of the three solvents: cyclohexane, toluene and dichloroethane. The values of the critical surface tension are listed in Table 10. The critical surface tension values for the three radial block polymers prepared by solution casting from cyclohexane were evaluated in Chapter V (48). Any differences that may result between the two studies could possibly be attributed to the redistribution of the total styrenic content over a larger number of blocks in the case of the radial copolymers possessing an average number of arms of 8-10 as opposed to 3-6.

Table 10. Critical Surface Tensions.

	γ_c (dynes/cm)
(S-I)*/Cyclohexane	30.1
(S-I)*/Toluene	31.0
(S-I)*/Dichloroethane	32.3

The extent of contact between adhesive and an adherend can depend on their relative surface energies (12,13). Adhesives with surface tensions less than the adherend's critical surface tension are expected to wet and spread, but this is also highly dependent on polymer viscoelasticity. The radial polymers are of hydrocarbon compositions, therefore, they naturally have low surface energies. The radial polymers having low surface energies are expected to exhibit good tack to a wide variety of adherends, including Ti 6-4 which is a high energy surface.

Angular dependent ESCA studies on the five polymer/solvent pairs revealed that there was no significant surface migration of a given phase from bulk to surface. Angular dependent ESCA experiments were also conducted on the respective homopolymers, which were used as controls (For ESCA results, see Appendix A).

ii. Bulk Polymer Characterization and Adhesive Performance

(S-I)*, (PMS-I)* and (TBS-I)* as Cast from Cyclohexane: A close connection exists between tack and adhesion, and viscoelasticity. The dynamic mechanical analysis of styrene, p-methylstyrene, and p-tert-butylstyrene and isoprene radial block copolymers solution cast from cyclohexane are shown in Figure 37.

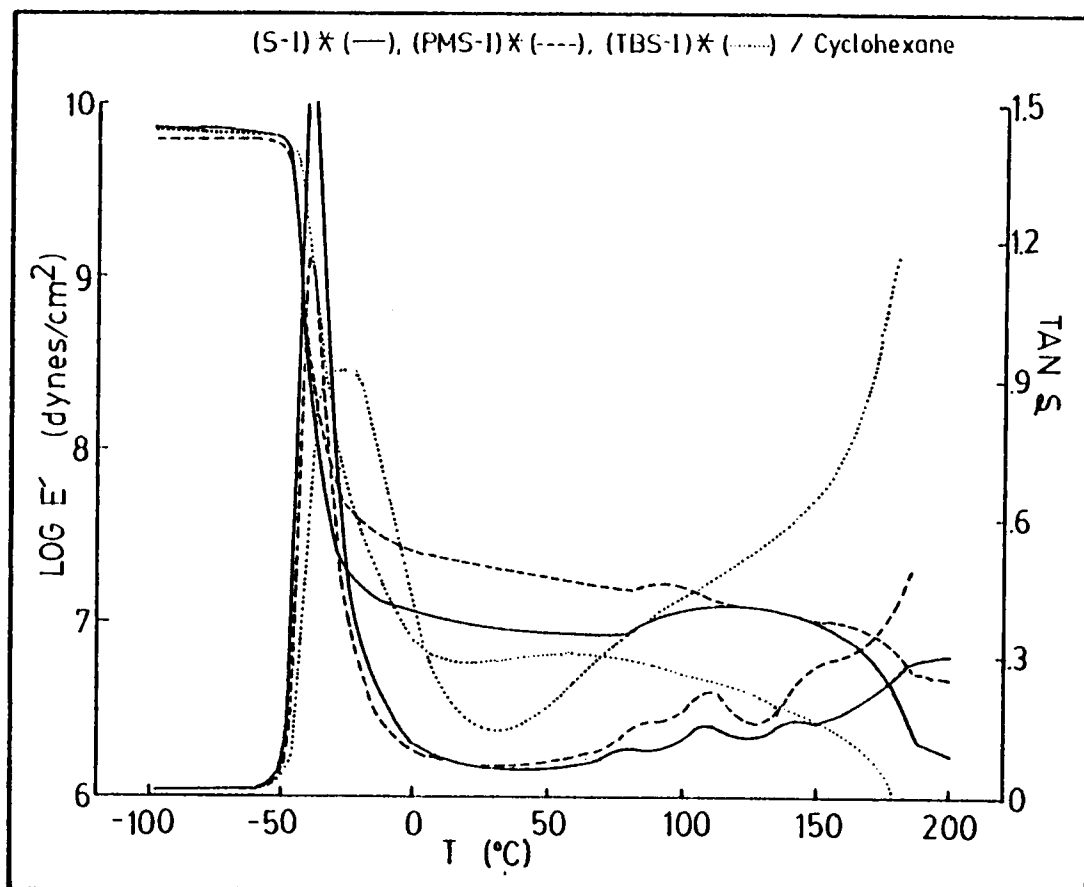


Figure 37. Viscoelastic properties of styrene, p-methylstyrene and p-tert-butylstyrene and isoprene radial block copolymers as cast from cyclohexane (1 Hz).

Examination of the $\tan \delta$ vs. temperature data in Figure 37 reveals that the styrene and isoprene and the p-methylstyrene and isoprene radial block copolymers exhibit a sharp low temperature (polyisoprene) dispersion very near that expected for the polyisoprene homopolymer. This observation is characteristic of a high degree of microphase separation. The upper (polystyrenic) transitions are not well resolved in either block copolymer; this appears to be due to morphological factors.

The styrene and isoprene, and p-methylstyrene and isoprene radial block copolymers do not meet the Dahlquist contact criterion. The room temperature tensile storage modulus (E') measured at 1 Hz is 1×10^7 dynes/cm² for (S-I)* and 3×10^7 dynes/cm² for (PMS-I)*. The measured peel strengths for the polymers (Table 11), where the application pressure was 8 psi, reflect their lack of appreciable tack. However, the polystyrenic domain structure of (S-I)* and (PMS-I)* effectively inhibits shear creep.

On the other hand, the p-tert-butylstyrene and isoprene radial block copolymer exhibits essentially a single broad primary dispersion centered at about -20°C , followed by a rising $\tan \delta$ as temperatures approach the melt region. The breadth and position of the low temperature transition and the lack of a distinct high temperature transition

Table 11. Peel Force¹ (lbs/in).

Solvent [$\delta(\text{cal/cm}^3)^{1/2}$]	Dichloroethane ($\delta = 9.2$)	Toluene ($\delta = 8.9$)	Cyclohexane ($\delta = 8.2$)
<u>Polymer</u> [$\delta(\text{cal/cm}^3)^{1/2}$]			
<u>(TBS-I)*</u> ($\delta = 8.1$)			9.3 + .8
<u>(PMS-I)*</u> ($\delta = 8.8$)			1.2 + .6
<u>(S-I)*</u> ($\delta = 9.0$)	.01	.08 + .05	4.1 + .3

¹ Application Pressure = 8 psi. Rate = 11.8 in/min. Temperature = 23°C.

corresponding to the poly(p-tert-butylstyrene) phase, are characteristic of a highly phase mixed system. The extent of compatibility effects the degree of microphase separation and hence the integrity of the domains, resulting in good tack and adhesion (Table 11), and poor shear resistance.

(S-I)* as Cast from Cyclohexane, Toluene and Dichloroethane: When block copolymers are cast from solution, the resulting polymer morphology, will in general, depend upon the solvent (17-19). Selective solvation of one block causes those chains to expand in solution, but leaves the chains from the other block in a collapsed state. This promotes the continuity of the block that is preferentially dissolved while casting, even though it may be the minor component.

The dynamic mechanical properties of the styrene and isoprene radial block copolymer reflect the change in the polymer morphology that results from solution casting the polymer from different solvents: cyclohexane, toluene and dichloroethane. It is apparent that polystyrene tends to be the more continuous phase when the solvent is relatively better for polystyrene than polyisoprene (Figure 38).

As Figure 38 reveals, when (S-I)* is cast from cyclohexane, which preferentially solvates polyisoprene, the upper (polystyrene) transition is not well resolved. However, as the casting solvent is increasingly better for

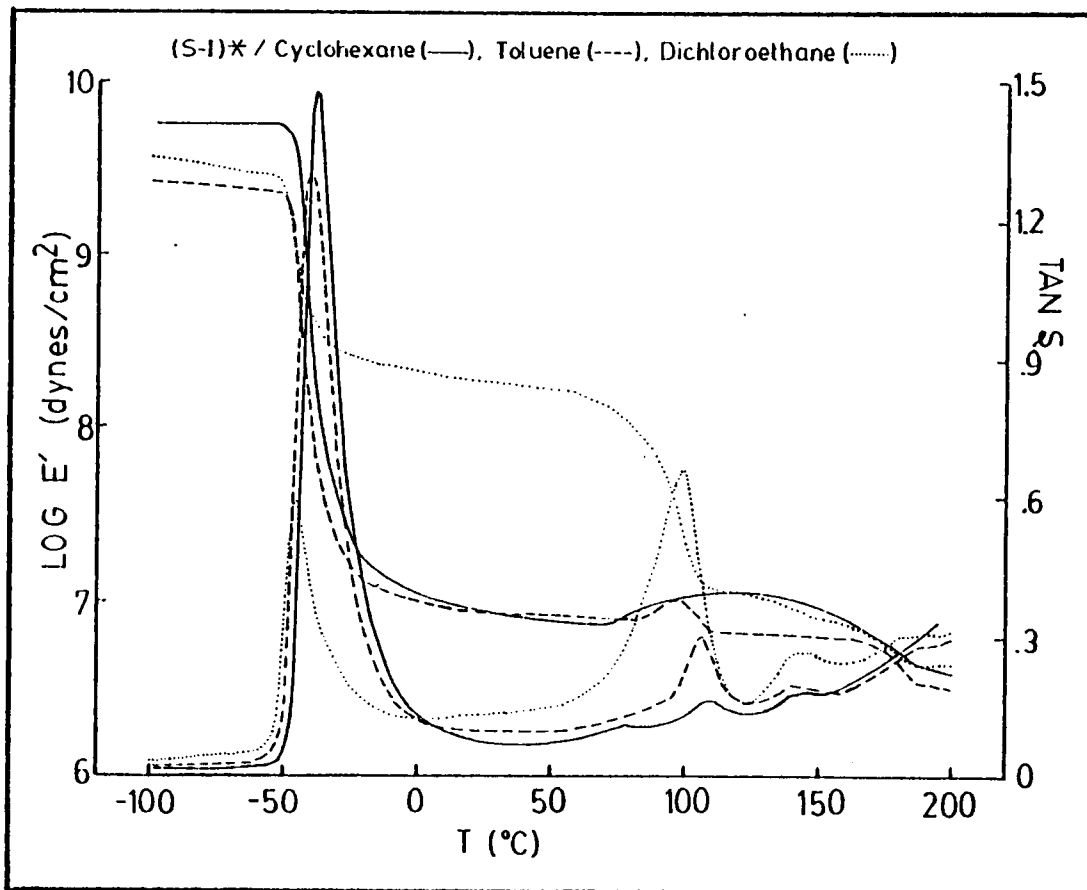


Figure 38. Viscoelastic properties of styrene and isoprene radial block copolymer are cast from cyclohexane, toluene and dichloroethane (1 Hz).

polystyrene there is a corresponding increase in the $\tan \delta$ dispersion of the polystyrene phase and decrease in the $\tan \delta$ dispersion of the polyisoprene phase. The value of the storage modulus between the two glass transitions is closely related to morphology; E' in the region increases concurrently with increasing connectivity of the polystyrene domains. In the case where (S-I)* was cast from dichloroethane, which preferentially solvates polystyrene, there is a one and a half order of magnitude increase in the plateau modulus value over that which occurs when (S-I)* is cast from cyclohexane or toluene; this is presumably a consequence of connectivity of the hard (polystyrene) phase.

As polystyrene tends to be the more continuous phase, when the casting solvent is relatively better for polystyrene than polyisoprene, there is more adherend-adhesive contact limitation; this results in low values of peel strength. As Table 11 reveals, when (S-I)* is cast from cyclohexane, which preferentially solvates polyisoprene over polystyrene, the adhesive possesses sufficient tack to result in some adhesion between the adhesive and the adherend. However as polystyrene tends to be the more continuous phase when (S-I)* is cast from toluene and dichloroethane, adhesion becomes contact limited resulting in near zero peel strength.

In general, the high level of chain anchoring provided by the polystyrenic domain formation and connectivity and the polymer radial topology gave rise to high shear resistant

adhesives at the expense of tack and adhesion. Whereas tack was low, adhesion can be developed by control of contact pressure. High peel strengths resulted for all five polymer/solvent pairs when the contact pressure was 1000 psi (Table 12). Special notice should be taken in the p-tert-butylstyrene and isoprene radial block polymer; the measured peel strength is unaffected by application pressure and absence of residual diblock.

In general, the styrene (and substituted styrene) and isoprene radial block polymers were inherently "low" tack and "high" shear resistant adhesives. The radial block copolymers were virtually free of diblock impurities and possessed a well defined number of branches. However, high peel strengths were measured for the p-tert-butylstyrene and isoprene radial block copolymer; the extent of phase compatibility resulted in good tack and adhesion. Furthermore, where tack was low, adhesion was developed by control of contact pressure.

C. Part II: Creep Phenomena

In a broad sense, the entire stress-strain behavior of a pressure sensitive adhesive can be treated as a creep phenomenon. Creep compliance of a pressure sensitive adhesive is significant in tack, peel and resistance to failure in loading. Both retarded elastic processes and

Table 12. Peel Force¹ (lbs/in).

Solvent [$\delta(\text{cal/cm}^3)^{1/2}$]	Dichloroethane ($\delta = 9.2$)	Toluene ($\delta = 8.9$)	Cyclohexane ($\delta = 8.2$)
<u>Polymer</u> [$\delta(\text{cal/cm}^3)^{1/2}$]			
<u>(TBS-I)*</u> ($\delta = 8.1$)			8.4 + .9
<u>(PMS-I)*</u> ($\delta = 8.8$)			5.7 + .7
<u>(S-I)*</u> ($\delta = 9.2$)	6.7 + .4	5.9 + .1	6.2 + .2

¹ Application Pressure = 1000 psi. Rate = 11.8 in/min.
Temperature = 23°C.

steady-flow viscosity play important roles, the former in tack and peel (short-term response), the latter in long-term creep (14). The design of block copolymers for use as pressure sensitive adhesives must be closely tied to morphology and the overall compatibility of the component blocks to give a balance of tack, peel adhesion and cohesive strength (shear creep resistance) (22).

Compressive creep compliance master curves have been constructed (50) for the styrene and isoprene (Figure 39) and p-tert-butylstyrene and isoprene (Figure 40) radial block copolymers (Chapter III) which were prepared by solution casting from cyclohexane. The master curves are utilized as a predictive tool for adhesive performance in relation to tack, peel and shear creep resistance. The master curves are interpreted in terms of the three PSA criteria of tack, peel and shear creep resistance below.

i. Tack

For good pressure sensitive tack and rapid bond formation, the adhesive should be easily deformed in the time frame of the bonding process (16). Dahlquist (16) found the 1-second compressive creep compliance of a pressure sensitive adhesive having good tack to be greater than or equal to 10^{-7} cm²/dyne. The compressive creep compliance master curves for (S-I)* and (TBS-I)* as cast from cyclohexane have been shifted, as dictated by their respective shift factor plots,

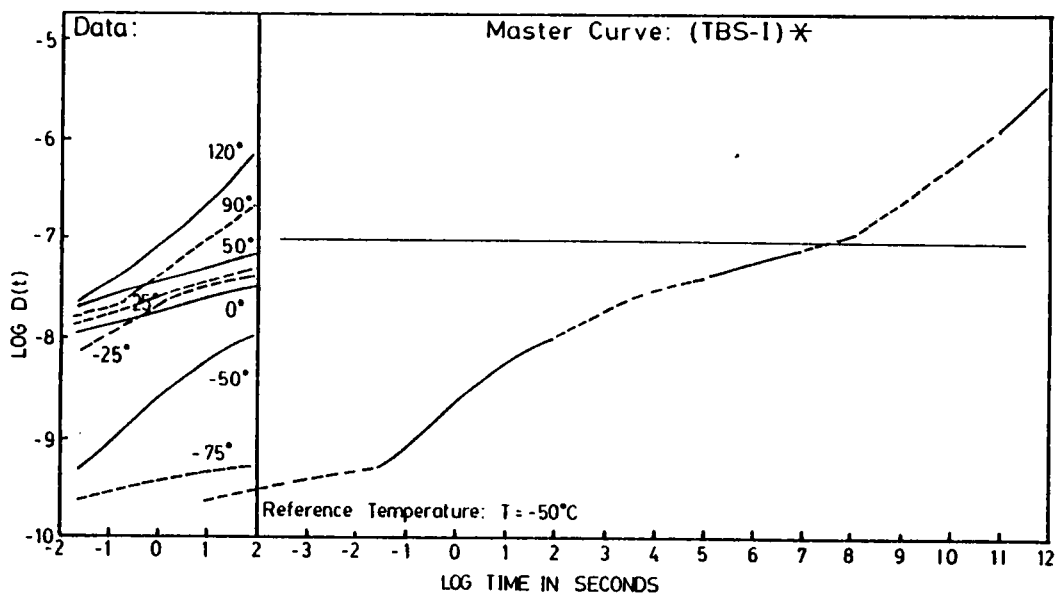


Figure 39. Compressive creep compliance data and master curve for p-tert-butylstyrene and isoprene radial block copolymers.

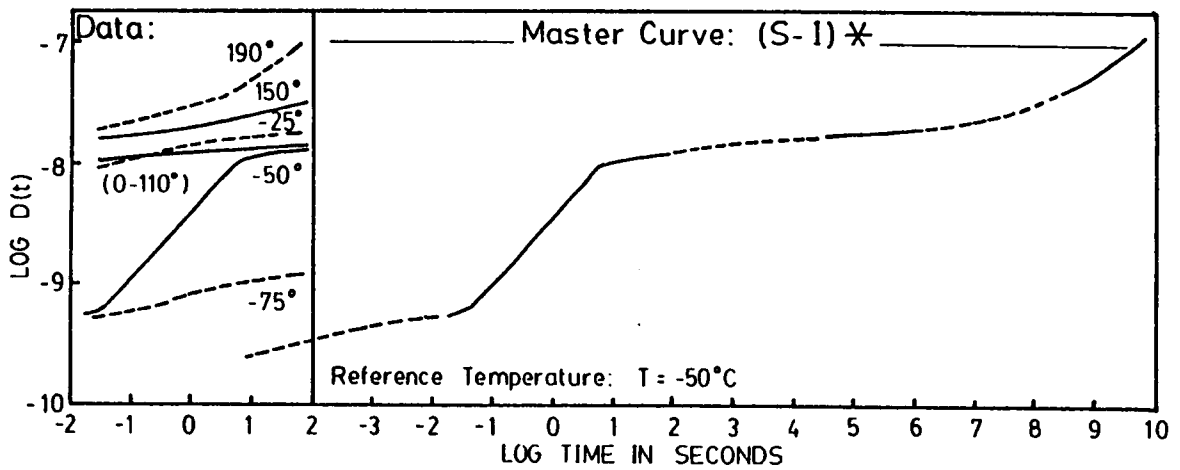


Figure 40. Compressive creep compliance data and master curve for styrene and isoprene radial block copolymer.

to represent the polymer response at 25°C. The styrene and isoprene radial block polymer does not meet the contact criterion, $D(1s)$ at 25°C is $1 \times 10^{-8} \text{ cm}^2/\text{dyne}$; as a result, the degree of conformability to solid surfaces was not sufficient to affect the desired adhesive bonding. On the other hand, $D(1s)$ at 25°C for the p-tert-butylstyrene and isoprene block polymer is very near $10^{-7} \text{ cm}^2/\text{dyne}$; therefore, the material is sufficiently deformable in the time frame of adhesive bonding to result in good adhesion.

ii. Peel

Peel strength depends on the adhesion, but it also depends on the viscoelastic properties of the adhesive. Peel strengths for pressure sensitive adhesives depend strongly upon the rate of detachment and test temperature because these materials are viscoelastic in character. The mechanical properties of simple elastomers depend upon the rate of deformation and upon temperature in a well known way. In peeling rupture of adhesive joints, changes in energy dissipated upon deformation are mainly responsible for the rate and temperature dependence of the observed strength (23).

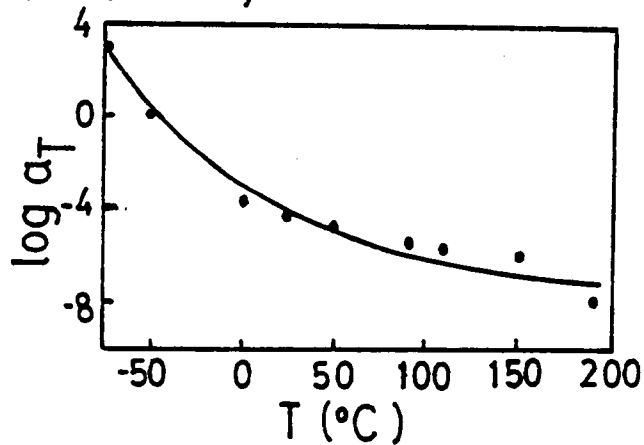
Examining the peel force as a function of pull rate (Figure 41) and the compressive creep compliance master curve (Figure 40) for the p-tert-butylstyrene and isoprene radial block polymer as solution cast from cyclohexane is

informative. At low pull rates, equivalent to long times of force application, the compressive creep compliance master curve at 25°C for (TBS-I)* reveals that the adhesive response is predominately viscous; the result is cohesive failure of the adhesive. Adhesive was visibly present on both the Ti 6-4 adherend and the mylar backing for the peel specimens pulled at the lower pull rates. Whereas, at the higher pull rates, corresponding to shorter times of force application, the master curve reveals that the (TBS-I)* polymer response is predominately elastic; the result is adhesive failure between the adhesive and the Ti 6-4 adherend.

Similar behavior can be illustrated by changing testing temperature. A change in temperature corresponds to a shift in the master curve along the long time axis as dictated by the shift factor plot (Figure 42). At high temperatures the response is predominately viscous and this would result in cohesive failure. As the temperature is decreased, the response becomes predominately elastic and failure would become adhesive.

On the other hand, the compressive creep compliance master curve at 25°C of the (S-I)* as solution cast from cyclohexane shows that the polymer exhibits predominately elastic response over the entire log time scale (Figure 39). The degree of conformability of the polymer is insufficient to result in good adhesive bonding, consequently, bond failure is strictly adhesive over the full range of pull

(S-I)* / Cyclohexane:



(TBS-I)* / Cyclohexane:

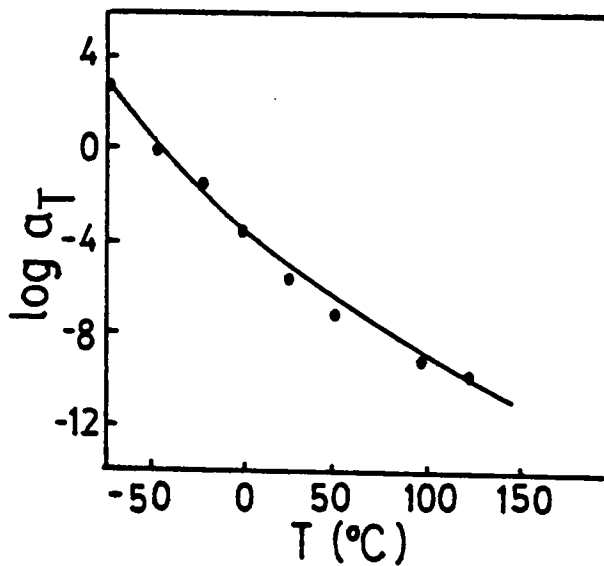


Figure 41. Shift factor plots for styrene and isoprene, and p-tert-butylstyrene and isoprene radial block copolymers.

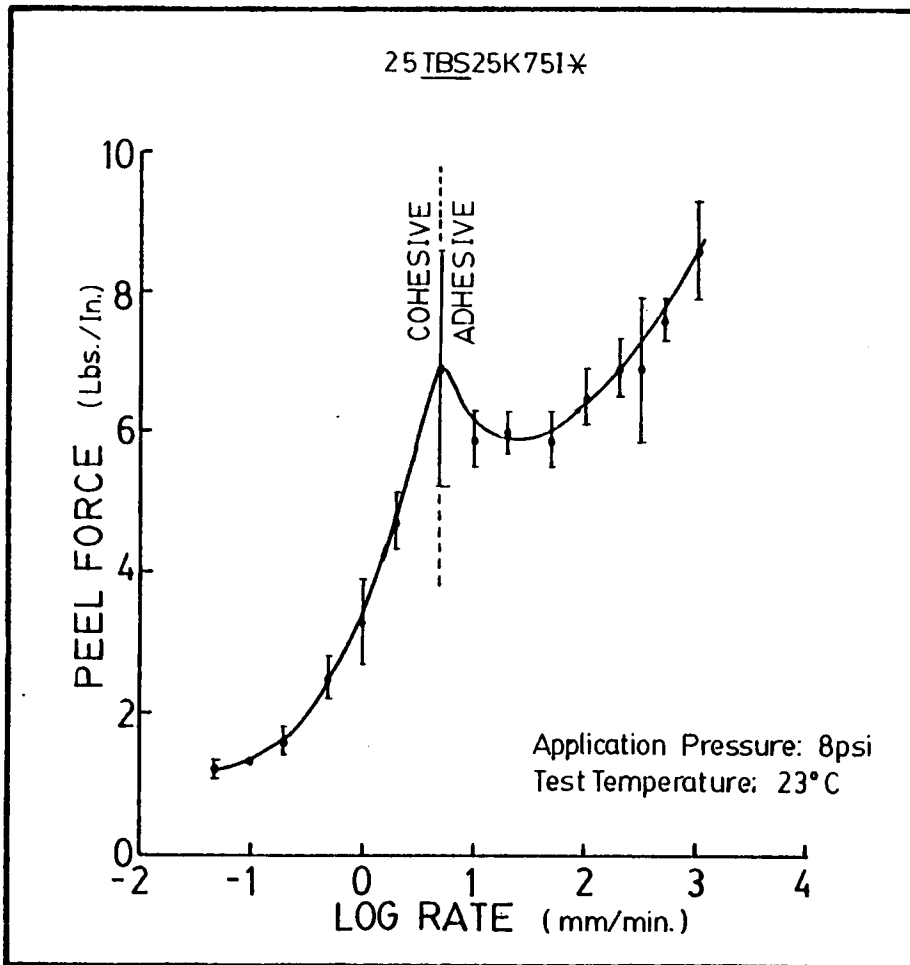


Figure 42. Peel force versus peel rate for p-tert-butylstyrene and isoprene radial block copolymer.

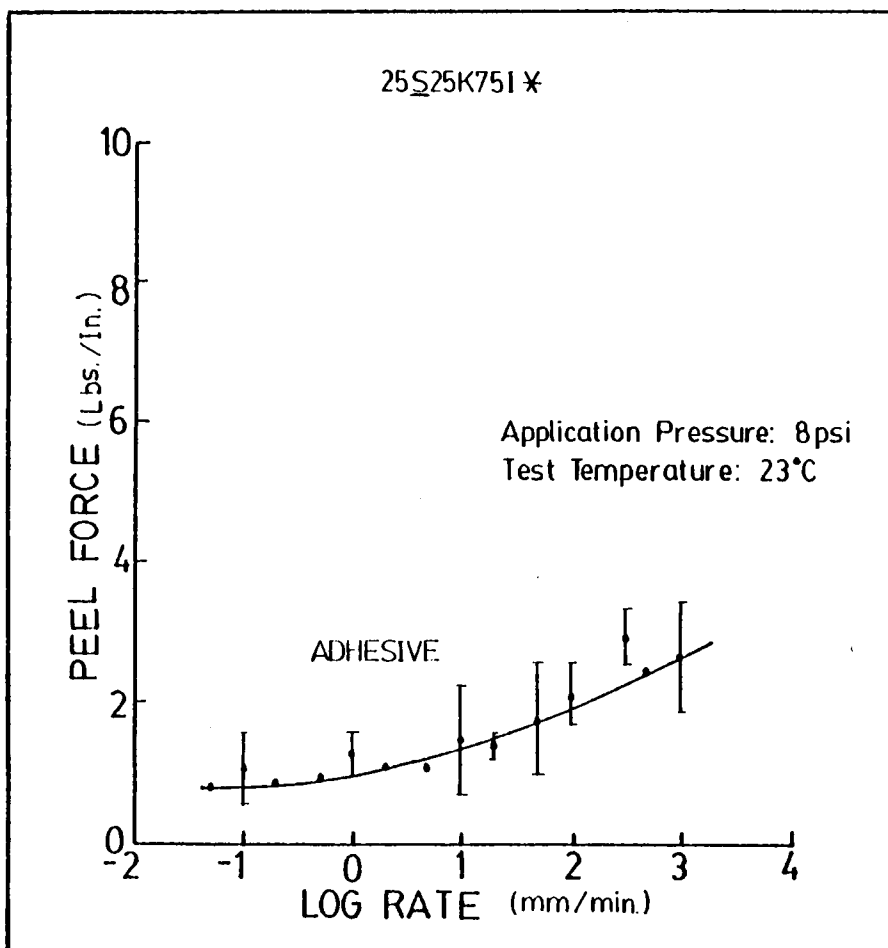


Figure 43. Peel force versus peel rate for styrene and isoprene radial block copolymer.

rates (Figure 43). The measured peel force is low because adhesive contact is limited.

iii. Shear Creep Resistance

Shear creep resistance is a long-term creep response (14). For the styrene and isoprene block copolymer, the polystyrene domain structure effectively inhibits viscous flow at temperatures below T_g of the styrene block. In contrast, the p-tert-butylstyrene and isoprene radial polymer exhibits some viscous behavior. However, the extent of phase compatibility affects the integrity of the domains resulting in poor shear resistance in the latter case.

Therefore, the overall adhesive performance of a pressure sensitive adhesive, the establishment and breakage of a bond and long-term creep resistance, can be evaluated based on the characteristic time response of the material. Furthermore, the compressive creep compliance master curves and the corresponding shift factor plots allow for predictions to be made on the adhesive performance of a material in terms of tack, peel and shear creep resistance over a full range of temperatures and times. However, strict quantitative correlations for block copolymer adhesives are more difficult to establish because of the thermorheological complexity and multiphase morphology of these systems.

REFERENCES

1. P. J. C. Counsell and R. S. Whitehouse, "Tack and Morphology of Pressure Sensitive Adhesives," Chapter 4, p. 99.
2. F. H. Hammond, Jr., "Tack," in "Handbook of Pressure Sensitive Adhesive Technology," D. Satas (ed.), Van Nostrand and Reinhold Co. Inc., N.Y. (1982).
3. J. J. Bikerman, J. Coll. Sci., 2, 163 (1947).
4. G. J. Crocker, Rub. Chem. and Tech., 42, 30 (1969).
5. J. R. Dann, J. Coll. and Inter. Sci., 32(2), 302 (1970).
6. J. R. Huntsberger, Chem. and Eng. News, 82 (1964).
7. Y. Iyengar and D. E. Erickson, J. Appl. Polym. Sci., 11, 2311 (1967).
8. M. Toyama, T. Ho, H. Moriguchi, J. Appl. Polym. Sci., 14, 2295 (1970).
9. F. Wetzel, Characterization of Pressure Sensitive Adhesives. ASTM Bulletin No. 221, 64 (1957).
10. G. Kraus and K. W. Rollmann, J. Appl. Polym. Sci., 21, 3311 (1977).
11. J. L. Gordon, J. Phys. Chem., 67, 1935 (1962).
12. F. H. Hammond Jr., Polyken Probe Tack Tester, ASTM Spec. Pub. 360 (1963).
13. M. Toyama, T. Ho, and H. Horiguchi, J. Appl. Polym. Sci., 14, 2039 (1970).
14. C. A. Dahlquist, "Creep," in "Handbook of Pressure Sensitive Adhesive Technology," D. Satas (ed.), Van Nostrand and Reinhold Co. Inc., N.Y. (1982).
15. D. H. Kaelble, Rub. Chem. and Tech., 45, 1604-1622.
16. C. A. Dahlquist, "Tack, Adhesion, Fundamentals and Practice," London: McLaren and Sons, Ltd., 1966.
17. G. Kraus, F. B. Jones, O. L. Marrs and K. W. Rollmann, J. Adhesion, 6, 235 (1977).

18. H. Kambe and K. Kamagata, *J. Appl. Polym. Sci.*, 13, 493 (1969).
19. G. Kraus, K. W. Rollmann and J. O. Gardner, *J. Polym. Sci., Physics Ed.*, 10, 2061 (1972).
20. G. Kraus and K. W. Rollmann, *J. Appl. Polym. Sci.*, 21, 3311 (1977).
21. G. Kraus, K. W. Rollmann and R. A. Gray, *J. Adhesion*, 10, 221 (1979).
22. G. Kraus, in "Block Copolymers: Science and Technology," D. J. Meier (ed.), MMI Press Symposium Series Vol. 3, Hardwood Academic Publishers (1983).
23. D. Satas, "Peel," in "Handbook of Pressure Sensitive Adhesive Technology," D. Satas (ed.), Van Nostrand and Reinhold Co. Inc., N.Y. (1982).
24. M. Toyama and T. Ito, *Polym.-Plast. Technol. Eng.*, 2 (2), 161 (1973).
25. D. D. McLaren and C. J. Seiler, *J. Polym. Sci.*, 4, 63 (1949).
26. J. R. Huntsberger, *J. Polym. Sci.*, A1, 2241 (1963).
27. J. O. Hendricks and C. A. Dahlquist, *Pressure Sensitive Adhesive Tapes, Adhesion and Adhesives*, Vol. 2, R. Houwink and G. Saloman (eds.), Amsterdam: Elsevier Publishing Co., 1967.
28. K. Kamagata, T. Saito and M. Toyama, *J. Adhesion*, 2, 279 (1970).
29. D. H. Kaelble, *J. Adhesion*, 1, 102 (1969).
30. A. N. Gent and R. P. Petrich, *Proc. Roy. Soc.*, A130, 433 (1969).
31. A. J. Duke, *J. Appl. Polym. Sci.*, 18, 3019 (1974).
32. G. Salomon, "Adhesion and Adhesives," R. Houwink and G. Saloman (eds.), Vol. 1, p. 119, Amsterdam: Elsevier Publishing Co., 1967.
33. S. S. Voyutskii, "Autoadhesion and Adhesion of High Polymers," p. 162, New York: Interscience Publishers, 1963.

34. M. Toyama, T. Ho, H. Nakatsuka and M. Ikeda, J. Appl. Polym. Sci., 17, 3495 (1973).
35. F. H. Hammond, ASTM Special Technical Publication No. 360, 123 (1963).
36. H-K. Chan and G. J. Howard, J. Adhesion, 9 279 (1978).
37. J. Johnston, Adhesives Age, 11(4), 20 (1968).
38. D. W. Aubrey, G. N. Welding and T. Wong, J. Appl. Polym. Sci., 13, 2193 (1969).
39. J. L. Gardon, J. Appl. Polym. Sci., 7, 625 (1963).
40. J. J. Bikerman, The Science of Adhesive Joints, 2nd ed., N.Y.: Academic Press (1968).
41. D. Satas and F. Egan, Adhesives Age, 9(8), 22 (1963).
42. C. A. Dahlquist, ASTM Special Technical Publication No. 360, 66th Annual Meeting Papers, Atlantic City, N.J., June 26, 1963.
43. F. Shoraka, Adhesion and Heat of Peeling of Pressure Sensitive Tapes. Ph.D. Thesis. State University of New York at Buffalo, May 1979.
44. R. J. Good, Aspects of Adhesion, D. J. Alner (ed.) Vol. 6, London: University of London Press, 1971.
45. K. Kamagata, H. Kosaka, K. Hino, and M. Toyama, J. Appl. Polym. Sci., 15, 483 (1971).
46. J. L. Gardon, Treatise on Adhesion, Vol. 1, R. L. Patrick (ed.) New York: Marcel Dekker, Inc. 1967.
47. D. H. Kaelble, Trans. Soc. Rheol., IV, 45 (1960).
48. Refer to Chapter IV.
49. ASTM Designation: D903-49, Standard Test Method for Peel or Stripping Strength of Adhesion Bonds, Volume 15.06, 29 (1984).
50. Refer to Chapter VI.
51. Polymer synthesis and molecular characterizations were carried out by Mr. Jim Hoover, a Ph.D. candidate in the Materials, Engineering and Science program at VPI&SU,

under the guidance of Drs. James E. McGrath and Thomas C. Ward.

CHAPTER VII

ROLE OF MICROPHASE SEPARATION IN ADHESION, III

ABSTRACT

Investigations were conducted on a series of hydrogenated forms of p-tert-butylstyrene and isoprene radial block copolymers (25% weight p-tert-butylstyrene) in order to evaluate their potential as adhesives. Hydrogenation of the isoprene phase converts the p-tert-butylstyrene and isoprene radial block polymer, (TBS-I)*, into essentially a p-tert-butylstyrene block plus an ethylene propylene alternating copolymer, overall having a radial structure. It is important that this operation converts a reasonably compatible pair of block components into a system likely to have a high degree of microphase separation.

The series is an excellent model system to study in terms of microphase separation-property response. The polymers in the series were found to vary in the degree of microphase separation as influenced by the degree of hydrogenation. Consideration was also given to the physical properties of the diene originating segment, having extreme compositions of polyisoprene and an ethylene propylene alternating copolymer as well as a number of partially unsaturated versions. The uniqueness of the investigated polymers lies in that it was possible to control tack and holding power, both necessary for pressure sensitive

adhesives, by controlling the degree of hydrogenation. The pressure sensitive adhesive properties of the polymers in this series are closely tied to the morphology and the overall compatibility of the component blocks as affected by the degree of hydrogenation.

INTRODUCTION

Block copolymers, ABA and $(AB)_x$, composed of non-crystallizable A and B block sequences form a two-phase, or a pseudo two-phase, texture in the solid state in which domains of one component are dispersed in a medium of the other component on a microscopic scale (1,2). Generally, there exists an interfacial region of an uncertain, somewhat fuzzy, thickness in which the incompatible sequences of A and B are intermixed in between the regions of pure A and B segments. The morphology and the arrangement of the two microphases are known to depend upon thermodynamic and molecular parameters (3-21) which affect the microphase separation of the block copolymers. Some of these are the chemical nature of the phases, the fraction of the A and B segments, preparation conditions of the films, the molecular weight of the block copolymers, and experimental conditions such as temperature and pressure histories.

Several studies of the mechanical properties of the block copolymers have also proposed existence of the interphase (22,26). The interphase can play an important

role on the mechanical properties of block copolymers, e.g., thermoplastic elastomers, in terms of Young's modulus, modulus of the rubber plateau, and its time and temperature dependencies, as well as flow behaviors. The same is equally true of adhesive compositions formulated from such systems. The design of block polymers for use as pressure sensitive adhesives (PSAs) is centered on the morphological uniqueness of these materials in terms of domain formation to give a balance of tack and adhesion, and holding power (shear creep resistance) (60).

Numerous studies (1,27-51) have been conducted on ABA block copolymers where A is polystyrene and B is polybutadiene or polyisoprene. The investigations have examined characteristic structural properties, the organization in spheres, cylinders, or lamellae, and the partial miscibility between the component blocks, known to depend on composition, preparation conditions of the films, molecular weight, and temperature. Kraus, et al. and others (74) have expressed the above in terms of their role in adhesion.

Few workers (52-56) have addressed the morphology of styrenic/diene block copolymers that results from modification of the chemical nature of the styrene and diene phases, either by replacement of polystyrene with a ring substituted styrenic polymer such as poly(p-tert-butyl styrene) or by a partial or full hydrogenation of the

polydiene in terms of eventual adhesive function. In the two previous chapters (57,58) some questions were answered as the chemical nature of the styrene phase was changed by replacement of polystyrene with a ring substituted styrenic polymer. The resulting polymer properties were analyzed in terms of their role in adhesive performance. In the present chapter the chemical nature of the isoprene phase of a p-tert-butylstyrene and isoprene radial block copolymer was modified by hydrogenation; the viscoelastic properties were examined, and adhesive qualities, particularly with respect to PSA potential, evaluated.

It has been demonstrated through a number of independent means in a previous paper (52) that the high miscibility of block copolymers of poly(p-tert-butylstyrene) with polydienes limits the degree of phase separation that can be conventionally achieved in more typical block copolymers, thus strongly influencing their physical properties. For example, Fetters, et al. (52), noted that hydrogenation of the polyisoprene block in triblock p-tert-butylstyrene and isoprene copolymers yields materials which exhibit tensile strengths comparable to the conventional SBS and SIS materials. This indicates that effective microphase separation occurs in the hydrogenated poly(p-tert-butylstyrene) and polyisoprene materials. Calculations of the respective solubility parameters also indicate that this should be the case.

Hydrogenation studies that enhanced phase separation of polystyrene and polybutadiene block copolymers have been conducted at Shell (54). Styrenic block polymers having an ethylene and butylene rubber (EB) midblock showed excellent properties. The high performance of these S-EB-S polymers was explained by a sharp phase separation between mid and end blocks.

In order to gain further insight into the role of microphase separation in overall adhesive performance of ABA and $(AB)_x$ block copolymers, a study was undertaken involving hydrogenation of a isoprene phase of a p-tert-butylstyrene and isoprene based radial block copolymer, (TBS-I)*. Hydrogenation of the isoprene phase converts the (TBS-I)* into essentially a block p-tert-butylstyrene and ethylene propylene alternating copolymer with a radial structure; thus, changing a reasonably compatible pair of components into a system of blocks of greater dissimilarity. By controlling the degree of hydrogenation it was possible to control the degree of microphase separation, as will be demonstrated below, and PSA behavior.

EXPERIMENTAL (73)

A. Synthesis and Characterization

The hydrogenated forms of the (TBS-I)*, containing 25% weight poly(p-tert-butylstyrene) having a number average

molecular weight of about 25,000 g/mole, were prepared by first synthesizing the (TBS-I)*, by a procedure described in Chapter IV (57). Then, following purging the system well with H₂, (53) a hydrogenation catalyst, a triethylaluminum nickel octanoate complex, was then added to the reactor, while maintaining 50 psi H₂ atmosphere. Aliquots of the sample were removed over time; the resulting polymers were isolated by precipitation in acidic methanol followed by a methanol wash and vacuum drying. FTIR was used to identify the degree of hydrogenation (Figure 44).

Figure 44 shows FTIR spectra of the parent p-tert-butylstyrene and isoprene radial block copolymer and a hydrogenated form. The notation is as follows: r = reference peak (1510 cm⁻¹), p = pendant 3,4-unsaturation of the polyisoprene originating block (1645 and 890 cm⁻¹) and b = backbone cis and trans 1,4-unsaturation (1665 and 830 cm⁻¹). In addition, the absorbance at 830 cm⁻¹ also has contributions from the poly(p-tert-butylstyrene) block.

The percent hydrogenation is calculated as described below. The absorbance peaks due solely to unsaturation in the polyisoprene phase (1665, 1645 and 890 cm⁻¹) are normalized with respect to the reference peak at 1510 cm⁻¹, first, for the unsaturated (TBS-I)* base polymer. This procedure is then repeated for the hydrogenated forms. The ratios of the normalized absorbance after hydrogenation to

FTIR SPECTRA OF 25TBS25K75I*

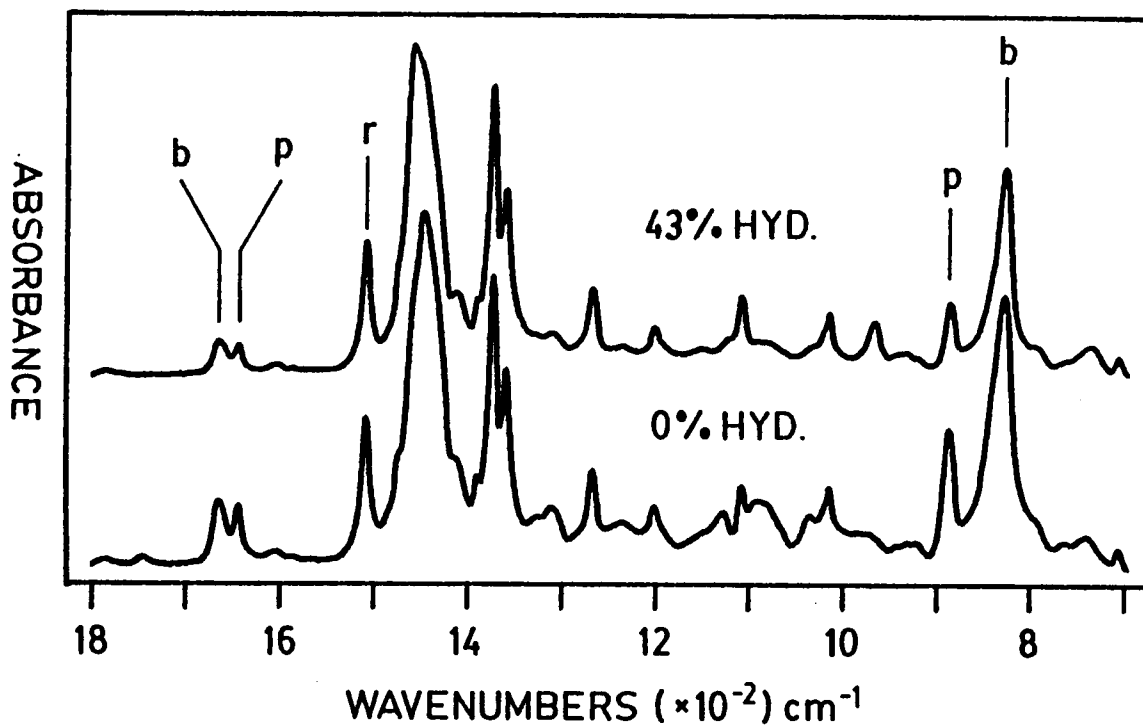


Figure 44. FTIR spectra of p-tert-butylstyrene and isoprene radial block copolymer and a hydrogenated form for determination of degree of hydrogenation (r=reference peak, b=backbone unsaturation, p=pendant unsaturation) (73).

that of the unsaturated (TBS-I)* base polymer for the respective peaks are added and divided by the number of peaks to give the percent hydrogenation. The results by FTIR agree very closely with those determined by NMR.

Size exclusion chromatography and molecular weight determinations of the parent (TBS-I)* polymer indicate 8-10 arms with the radial block polymer being virtually free of residual diblock (2-3 % by weight). FTIR and FT proton NMR analysis indicate that the polydiene microstructure consisted of 72% cis-1,4-, 22% trans-1,4- and 5% 3,4-polyisoprene.

B. Characterization of Bulk Polymer Properties

i. Dynamic Mechanical Thermal Analysis

Isochronal dynamic mechanical measurements were made in the shear mode and the tensile mode with a Polymer Laboratory Dynamic Mechanical Thermal Analyzer (PL-DMTA). Measurement frequency was 1 Hz and the heating rate was 5°C/minute.

ii. Thermal Mechanical Analysis

Thermal mechanical measurements were made in the penetration mode as a function of temperature with a Perkin Elmer Thermomechanical Analyzer System (TMS-2). The heating rate was 10°C/minute.

Polymer films for measurement were solution cast from 20 weight % solutions in cyclohexane. Solutions were poured

into teflon troughs and evaporated slowly at ambient temperature. After films were visibly dry, approximately 72 hours, they were vacuum dried at 60°C for 48 hours.

C. Adhesive Performance Testing

A 180° peel test, in close agreement with an ASTM test (59), was conducted on an Instron Model 1122. The peel test was done at room temperature and the pull rate ranged from 0.05 mm/minute to 1000 mm/minute.

Test specimens were prepared as described in Chapters V and VI. The casting solvent was cyclohexane and the application pressure was 8 psi.

RESULTS AND DISCUSSION

The parent (TBS-I)* polymer possessed an average of 8-10 arms, and the radial block polymer was virtually free of residual diblock (2-3 % by weight). The series of hydrogenated p-tert-butylstyrene and isoprene radial block copolymers included polymers containing 0%, 5%, 23%, 43%, 68% and 90% hydrogenation of the isoprene phase. The polymers were 25 weight % poly(p-tert-butylstyrene) of a number average molecular weight of 25,000 g/mole. The composition of the radial block polymers is such that the polymers have application as PSAs since the poly(p-tert-butylstyrene) is dispersed in a matrix varying from rubbery to plastic (73).

Dynamic mechanical analysis was conducted on a separate series of (TBS-I)* materials that varied in the number average molecular weight of the styrenic block. Four polymers were investigated; the "hard" block molecular weights were 10,000, 15,000, 20,000 and 25,000 g/mole. The viscoelastic properties of the four polymers (Figure 45) are essentially identical. Therefore, at a poly(p-tert-butylstyrene) block molecular weight of 25,000 g/mole used in the present investigation, apparently the critical molecular weight of poly(p-tert-butylstyrene) for domain formation has been exceeded. Fetters, et al. (52), reported the critical molecular weight of poly(p-tert-butylstyrene) for apparent domain formation to be 15,000 g/mole.

The study being presented is a result of a two part investigation. The first experiments (part I) defined the mechanical properties of the limits, p-tert-butylstyrene and isoprene radial block copolymer and p-tert-butylstyrene and ethylene propylene alternating copolymer. For this initial investigation, the hard block molecular weight was fixed at 15,000 g/mole, and the radial polymers possessed an average of 4-6 arms. These materials contained 5-10% by weight residual diblock by GPC. In part II, the degree of hydrogenation of the isoprene phase of the (TBS-I)*, having a hard block number average molecular weight of 25,000 g/mole, was systematically varied from 0% to 90%; the

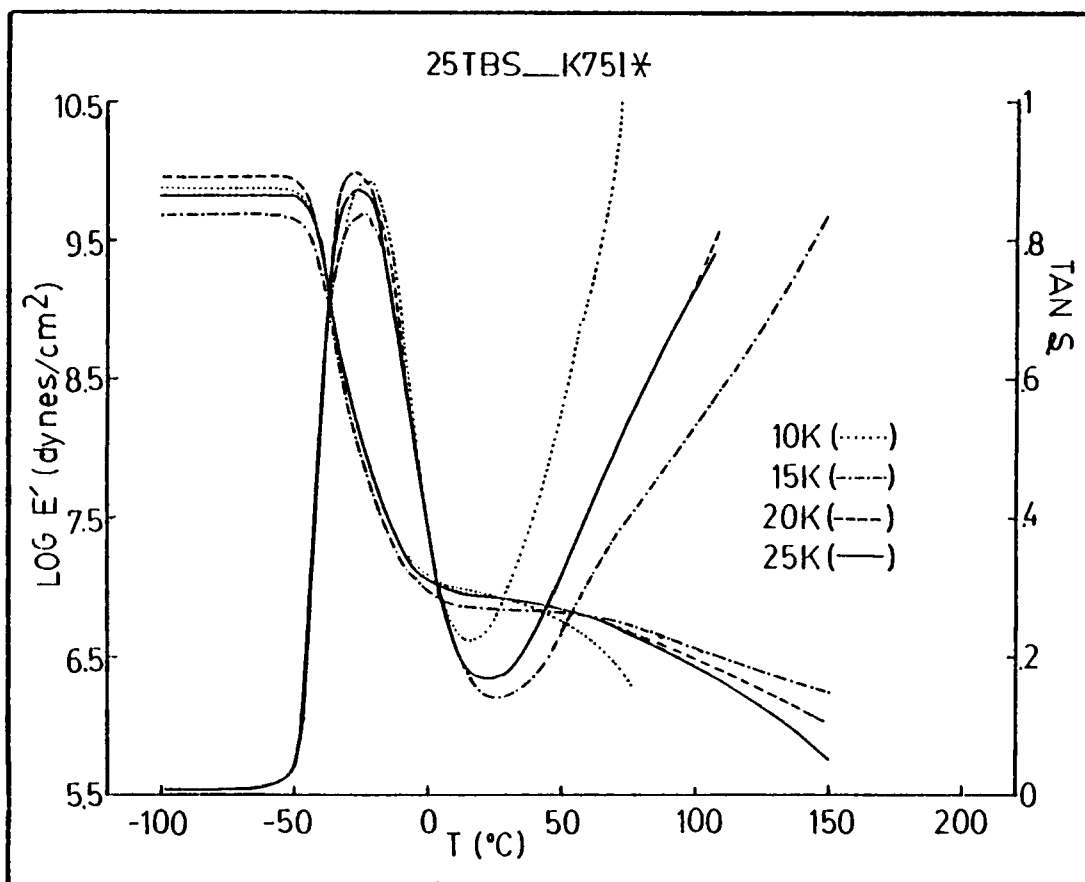


Figure 45. Viscoelastic properties of p-tert-butylstyrene and isoprene radial block copolymers having poly(p-tert-butylstyrene) molecular weights of 1.0×10^4 , 1.5×10^4 , and 2.5×10^4 g/mole (1 Hz).

resulting viscoelastic properties were examined and related to the overall adhesive performance of the material.

A. Part I

The dynamic mechanical (Figure 46) and thermal mechanical analysis (Figure 47) of the p-tert-butylstyrene and isoprene radial block copolymer, and the p-tert-butylstyrene and ethylene propylene alternating copolymer, reveal the effect of hydrogenation on the compatibility of the two components.

Figure 46 shows the shear storage modulus (G') and $\tan \delta$ as a function of temperature at 1 Hz for the two polymers. The (TBS-I)* $\tan \delta$ exhibits essentially a single broad primary dispersion at -20°C , followed by a rising $\tan \delta$ approaching the melt region. The breadth and position of the low temperature transition and the lack of a distinct high temperature transition, corresponding to the poly(p-tert-butylstyrene) phase, are characteristic of a highly phase mixed system.

Quantitative hydrogenation of the (TBS-I)* resulted in a narrowing and a shift to lower temperatures of the low temperature relaxation, a half order of magnitude increase in G' , and the appearance of a high temperature $\tan \delta$ dispersion. These changes suggest that demixing has resulted, upon hydrogenation, in more homogeneous or pure

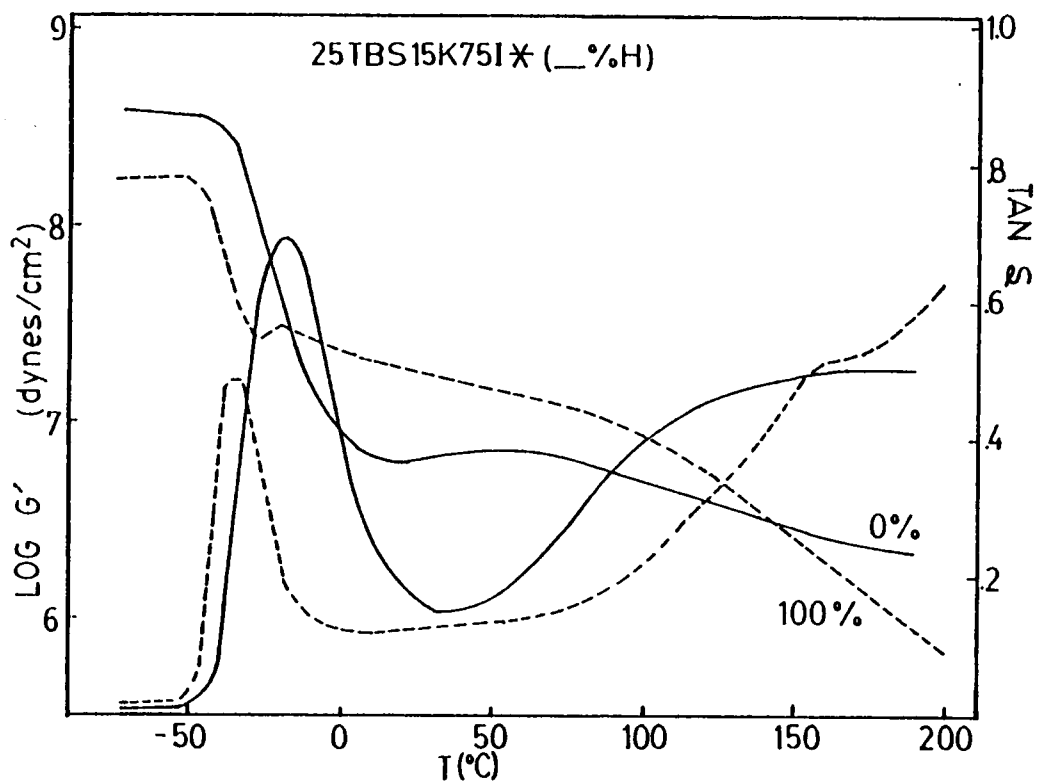


Figure 46. Viscoelastic properties of p-tert-butylstyrene and isoprene radial block copolymer, and p-tert-butylstyrene and ethylene propylene alternating copolymer (1 Hz).

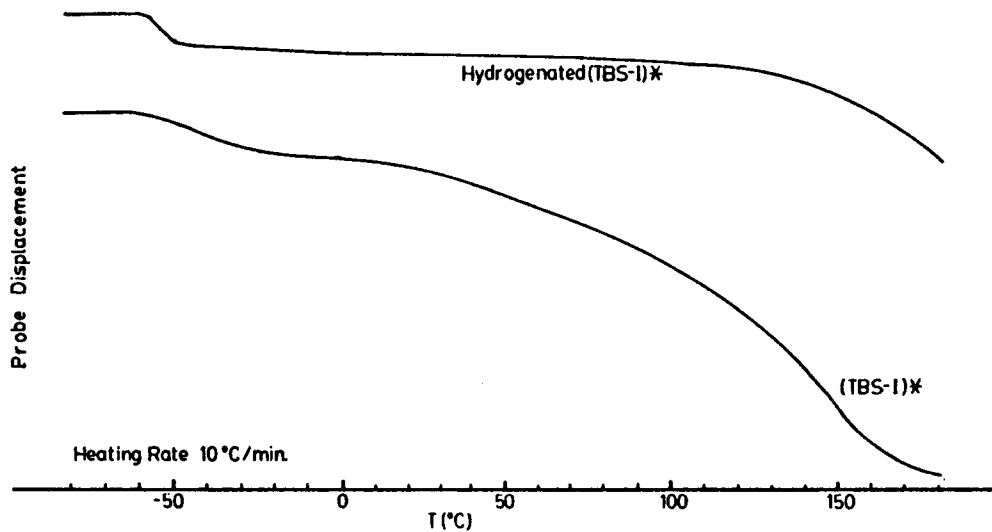


Figure 47. Thermal mechanical analysis of p-tert-butylstyrene and isoprene radial block copolymer and p-tert-butylstyrene and ethylene propylene alternating copolymer.

Table 13. Glass Transitions of Homopolymers (DMTA, 1 Hz).

Poly(p-tert-butylstyrene)	2.5×10^4 g/mol	157°C
Polyisoprene	7.5×10^4 g/mol	-45°C
Hydrogenated polyisoprene	7.5×10^4 g/mol	-45°C

phases with thermal properties more characteristic of the individual block components (Table 13).

Table 13 lists the glass transition temperatures, determined by dynamic mechanical analysis, of poly(p-tert-butylstyrene), polyisoprene and hydrogenated polyisoprene (ethylene propylene alternating copolymer). These polymers are of comparable chemistry and molecular weight to the individual block components of the radial block copolymer.

The increase in G' upon hydrogenation of (TBS-I)* is a result of an increase in the degree of microphase separation as well as a change in the viscoelasticity of the diene originating phase due to the change in the chemical nature of that phase. Both polyisoprene and an ethylene propylene alternating copolymer have a glass transition temperature of -46°C as determined by dynamic mechanical analysis at 1 Hz (Figure 48). However, polyisoprene has a plateau modulus of 10^7 dynes/cm², whereas the ethylene propylene copolymer has a plateau modulus of 10^8 dynes/cm².

The thermal mechanical analysis (Figure 47) of the (TBS-I)* and its hydrogenated form compliment the dynamic mechanical analysis. The poly(p-tert-butylstyrene) and isoprene polymer exhibits a broad low temperature transition followed by a continual decrease in modulus. Whereas, upon hydrogenation, the polymer exhibits a sharp low temperature

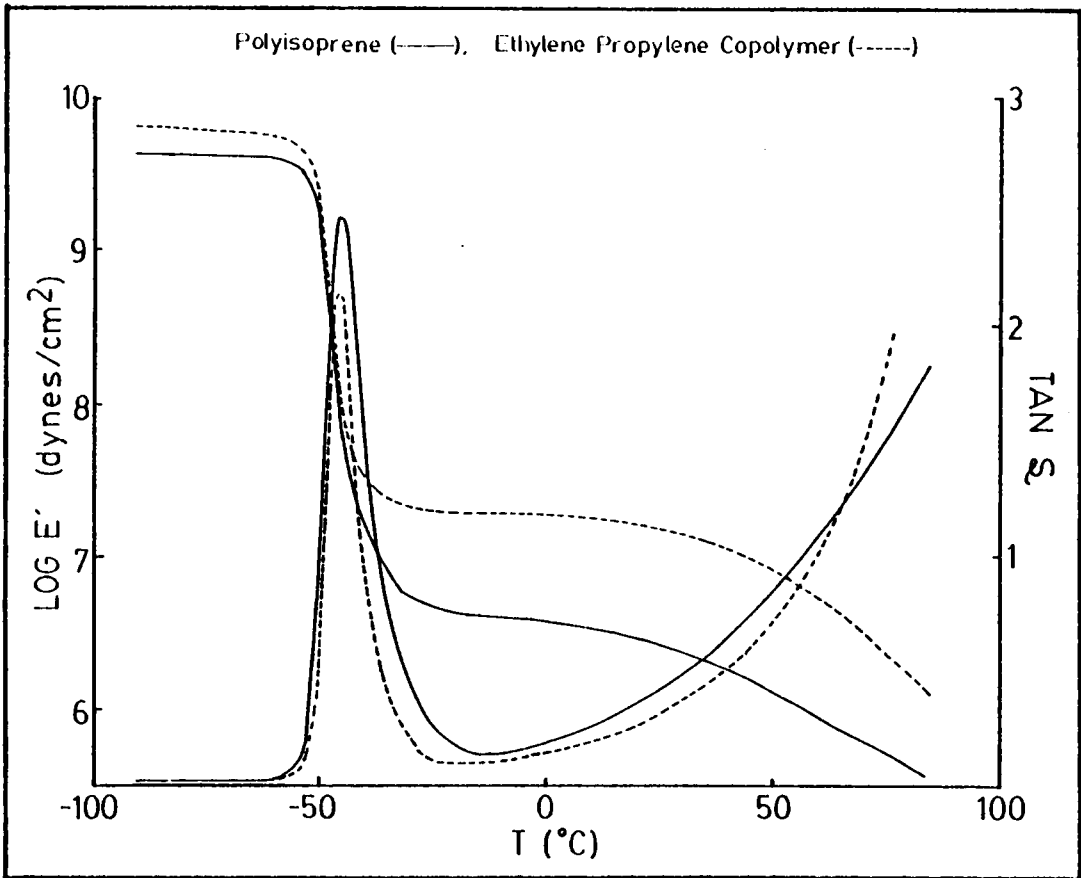


Figure 48. Viscoelastic properties of polyisoprene and ethylene propylene alternating copolymer (1 Hz).

transition near that of the ethylene propylene alternating copolymer and a retention of the plateau modulus over a temperature range covering 200°C. Thus, hydrogenation of the isoprene phase converts the material from one in which a reasonably compatible pair of components becomes a system having a high degree of microphase separation.

B. Part II

i. Dynamic Mechanical Properties

Figure 49 and Figure 50 show $\tan \delta$ and the tensile storage modulus at 1 Hz as a function of temperature for the full series of (TBS-I)* copolymers.

At 0% hydrogenation the unsaturated (TBS-I)* exhibits essentially a single broad primary dispersion at -20°C, followed by a rising $\tan \delta$ approaching the melt region (Figure 49). As the polymer is hydrogenated from 5% to 23% to 43% the low temperature transition broadens towards higher temperatures with the $\tan \delta$ maximum positioned at about -20°C; and, there is increasing evidence for the upper poly(p-tert-butylstyrene) transition as a shoulder on the rapidly rising $\tan \delta$ peak approaching the melt region.

Whereas, at 68% hydrogenation, this radial polymer exhibits $\tan \delta$ dispersions of the two phases, a sharp low temperature transition characteristic of the soft phase and

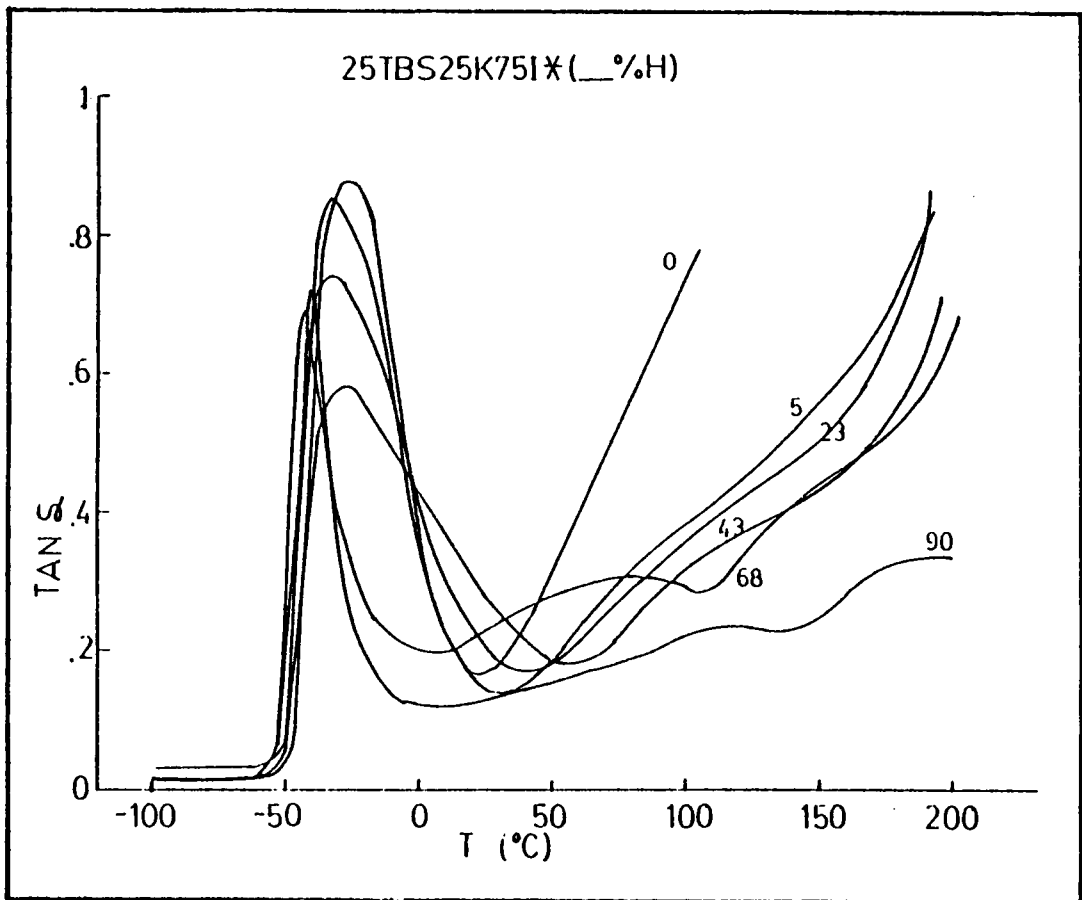


Figure 49. Tan δ of series of hydrogenated p-tert-butylstyrene and isoprene radial block copolymers (1 Hz).

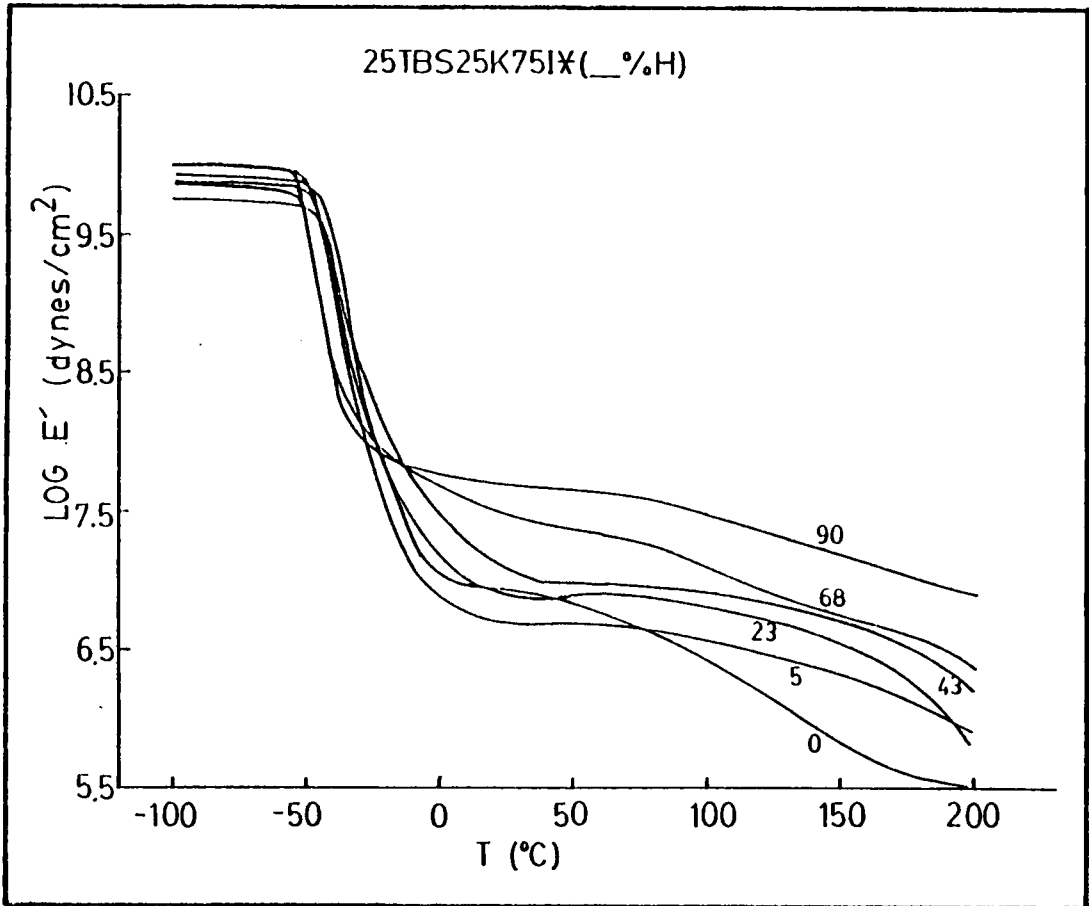


Figure 50. Dynamic storage moduli of series of hydrogenated p-tert-butylstyrene and isoprene radial block copolymers (1 Hz).

the onset of a high temperature transition at about 150°C corresponding to the p-tert-butylstyrene derived phase. At 90% hydrogenation the $\tan \delta$ spectrum shows even greater evidence for a two phase structure; the diene based phase being predominately an ethylene propylene alternating copolymer.

The corresponding tensile storage modulus (E') versus temperature plots show an increase in the plateau modulus value and the temperature range over which the plateau modulus is retained with increasing hydrogenation. The polymer exhibits less viscous and more elastic character with increasing formation of a two phase domain structure. At near quantitative hydrogenation of the polyisoprene phase, the polymer exhibits stress-strain behavior comparable to conventional SBS and SIS materials (Figure 51), possibly with improved high temperature performance. The enhanced phase separation with hydrogenation resulted in increased cohesiveness and greatly improved stress-strain behavior (Figure 51).

ii. Adhesive Performance

Pressure sensitive adhesives (1-14) require rather specialized and characteristic rheological properties; a pressure sensitive adhesive must adhere when brought into contact with a surface under light pressures and have sufficient cohesiveness that it can be peeled away from the

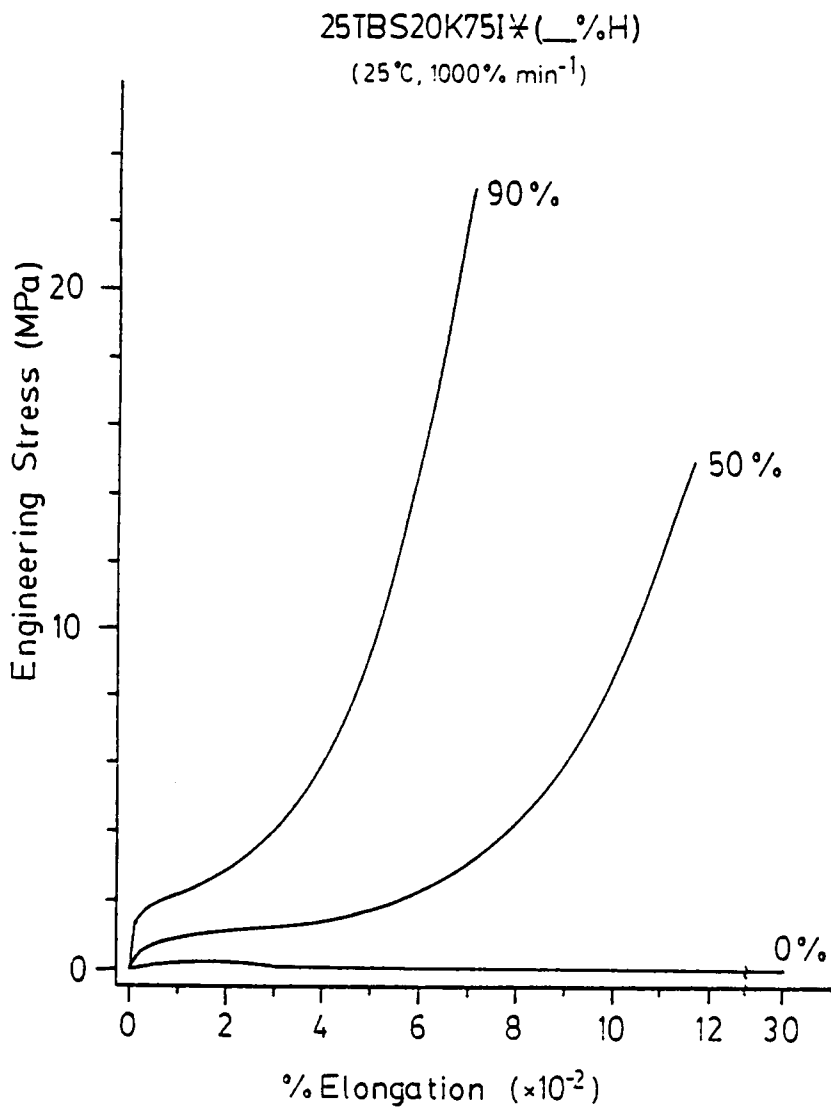


Figure 51. Typical stress-strain relations of a series of hydrogenated p-tert-butylstyrene and isoprene radial block copolymers (74).

surface without leaving a residue. It must have sufficient compliance to conform to surface rugosity, and it must undergo relaxation so that the stored energy due to elastic forces will be dissipated before they can overcome the forces of adhesion. Yet a satisfactory pressure sensitive adhesive must exhibit an elastic cohesiveness and a resistance to flow under stress. It is clear from the above that an important trade-off exists between tack and holding power, this is particularly true for block copolymer based PSAs.

There was good evidence for the development of a two phase structure in the (TBS-I)* copolymer upon hydrogenation, resulting in increased elasticity. Thus, hydrogenation of the isoprene phase to convert a reasonably compatible pair of components which exhibit "high" tack and "low" shear creep resistance into a system that has a high degree of microphase separation and exhibits "low" tack and "high" elastic cohesiveness was expected to provide a wide range of variation in PSA properties.

The peel results for the unsaturated (TBS-I)* base polymer (Figure 52) and its hydrogenated forms of 5% (Figure 53), 23% (Figure 54), radial block copolymer. and 43% (Figure 55) hydrogenation exhibit a shift, and also a broadening in some cases, of the transition region from cohesive to adhesive failure towards the lower peel rates. This corresponds to increasing elasticity of this set of polymers. At 68% hydrogenation, the polymer does not meet

the Dahlquist contact criterion (72); upon application of the polymer to the adherend no measurable adhesion resulted.

Increased hydrogenation of the polyisoprene block in the (TBS-I)* led to increased formation of a two phase domain structure and to increased elastic characteristics of the polymer, eventually, at the expense of tack and adhesion. Yet, up to 43% hydrogenation, the polymer had sufficient compliance to result in "good" tack and adhesion. With increased hydrogenation from 0% to 5% to 23% to 43% there is an increase in the measured peel force of cohesive failure due to the increased elasticity of the polymer with hydrogenation. At higher pull rates, where failure was adhesive, the measured peel force is independent of percent hydrogenation; the viscoelastic response of these polymers, at these higher pull rates, is not significantly different. Whereas, at 68% hydrogenation, the polymer did not have adequate tack to perform as a PSA.

The uniqueness of the investigated polymers lies in the ability to controllably affect the morphology and viscoelastic properties of the p-tert-butylstyrene and isoprene radial block copolymer by the extent of hydrogenation of the isoprene phase and in that way dictate the desired adhesive properties.

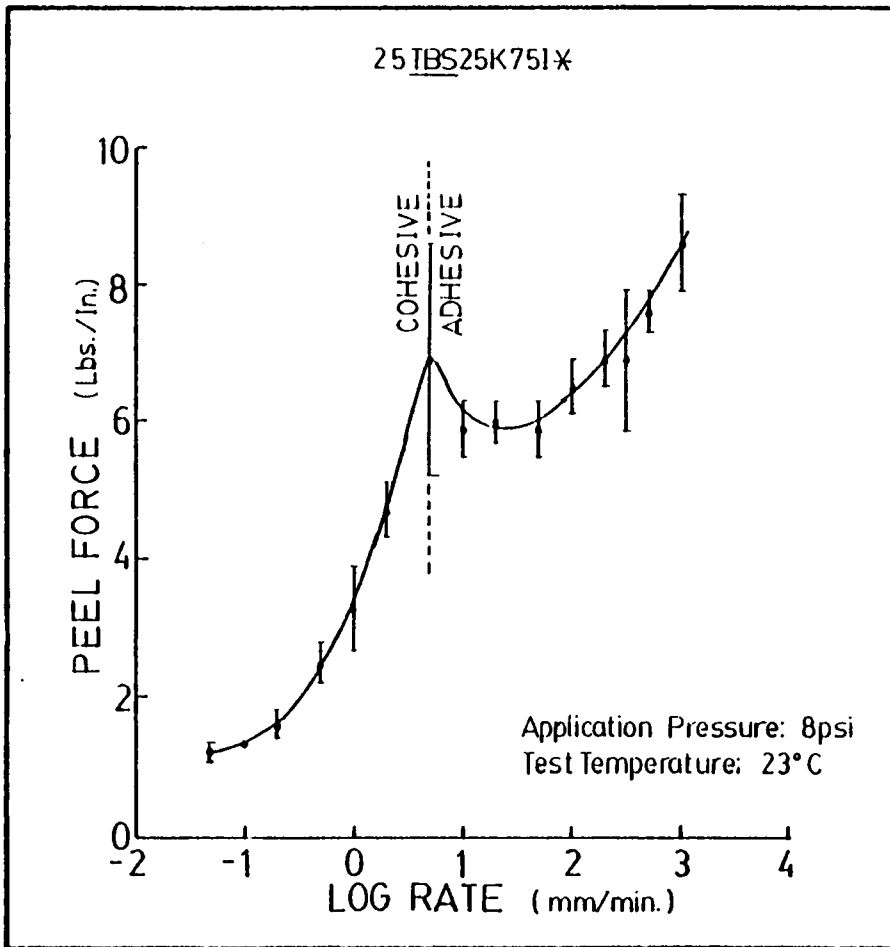


Figure 52. Peel force versus peel rate of p-tert-butylstyrene and isoprene radial block copolymer.

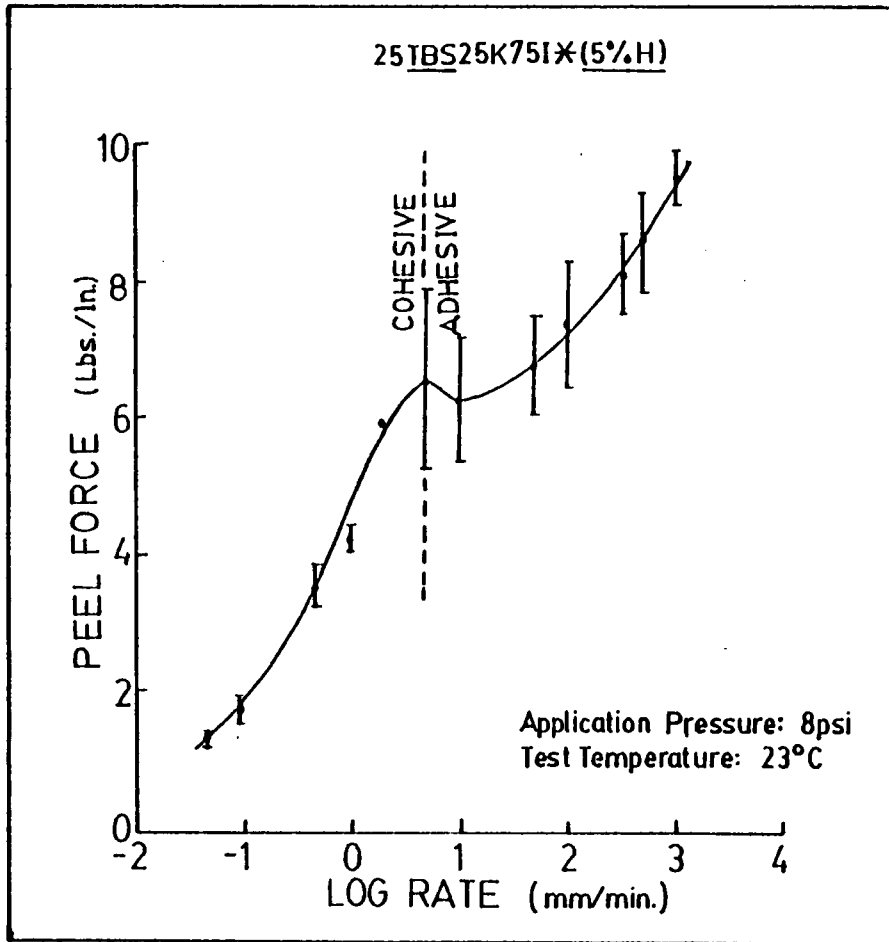


Figure 53. Peel force versus peel rate of p-tert-butylstyrene and isoprene radial block copolymer hydrogenated 5%.

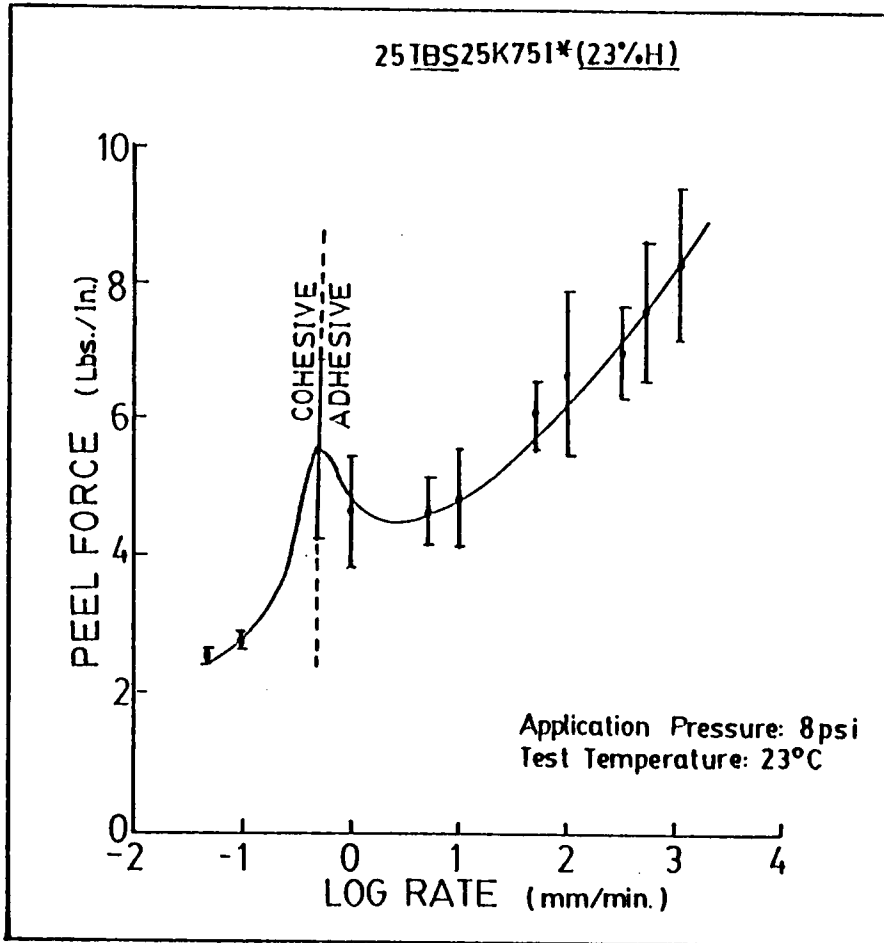


Figure 54. Peel force versus peel rate of p-tert-butylstyrene and isoprene radial block copolymer hydrogenated 23%.

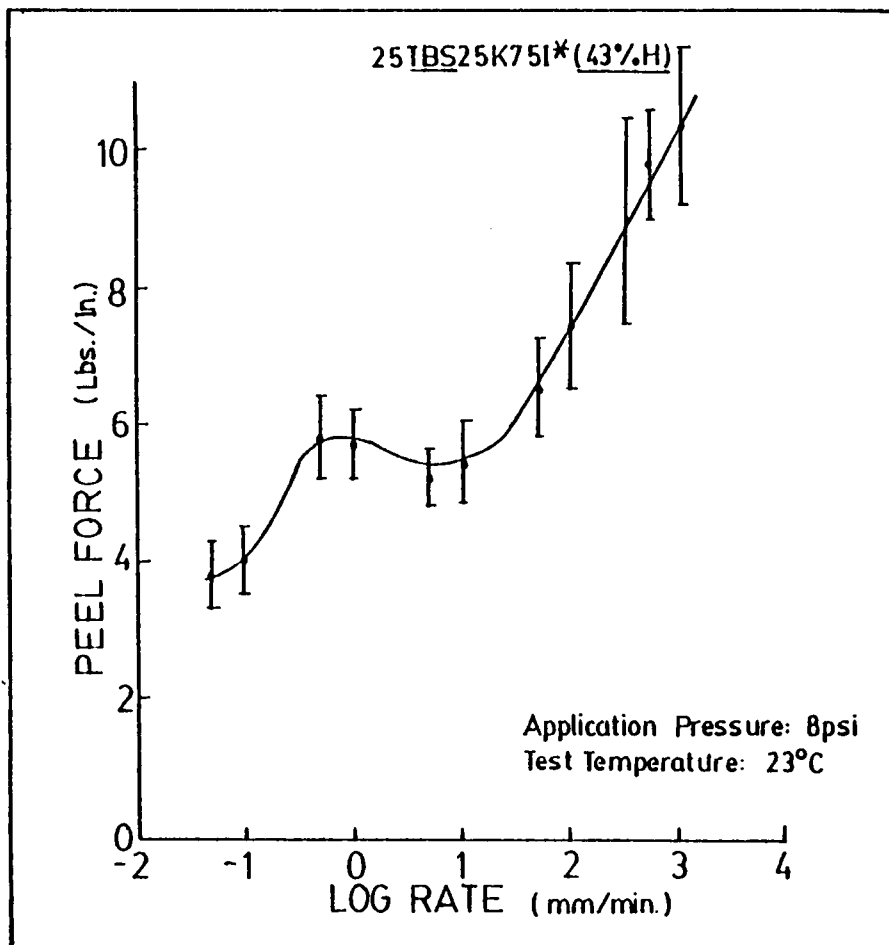


Figure 55. Peel force versus peel rate of p-tert-butylstyrene and isoprene radial block copolymer hydrogenated 43%.

REFERENCES

1. G. E. Molau, "Block Polymers," pp. 79-106, S. L. Aggarwal, ed., Plenum Press, New York (1970).
2. E. Vanzo, J. Polym. Sci., A-1, 4, 1727 (1966).
3. T. Inoue, T. Soen, H. Kawai, M. Fukatsu and M. Kurata, J. Polym. Sci., B, 6, 75 (1968).
4. T. Inoue, T. Soen, T. Hashimoto and H. Kawai, J. Polym. Sci., A-2, 7, 1283 (1969).
5. T. Inoue, T. Soen, T. Hashimoto and H. Kawai, Macromolecules, 3, 87 (1970).
6. T. Soen, T. Inoue, K. Miyoshi and H. Kawai, J. Polym. Sci., A-2, 10, 1757 (1972).
7. D. J. Meier, J. Polym. Sci., C26, 81 (1969).
8. D. J. Meier, Polym. Prepr.; ACS, Div. Polym. Chem., 11, 400 (1970).
9. D. J. Meier, "Block and Graft Copolymers," pp. 105-139, J. J. Burke and V. Weiss, ed., Syracuse University Press, N.Y. (1973).
10. D. J. Meier, Polym. Prepr., ACS, Div. Polym. Chem., 15, 171 (1974).
11. E. Helfand, Polym. Prepr., ACS, Div. Polym. Chem., 15, 970 (1973).
12. E. Helfand, "Recent Advances in Blends, Grafts and Blocks," L. H. Sperling, ed., Plenum Press, New York (1974).
13. E. Helfand, Macromolecules, 8, 552 (1975)
14. E. Helfand and Z. R. Wasserman, Macromolecules, 9, 879 (1976).
15. D. F. Leary and M. C. Williams, J. Polym. Sci., Polym. Phys. Ed., 11, 345 (1973); 12, 265 (1974).
16. W. R. Krigbaum, S. Yazyan and W. R. Talbert, J. Polym. Sci., Polym. Phys. Ed., 11, 511 (1973).

17. R. E. Boehm and W. R. Krigbaum, *J. Polym. Sci.*, C54, 153 (1976).
18. S. Kraus, *J. Polym. Sci.*, A-2, 7, 249 (1969).
19. S. Kraus, *Macromolecules*, 3, 84 (1970).
20. U. Bianchi, E. Pedemonte and A. Turturro, *Polymer*, 11, 268 (1978).
21. L. Marker, *Polym. Prepr.*, ACS Div. Polym. Chem., 10, 524 (1969).
22. S. L. Aggarwal, R. A. Livigni, L. F. Marker and T. J. Dudek, "Block and Graft Copolymers," pp. 157-194, J. J. Burke and V. Weiss, ed., Syracuse University Press, N.Y. (1973).
23. M. Shen and D. H. Kaelble, *J. Polym. Sci.*, B8, 149 (1970).
24. D. G. Fesko and N. W. Tschoegl, *Intern. J. Polymeric Mater.*, 3, 51 (1974).
25. T. Soen, M. Shimomura, T. Uchida and H. Kawai, *Colloid and Polym. Sci.*, 252, 933 (1974).
26. G. Kraus and K. W. Rollman, *J. Polym. Sci.*, Polym. Phys. Ed. 14, 1133 (1976).
27. G. Kraus, F. B. Jones, O. L. Marrs and K. W. Rollmann, *J. Adhesion*, 6, 235 (1977).
28. R. P. Zelinski and C. W. Childers, *Rubb. Chem. Technol.*, 41(1), 161 (1968).
29. R. J. Ceresa, ed., "Block and Graft Copolymerization," John Wiley and Sons, N.Y. (1973).
30. M. Matsuo, et al., *Polymer*, 9, 425 (1968).
31. G. Kraus, K. W. Rollmann and J. O. Gardner, *J. Polym. Sci.*, Physics Ed., 10, 2061 (1972).
32. T. Uchida, et al., *J. Polym. Sci. A-2*, 10, 101 (1972).
33. T. Hashimoto, et al., *Macromolecules*, 7, 362 (1974).
34. B. Gallot, *Pure and Applied Chem.*, 38(4), 1 (1974).

35. E. Campos-Lopez, D. McIntyre and L. J. Fetters, *Macromolecules*, 6, 415 (1973).
36. J. C. Kelterborn and D. S. Soong, *Polym. Eng. Sci.*, 22(11), 654 (1982).
37. A. Todo, Hiroyukiuno, K. Miyoshi, T. Hashimoto and Hiromichikawai, *Polym. Eng. Sci.*, 17(8), 587 (1977).
38. T. Hashimoto, Y. Tsukahara and H. Kawai, *Polymer J.*, 15(10), 699 (1983).
39. E. J. Amix, O. J. Glinka, . C. Han, H. Hasegawa, T. Hashimoto, T. P. Lodge and Y. Matsushita, *Polym. Prepr. (ACS, Div. Polym. Chem.)*, 24(2), 215 (1983).
40. H. Hashimoto, M. Fujimura, T. Hashimoto and H. Kawai, *Macromolecules*, 14, 844 (1984).
41. T. Hashimoto, Y. Tsukahara and H. Kawai, *Macromolecules*, 14, 708 (1981).
42. C. I. Chung, H. L. Griesbach and L. Young, *J. Polym. Sci., Polym. Phys. Ed.*, 18, 1237 (1980).
43. C. I. Chung and J. C. Gale, *J. Polym. Sci., Polym. Phys. Ed.*, 14, 1149 (1976).
44. C. I. Chung and M. I. Lin, *J. Polym. Sci., Polym. Phys. Ed.*, 16, 545 (1978).
45. T. Hashimoto, M. Fujimura and H. Kawai, *Macromolecules*, 13, 1660 (1980).
46. E. V. Gouinlock and R. S. Porter, *Polym. Eng. Sci.*, 17, 535 (1977).
47. A. Ghijsels and J. Raadsen, *Pure Appl. Chem.*, 52, 1361 (1980).
48. G. Kraus and K. W. Rollmann, *J. Appl. Polym. Sci.*, 21, 3311 (1977).
49. G. Kraus and T. Hashimoto, *J. Appl. Polym. Sci.*, 27, 1745 (1982).
50. J. M. Widmaier and G. C. Meyer, *J. Polym. Sci., Polym. Phys. Ed.*, 18, 2217 (1980).
51. N. Sivashinsky, T. J. Moon and D. S. Soong, *J. Macromol. Sci. - Phys.*, 822(2), 213 (1983).

52. L. J. Fetters, E. M. Firer and M. Dafauti, *Macromolecules*, 10, 1200 (1977).
53. J. M. Hoover, T. C. Ward and J. E. McGrath, *Polym. Prepr. (ACS, Div. Polym. Chem.)*, 25(1), 253 (1985).
54. W. P. Gergen, *Kautsch Gummi, Kunstst.*, 37(4), 284 (1984).
55. E. R. Pico and M.C. Williams, *Polym. Eng. Sci.*, 17, 573 (1977).
56. O. J. Chung, H. L. Griesbach and L. Young, *J. Polym. Sci. Phys. Ed.*, 18, 1237 (1980).
57. Refer to Chapter IV.
58. Refer to Chapter V.
59. P. J. C. Counsell and R. S. Whitehouse, "Tack and Morphology of Pressure Sensitive Adhesives," Chapter 4, p. 99.
60. F. H. Hammond, Jr., "Tack," in "Handbook of Pressure Sensitive Adhesive Technology," D. Satas (ed.), Van Nostrand and Reinhold Co. Inc., N.Y. (1982).
61. J. J. Bikerman, *J. Coll. Sci.*, 2, 163 (1947).
62. G. J. Crocker, *Rub. Chem. and Tech.*, 42, 30 (1969).
63. J. R. Dann, *J. Coll. and Inter. Sci.*, 32(2), 302 (1970).
64. J. R. Huntsberger, *Chem. and Eng. News*, 82 (1964).
65. Y. Iyengar and D. E. Erickson, *J. Appl. Polym. Sci.*, 11, 2311 (1967).
66. M. Toyama, T. Ho, H. Moriguchi, *J. Appl. Polym. Sci.*, 14, 2295 (1970).
67. F. Wetzel, *Characterization of Pressure Sensitive Adhesives. ASTM Bulletin No. 221*, 64 (1957).
68. G. Kraus and K. W. Rollmann, *J. Appl. Polym. Sci.*, 21, 3311 (1977).
69. J. L. Gordon, *J. Phys. Chem.*, 67, 1935 (1962).
70. F. H. Hammond Jr., *Polyken Probe Tack Tester, ASTM SPec. Pub. 360* (1963).

71. M. Toyama, T. Ho, and H. Horiguchi, J. Appl. Polym. Sci., 14, 2039 (1970).
72. C. A. Dahlquist, "Creep," in "Handbook of Pressure Sensitive Adhesive Technology," D. Satas (ed.), Van Nostrand and Reinhold Co. Inc., N.Y. (1982).
73. Polymer synthesis and molecular characterization were carried out by Mr. Jim Hoover, a Ph.D. candidate in the Materials, Engineering and Science program at VPI & SU, under the guidance of Drs. James E. McGrath and Thomas C. Ward.
74. G. Kraus, T. Hashimoto, J. Appl. Polym. Sci., 27, 1745 (1982).

CHAPTER VIII

CONCLUSIONS

The fundamental adhesive studies of block copolymers presented in this dissertation demonstrate the very important relationship that exists between morphology and adhesive performance. The investigated model systems were multiple component, multiple phase adhesives, representative of most real adhesives. The structure of the microphase separated morphology of the materials was found to influence the adhesive behavior in applications as hot melt/structural type adhesives and as pressure sensitive adhesives.

The dynamic mechanical behavior of the thermosetting and thermoplastic adhesives determined for free films and for films bonding together two rigid adherends, indicated a broader mechanical relaxation spectrum occurring at higher temperatures in the bonded assemblies. Microphase separation in the melts of the linear styrene/isoprene/styrene triblock copolymers was interpreted as contributing to the formation of residual stresses in both the free films and the bonded joints, under appropriate thermal and pressure histories; thus, illustrating the importance of sample preparation in the evaluation of multiple phase adhesive systems.

The need for a fundamental adhesive performance testing method led to the development of the modified probe tack test. The design of the Perkin Elmer DMA-2 permitted a new

experimentally more fundamental approach to be taken to the evaluation of tack and pressure sensitive adhesion. Compressive creep compliance master curves were constructed and utilized as predictive tools for pressure sensitive adhesive performance in relation to the three primary requirements of a good pressure sensitive adhesive, PSA: tack, peel adhesion and shear creep resistance. The compressive nature of the experiment was the key to the evaluation because it is the form of application of typical PSAs. Then, the value of the master curve is that predictions of a materials performance as a PSA can be made over an extended period of time and range of temperatures.

In the styrene (and substituted styrene) and isoprene radial block copolymer series, the presence or absence of diblock copolymer influenced the mechanism of performance of the materials as pressure sensitive adhesives. In the absence of residual diblock, the styrene (and substituted styrene) and isoprene radial block polymers were, in general, inherently "low" tack and "high" shear resistant adhesives. This was the expected behavior because typical styrene and isoprene block copolymer based PSAs require the addition of a sufficient quantity of a polydiene compatible tackifier to bring about sufficient tack for the material to perform well as a PSA. However, the high degree of compatibility in the p-tert-butylstyrene and isoprene radial block copolymer was responsible for the high tack and adhesion exhibited by this

adhesive. For the other materials where tack was low, adhesion was developed by control of contact pressure.

On the other hand, when the radial block polymers contained 20-30% by weight diblock copolymer, the diblock material served to "plasticize" the compositions and result in the materials meeting the Dahlquist contact criterion (1), in most cases. As a result of the plasticizing effect of the residual diblock, these materials were, in general, inherently "high" tack and "low" shear resistant adhesives. Overall, the measured peel strengths were well near the maximum of observed performance of industrial PSAs of similar formulation. The highest peel strengths were for those systems whose morphology contained well defined hard segment domains within the rubber matrix, where the domains served to reinforce the compositions.

Furthermore, the series of hydrogenated forms of the p-tert-butylstyrene and isoprene radial block copolymer clearly demonstrates the use of multiple component, multiple phase adhesives to meet the conflicting demands placed on modern adhesives. By controlling the extent of hydrogenation of the isoprene phase one can controllably affect the morphology and viscoelastic properties of the p-tert-butylstyrene and isoprene radial block copolymer and in that way control the trade-off between tack and holding power, dictating the desired adhesive properties.

In summary, the conflicting demands placed on modern adhesives are met through the use of multiple component, multiple phase adhesive systems. And, it is the compatibility of the adhesive components, as affected by the chemistry of the phases, composition, solvent, thermal and pressure histories, and the like, which influence the materials overall adhesive performance.

REFERENCES

1. C. A. Dahlquist, "Tack, Adhesion, Fundamentals and Practice," London: McLaren and Sons, Ltd. (1966).

CHAPTER IX

FUTURE WORK

Along the same lines as the work presented in this dissertation on "Fundamental Adhesive Studies of Block Copolymers," there is an immediate need to establish the morphology of the radial block copolymers. Information is needed on the structure of the domains, the size of the domains and also, on the degree of miscibility of the two materials that make up the respective block copolymers.

The question of the morphology can be convincingly answered by electron microscopy, through the use of staining techniques, and by the small angle x-ray scattering (SAXS) technique. Preliminary SAXS investigations showed evidence for a high degree of compatibility between poly(p-tert-butylstyrene) and polyisoprene, the results gave no indication of the formation of domains. Whereas, for the p-methylstyrene and isoprene, and the styrene and isoprene radial block copolymers, SAXS results presented evidence in support of a domain structure.

Two other areas for future work consideration include: i.) the investigation of the adhesive properties of further multiple component, multiple phase adhesives, either in the form of physical blends of the studied radial block copolymers or anionically synthesized terpolymers, and ii.) the "science of tackification."

Curiosity, early on, led to a brief investigation of the dynamic mechanical properties of polymer blends of various combinations of the styrene and isoprene based block copolymers. The materials proved to have interesting viscoelastic properties, promoting further interest in the adhesive performance side of this work. In addition, pentablock copolymers, ABCBA, where A is a polystyrene block, B is a poly(p-tert-butylstyrene block and C is a polybutadiene block have been anionically synthesized by Fetters et al. (1), should possess interesting morphologies and viscoelastic properties, and unique combinations of adhesive properties.

Lastly, one question that is not often addressed, but is of primary concern in the real world pressure sensitive adhesive industry is: "What is the mechanism of tackification?" Typical commercial pressure sensitive adhesives (PSAs), based on styrene and isoprene require the addition of a tackifier to bring about sufficient tack for the material to perform well as a PSA. To date, the process of tackification (i.e., the selection of an appropriate tackifier) is much more an art than it is a science. There is a strong need to develop the "science of tackification." One possible approach is to examine PSA formulations based on model tackifiers and model adhesives by solid state NMR (nuclear magnetic resonance). Isotopically labelled tackifiers can further help elucidate the process. In

addition, the accessibility of variable temperature magic angle spinning makes possible the investigation of structural and motional features of the adhesive compositions above and below their transition temperatures. From such a fundamental approach, an effort can be made to begin to understand the mechanism of tackification.

REFERENCES

1. L.J. Fetters, Proc. IUPAC, I.U.P.A.C., Macromol. Symp., 28th, Int. Union Pure Appl. Chem.: Oxford, UK (1982).

APPENDIX A
ESCA TAKE-OFF ANGLE STUDIES

INTRODUCTION

Surface chemistry plays a major role in the science of adhesion; therefore, in order to come to some understanding of the role of the surface in the adhesion studies undertaken in this dissertation, a knowledge of the nature of the film surfaces was needed. The pertinent question that needed to be answered was: "Is there any preferential surface migration of a given phase in the radial block copolymers to the surface?"

ESCA (electron spectroscopy for chemical analysis) take-off angle studies were conducted to resolve this question. However, detailed ESCA analysis of block copolymers requires considerable expertise beyond that of the author, therefore, the experimental details and results are presented without interpretation. The polymers which were investigated include: the p-tert-butylstyrene and isoprene, (TBS-I)*, the p-methylstyrene and isoprene, (PMS-I)*, and the styrene and isoprene, (S-I)*, radial block copolymers (studied in Chapter VI) as cast from either cyclohexane (CH), toluene (T) or dichloroethane (DCE).

EXPERIMENTAL

The number average molecular weight $\langle M_n \rangle$ of the styrenic block of the three radial block copolymers was ca. 25,000 g/mole. The polymers were 25% by weight styrenic block - 75% hydrocarbon block. The star block copolymers were virtually free of diblock impurities (2-3% by weight) and possessed a well-defined number of branches (ca. 8-10).

The take-off angle dependent ESCA studies were conducted using a Kratos XSAM 800 x-ray photoelectron spectrometer with a MgK x-ray source. The take-off angle was varied from 10° to 30° to 90° . Polymer films used for surface characterization were spin coated from 2% by weight polymer solutions. The polymer films were ca. 1000 Å thick, as measured by interferometry, and of uniform thickness. Studies were conducted on the five polymer-solvent pairs discussed in Chapter VI: (TBS-I)* and CH, (PMS-I)* and CH, (S-I)* and CH, (S-I)* and T, and (S-I)* and DCE.

Furthermore, ESCA experiments were also conducted on polystyrene, PS, poly(p-methylstyrene), PPMS, and poly(p-tert-butylstyrene), PTBS, as controls. The homopolymers were anionically synthesized and each had a number average molecular weight ca. 25,000 g/mole. Polymer films, for ESCA analysis, were spin coated from 2% by weight polymer solutions in cyclohexane.

RESULTS

Results of the study for the homopolymers, as prepared from cyclohexane, are listed in Table A-1 and the results for the radial block copolymers, as prepared from the specific solvents, are listed in Table A-2. Oxygen was present as a contaminant on many of the radial block copolymer films. A typical ESCA spectrum, the (S-I)* as prepared from cyclohexane, is shown in Figure A-1.

Table A-1

Homopolymer ESCA Take-Off Angle Dependence Results

<u>C_{main}/C_{shake up}</u>	<u>PS</u>	<u>PPMS</u>	<u>PTBS</u>
@10°	14.33	17.55	26.08
30°	14.35	18.00	29.70
90°	15.68	18.70	30.09

Table A-2

Radial Block Copolymer ESCA Take-Off Angle Dependence Results

$C_{\text{main/}}/$ $C_{\text{shake up}}$	(S-I)*/ DCE	(S-I)*/ T	(S-I)*/ CH	(PMS-I)*/ CH	(TBS-I)*/ CH
@10°	28.78	36.39	30.26	26.02	27.75
30°	34.90	30.06	33.47	35.35	26.14
90°	31.39	29.13	31.23	37.34	32.38
$C_{\text{main/0}}$					
@10°	15.59	13.46	14.21	12.83	-
30°	34.13	46.94	37.92	31.77	-
90°	59.15	65.79	52.71	54.24	-

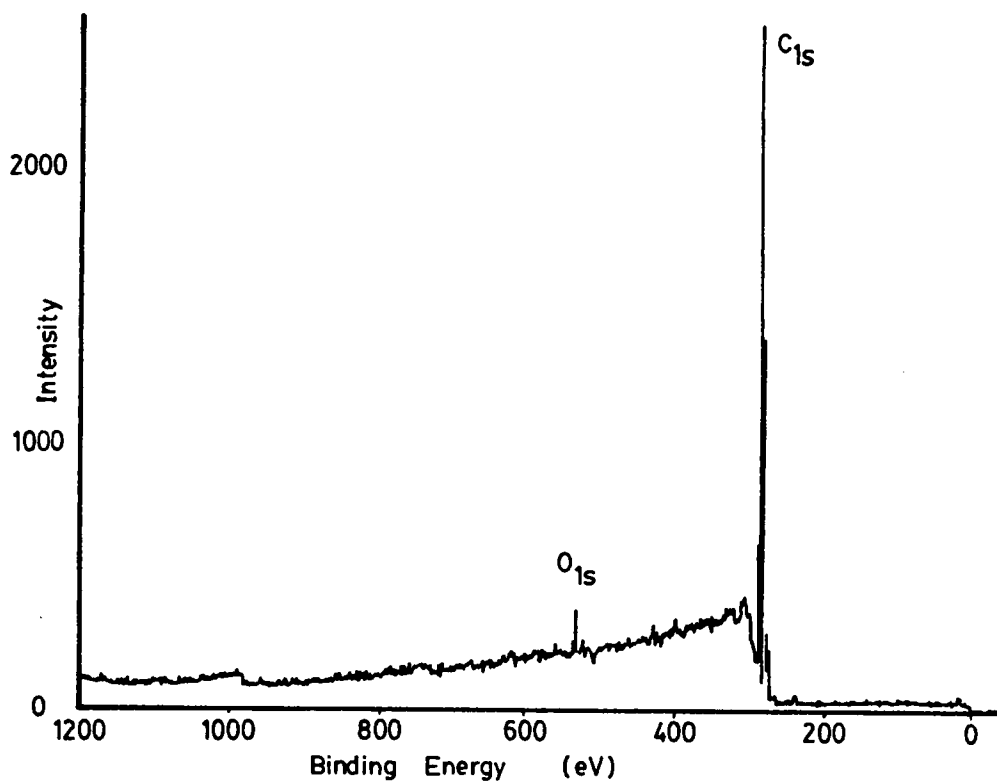


Figure A-1. ESCA spectrum for the styrenic and isoprene radial block copolymer as prepared from cyclohexane.

APPENDIX B
POLYMER BLENDS

INTRODUCTION

The multiple component, multiple phase adhesives based on styrene and isoprene proved to be excellent model adhesive systems. Therefore, additional multicomponent, multiphase materials prepared from physical blended combinations of the radial block copolymers were of interest. Initial investigations in this direction involved examination of the viscoelastic properties of physical blends of combinations of the p-tert-butylstyrene and isoprene, (TBS-I)*, the p-methylstyrene and isoprene, (PMS-I)*, and the styrene and isoprene, (S-I)*, radial block copolymers studies in Chapter V.

EXPERIMENTAL

The number average molecular weight $\langle M_n \rangle$ of the styrenic block of the three polymers was ca. 25,000 g/mole and the calculated average number of arms per "star", as determined by GPC analysis was ca. 3-6. The polymers were 25% by weight styrenic block - 75% hydrocarbon block. Each polymer was found to contain ca. 20-30% by weight residual diblock.

Polymer solutions, 20% by weight, in cyclohexane were prepared from each of the polymers. Physical blends of various polymer combinations were made by blending

predetermined amounts of the different solutions. The solutions were then poured into teflon trays and allowed to slowly dry under room conditions for 72 hours (while partially covered with a watchglass), followed by vacuum drying at 60°C for 48 hours. Films of the individual radial block copolymers were also prepared in the same manner.

The polymer films were tested on a Rheovibron DDV-II-C at 35 Hz in the tensile geometry. The heating rate was 1°C/minute. Approximate sample dimensions were: 5 mm width, 0.2 mm thickness and 30 mm length.

Furthermore, a polymer blend of poly(p-tert-butylstyrene), PTBS, and polystyrene, PS, was prepared. A 50/50 blend, by weight, was repeatedly molded at 180°C for 5 minutes under 20,000 psi and slowly cooled to room temperature under atmospheric pressure. In addition, a second, identical, blend was prepared by the solution method previously described. The number average molecular weight of the PTBS was ca. 25,000 g/mole and the number average molecular weight of the PS was ca. 100,000 g/mole. The PTBS was anionically synthesized at Virginia Tech and the PS was obtained from the Union Carbide Corporation.

The 50/50 blends of PTBS and PS were used to test the compatibility of the two homopolymers. A DSC (differential scanning calorimeter) thermogram was collected on the Perkin-Elmer DSC-2 for the blend prepared by the compression molding method. The heating rate was 10K/minute.

RESULTS

Figure B-1 shows the dynamic mechanical response for each radial block copolymer: (TBS-I)*, (PMS-I)* and (S-I)*. The results are similar to those found using the Polymer Laboratory DMTA, presented in Chapter V.

Figures B-2 and B-3 reveal the viscoelastic response of two different blends. Figure B-2 shows the results for a 50/50 blend by weight of (PMS-I)* and (TBS-I)*, and Figure B-3 shows the response for an equal blend by weight of the three block copolymers. Blending the various radial block copolymers creates additional multiple component, multiple phase materials whose dynamic mechanical response appears to be a combination of the individual responses of the respective block copolymers.

There was question of the compatibility of the hard blocks of the respective block copolymers in the blends. However, the DSC thermogram of the 50/50 blend of the PTBS and PS (Figure B-4), prepared by compression molding, indicates that the two homopolymers are not compatible. Furthermore, the same 50/50 blend prepared by the solution method, resulted in an opaque film, indicating again, that the two materials are non-miscible.

The viscoelastic response of the radial block copolymer blends, representing a combination of the individual

responses of the respective block copolymers, promotes interest in the adhesive performance side of this work. Various combinations of the individual radial block copolymers, as blends, should result in adhesive materials which possess a unique combination of properties.

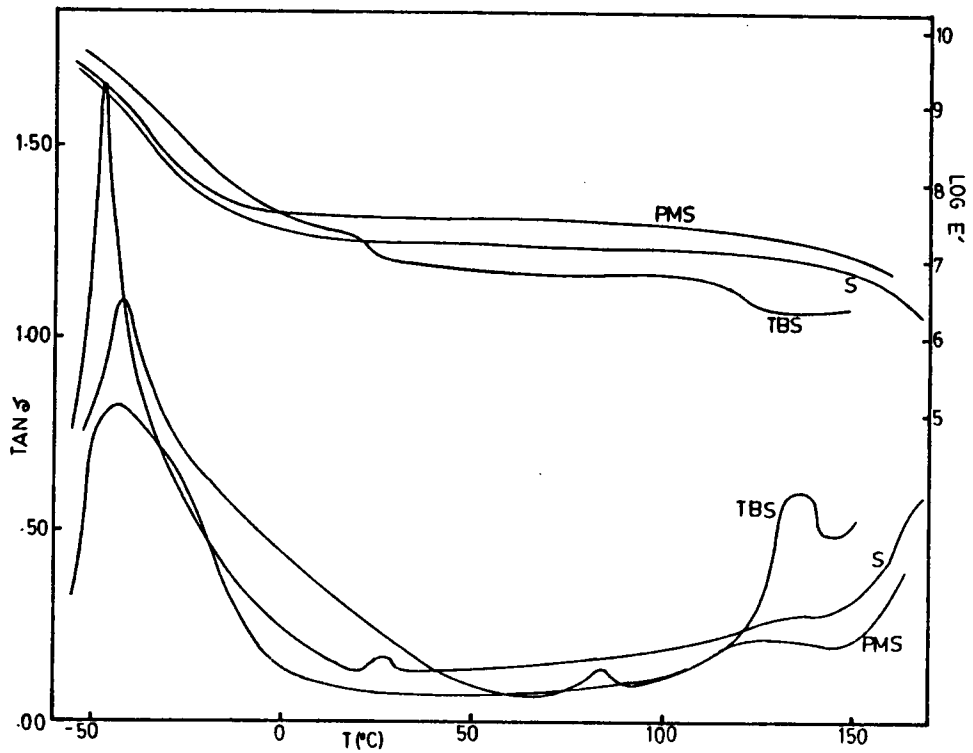


Figure B-1. Dynamic mechanical storage modulus and damping for (S-I)*, (PMS-I)* and (TBS-I)* radial block copolymer films (at 35 Hz).

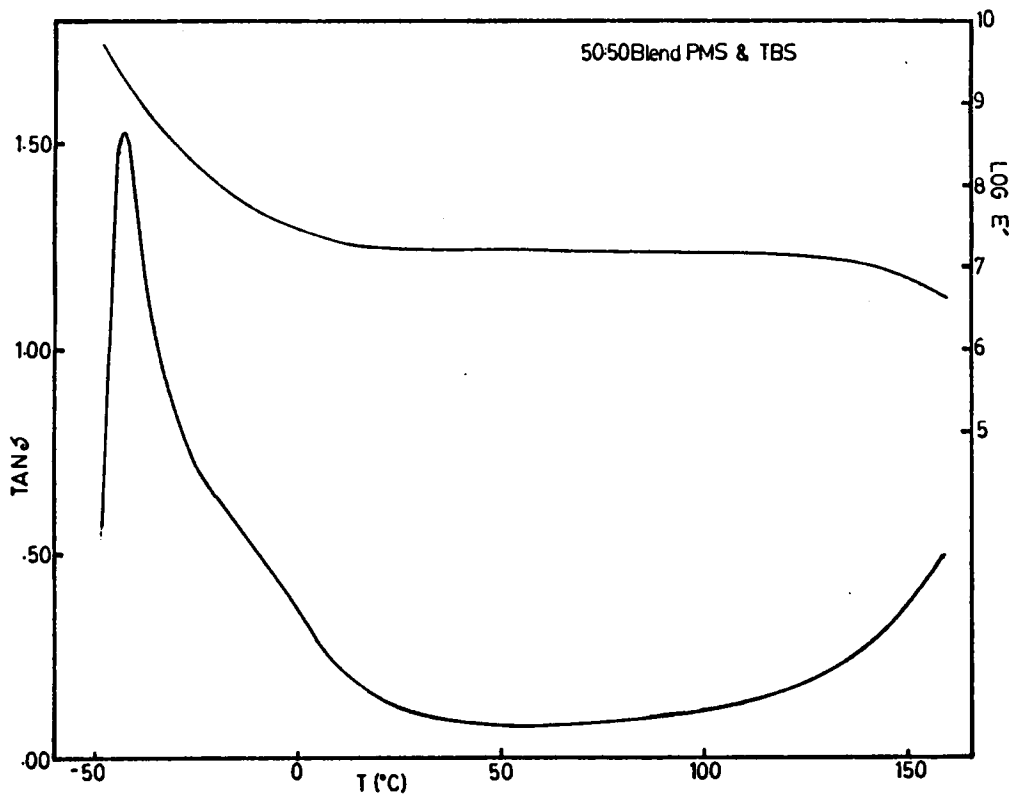


Figure B-2. Dynamic mechanical storage modulus and damping for a 50/50 blend by weight of (PMS-I)* and (TBS-I)* polymer film (at 35 Hz).

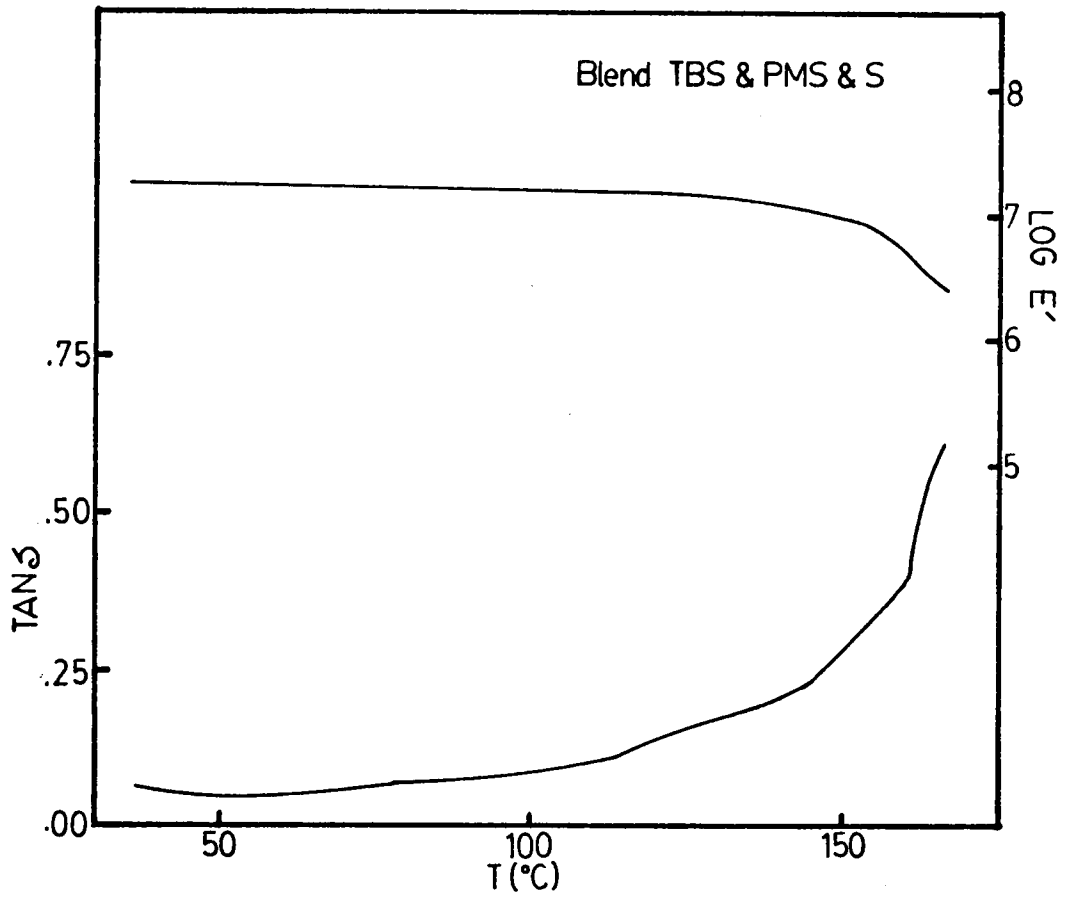


Figure B-3. Dynamic mechanical storage modulus and damping for an equal blend of (S-I)*, (PMS-I)* and (TBS-I)* polymer film (at 35 Hz).

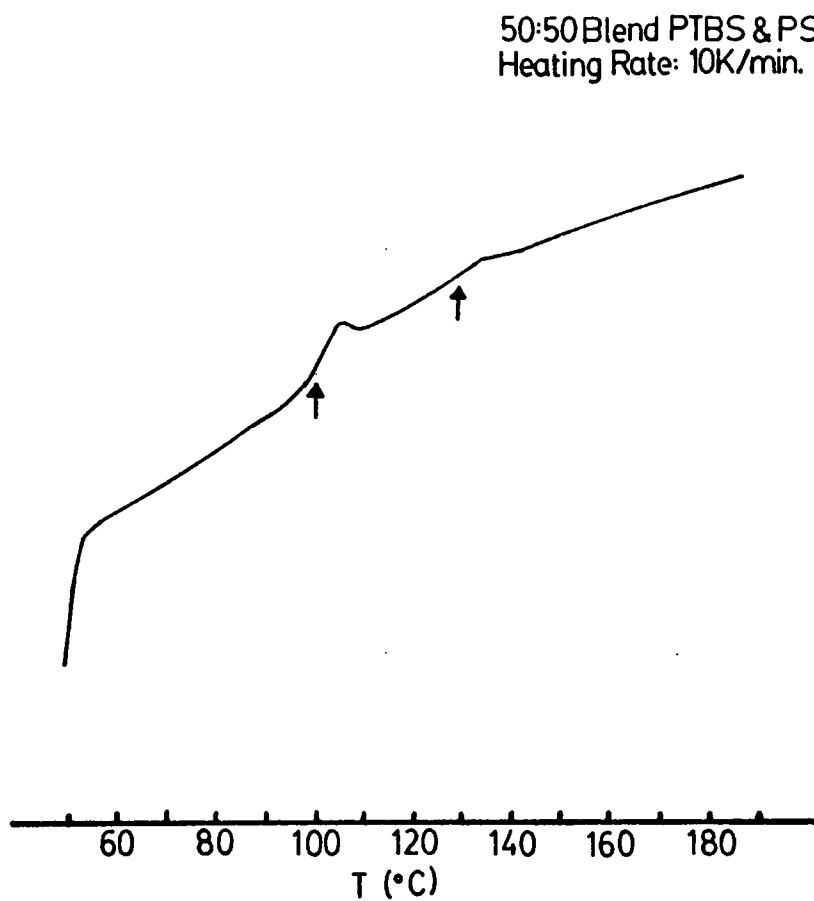


Figure B-4. DSC thermogram of 50/50 blend of PTBS and PS, prepared by compression molding.

APPENDIX C
SOLID STATE NMR

INTRODUCTION

High resolution NMR (Nuclear Magnetic Resonance) spectra for solid polymers can be obtained by employing a combination of resolution (DD-Dipolar Decoupling and MAS-Magic Angle Spinning) and sensitivity (CP-Cross Polarization) enhancement techniques. Such work, at ambient temperatures, has been conducted in our laboratory on various styrene/isoprene/styrene triblock copolymers (SIS) and polyurethanes in the bulk state (1); thus, similar work on a filled polymer sample or perhaps a modified bonded configuration could reveal information on polymer molecular motion as it occurs in a bonded specimen. Such an approach could further elucidate the adhesion studies being conducted here at Virginia Tech.

Preliminary investigations in this area involved collecting solid state NMR spectra of an SIS linear triblock copolymer and of the same polymer filled with a titanium alloy powder, thus, simulating a bonded specimen. The results were very intriguing, but, due to instrumental problems, the study was not continued. The experimental details and the results are presented without interpretation.

EXPERIMENTAL

A. Samples

i. SIS Copolymers

The SIS linear triblock copolymer was composed of 60% by weight styrene. The block number average molecular weights were 23,000/31,000/23,000 (g/mole), and the dispersity ratio (M_w/M_n), as determined by gel permeation chromatography, was 81,000/77,000. The polymer sample was obtained from the Phillips Petroleum Company. No evidence of homopolymer, diblock, or stabilizer additives could be seen in the chromatograms.

ii. Titanium Alloy Powders

The titanium alloy filler was 100 mesh and contained 6% by weight aluminum and 4% by weight vanadium. The Ti 6-4 (Al-V) powder was not pretreated prior to its use.

B. Sample Preparation

i. Ti(6-4) Filled Polymer Sample

The Ti 6-4 powder and the SIS triblock copolymer were physically blended in their powdered forms and compression molded at 180°C for 5 minutes under 20,000 psi. The film was cooled slowly to room temperature under atmospheric pressure.

The titanium powder was not uniformly distributed throughout the film, there were many areas where small islands of the Ti 6-4 powder had formed. The weight percent Ti 6-4 powder was ca. 40%. The film was punched into disks for the NMR experiment.

ii. Bulk Polymer Sample

The SIS triblock copolymer was compression molded in its powdered form at 180°C for 5 minutes under 20,000 psi. The film was slowly cooled to room temperature under atmospheric pressure. The film was then punched into disks for the solid state NMR experiment.

The filled and bulk polymer samples, contained in their respective rotors for the solid state NMR experiment, each possessed .35 g of polymer. The Ti 6-4 filled polymer film was evidently more densely packed than the bulk polymer film.

C. NMR

The solid state carbon-13 NMR experiment was carried out at 15.0 MHz on a Joel-60Q spectrometer at room temperature. Dipolar decoupled, magic angle spinning, cross polarization (CP-DD-MAS) NMR spectra were obtained from 10,000 FID accumulations with a selected contact time of 5.0 ms and a pulse delay time of 4s. A spectral width of 8000 Hz and an acquisition time of 64 ms were selected. NMR spectra were

collected for both the Ti 6-4 filled SIS triblock copolymer sample and the bulk SIS triblock copolymer sample.

RESULTS

Figure C-1 shows the CP-DD-MAS spectra of the SIS triblock copolymer (a.) in the bulk form and (b.) filled with Ti 6-4 powder. Peak assignments were not made and the results were not interpreted. Yet, there is a dramatic difference in the relative intensities of the peaks within the respective spectra, thus, promoting further interest in the use of NMR as a tool to uncover new details concerning polymer molecular motion as it may occur in a bonded joint and the interactions at the adhesive/adherend interface.

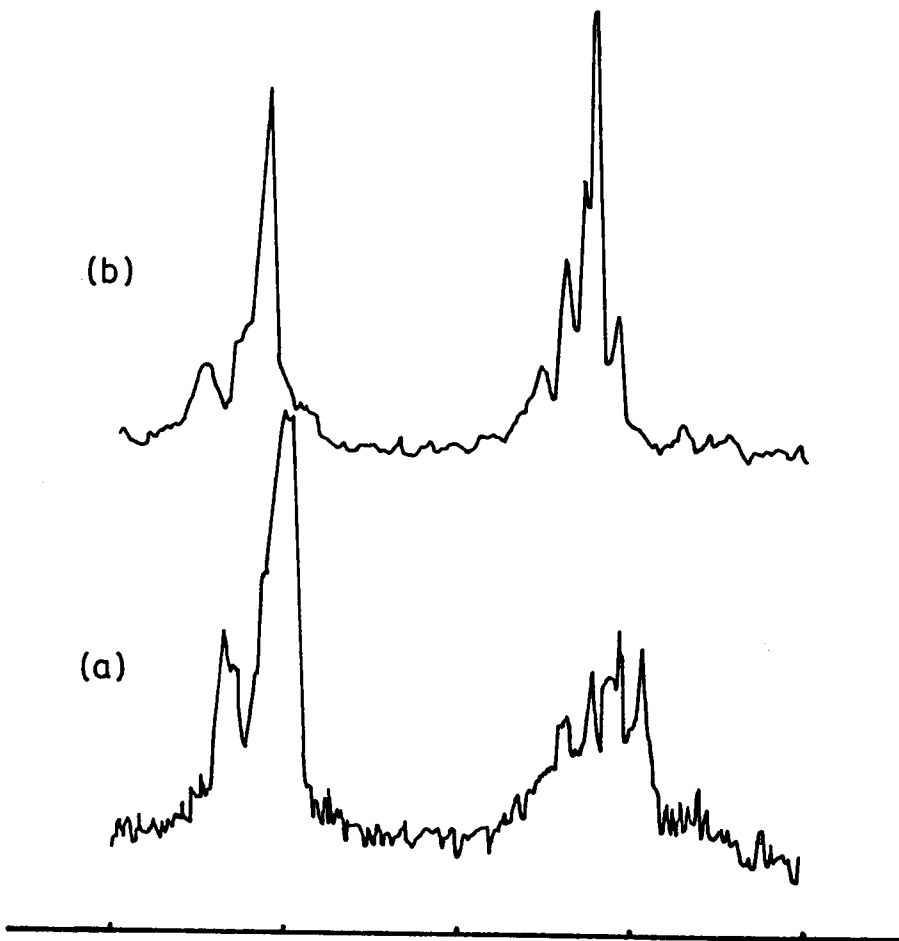


Figure C-1. CP-DD-MAS spectra obtained from 10,000 FID accumulations of SIS (60% S) triblock copolymer (a.) in the bulk form and (b.) filled with ca. 40% by weight Ti 6-4, with a selected contact time of 5.0 ms and a pulse delay time of 4s.

References

1. T.S. Lin, Ph.D. Dissertation, Virginia Polytechnic Institute and State University, Blacksburg, Virginia 24061 (1983).

**The two page vita has been
removed from the scanned
document. Page 1 of 2**

**The two page vita has been
removed from the scanned
document. Page 2 of 2**